Nickel (II) - Citric Acid Complex Formation in Aqueous Solution

A Thesis

presented in partial fulfilment of

the requirements for the degree of

Master of Science in Chemistry

at

Massey University

John Raymond Liddle

1979

Abstract

Titrimetric analysis of solutions of nickel(II) chloride and citric acid, H_3L, has led to the characterization of four complexes in the acidic pH range NiL^-, $NiHL$, NiH_2L^+, and NiL_2^{4-}.

Equilibrium constants for the formation of these complexes are reported. Results from a visible spectrophotometric study are analysed in terms of these four complexes.

The stability and possible structures of the complexes are discussed and compared with other nickel-carboxylic acid complexes.

Acknowledgements

I would like to express my gratitude to my co-supervisors, Dr. G. R. Hedwig and Dr. R. D. Reeves, for their advice and encouragement throughout the period of this work.

Thanks are also due to various members of the Chemistry Department, University Library and Computer Unit for advice and assistance, to Mr. R. S. Morrison for proof-reading the final scipt, to Mrs. J. Trow for assistance with diagrams, and to Mrs. J. V. Donnelly for endless typing efforts.

My grateful thanks go to my wife, Gabrielle, for her encouragement, support, and assistance throughout the past two years, and for the seemingly endless proof-reading of the past two months.

Table of Contents

List of Figures

List of Tables

1

Introduction

Nickel (atomic number 28) is a member of the first transition series of elements. This series includes the elements vanadium, chromium, manganese, iron, cobalt and copper, all of which are considered as essential elements for plant and animal nutrition (1-5). Nickel and titanium are the only members of this series of elements not yet universally considered as essential, although there is mounting evidence that nickel may be essential (2, 6-10, 100).

1.1 NICKEL IN VEGETATION

Nickel is ubiquitous in the earth and its waters. It constitutes about 0.008% of the earth's crust, the highest levels being found in igneous rocks, which average approximately 0.1% nickel. Of the igneous rocks, the ultrabasic rocks provide the principal sources of nickel. These rocks are high in magnesium and iron, but contain little silica, and the nickel level varies from 0.016% in basalt up to an average of 0.20% in peridotite (11).

Rocks forming the upper part of the earth's crust supply most of the material from which the soils are formed, and therefore the composition of the soils depends on the composition and distribution of various rock types. Farm soils throughout the world contain nickel in the range 0.0003 to 0.1% (11). The higher levels of nickel are found in soils of ultrabasic origin (92), and levels of nickel in soils derived from serpentinite and peridotite substrates have been reported as high as 0.8% (12, 13).

Nickel is widely distributed in plant tissues and has long been considered a normal constituent (14). The nickel concentration in most natural vegetation is in the range 0.05 to 5 ug/g on a dry weight basis (15). Nickel is normally toxic at levels greater than 50 ug/g (15), and the desire to make fertile large areas of barren ultrabasic land has led to wide research on the toxicity of nickel. This field has recently been reviewed by Mishra and Kar (14). All trace elements found in plant and animal tissues, whether essential or not, result in symptoms of toxicity. Nickel is no exception. Symptoms of nickel toxicity include: chlorosis of the leaves, necrosis, stunted growth of roots and shoots, deformation of various plant parts, unusual spottings; and are usually accompanied by a host of growth abnormalities (14).

Several plant species are known to thrive in ultrabasic soils and generally accumulate nickel to abnormally high levels, levels far in excess of those considered toxic. These species form a unique group of plants and there has been interest in their plant chemistry as a result of this accumulation. Brooks (16), has reviewed the accumulation of nickel by plants and has listed thirty-five species which are regarded as hyperaccumulators; that is, the nickel content of the dried leaf material is greater than 0.1%. Several of these species are recorded in Table 1.1, along with several non-accumulating species found over similar substrates. Most of these species are of the genera Alyssum and Homalium. Recent work has resulted in the discovery of further Alyssum accumulators and identified a further genus, Phyllanthus, as a dominant hyperaccumulator (17, 18). These three genera account for about two thirds of the nickel-accumulating species, leaving the other third spread roughly evenly throughout about a dozen other genera.

The geographical distribution of the species is also of interest, in that the Alyssum hyperaccumulators are to be found almost exclusively over the serpentine substrates of the Eastern Mediterranean, and the Homalium and Phyllanthus

Table 1.1 Representative Nickel-Accumulating Plant Species

1. Non-Accumulating

Species	ug/g Ni dry weight	Reference
Hebe odora	11.6	29
Cassinia vauvilliersii	12.0	29
Leptospermum scoparium	8.6	29
Artemisia scoparia	10.0	14
Avena sativa	7.2 - 30 [1]	14
Spinnacia oleraca	4.2	14

2. Hyperaccumulators

Species	ug/g Ni dry weight	Reference
Homalium francii	14500	32
mathienanum	1694	32
kanaliense	9420	32
Hybanthus austrocaledonius	13750	32
Alyssum alpestre	3640	17
bertolonii	13400	17
corsicum	10000	17
Rinorea bengalensis	17500	16
Psychotria dovarrei	47000	16
Sebertia accuminata	11700 [2]	12

1. Plants showed signs of nickel toxicity.
2. Latex was 25.7% Ni on a dry weight basis.

species over similar ultrabasic soils in New Caledonia. Other accumulating species have been found sparingly in South East Asia, Western Australia, and Central Africa.

Plant species which survive in hostile environments are able to do so as a result of tolerance mechanisms. These mechanisms generally take the form of either rejection of the metal so that no nickel is absorbed by the roots; or the storage of the metal at a particular site where it may be sequestered by complexation with naturally occurring ligands (30).

In the case of the nickel accumulators, the former mechanism is obviously not operating. There is evidence that nickel is readily absorbed by the plants as the divalent hexaquo-cation, and is not strongly absorbed when chelated (14). The absorption of nickel by plants is regulated by: (a) the total amount of available nickel in the soil; and (b) the properties of the soil, notably pH and organic matter content. These two conditions appear to be interdependent, in that the soil conditions regulate the amount of exchangeable nickel present.

Once absorbed by the plant, the nickel is probably complexed immediately in order to reduce its toxicity. Nickel is known to form chelate complexes with proteins, amino acids and organic acids (53, 89). Unidentified anionic complexes of nickel occur in xylem exudates of such plants as tomato, cucumber, corn, carrot and peanut (19). Tiffin found that iron (III) in several plant exudates showed the same electrophoretic behaviour as anionic iron (III)-citrate complexes, but suggested that amino acids may act as carriers for nickel, as nickel shows a particular affinity for nitrogen containing ligands (20, 21). However, no association between nickel and amino acids was found in studies of Hybanthus species from New Caledonia (22). Recent work on a number of Alyssum species suggests that the nickel is bound to the dicarboxylic acids, malic and malonic acids (23, 24,25,). The presence of an anionic citrato complex of nickel has been suggested in several species of the genera Sebertia,

Figure 1.1 The Structure of Carboxylic Acids Implicated in Studies of Nickel-Accumulating Plants

Common Name	Structure	Systematic Name [103]
Citric acid	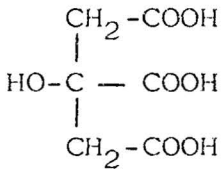	2-hydroxy 1,2,3 propane-dicarboxylic acid
Malonic acid	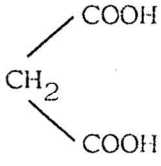	methane-dicarboxylic acid
Malic acid	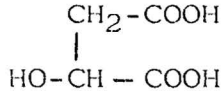	hydroxy-1,2 ethane dicarboxylic acid

Hybanthus, Homalium and Geissois, all from New Caledonia (16, 25,26,27). Spectral results suggest that in the hyperaccumulators where the nickel/citric acid ratio is generally greater than one, a 1:1 nickel:citrate species exists.

There is some speculation that the nickel is not immediately chelated by citric acid, although it is probably stored as such (27). If the nickel is translocated as the citrato complex, then unless the plant has other specific mechanisms for the exclusion of both copper and iron, one would expect these two elements to be accumulated also, as they form chelate complexes with citrate of greater stability. This assumes that the stability of the complex is important in translocation. However, this may not necessarily be so. A carrier and exchange mechanism for the uptake and storage of nickel has been suggested (27). A similar mechanism has been postulated for zinc resistant plants (28). However, this suggestion appears to overlook the availability of the metal ions for the uptake by the roots. The pH of serpentinite substrates is near neutral (pH is in the range 6.5 to 7.0) (29), hence the concentrations of the aquo ions of iron (III) and copper (II) will be considerably reduced because of the formation of hydroxides. In vitro, nickel hydroxide does not precipitate until a much higher pH than do iron (III) and copper hydroxides (90).

Due to these suggestions of the possible role of nickel-citrate complexes in some of the nickel-accumulating plant species, it was considered that a more complete study of nickel and citric acid complex formation would be in order.

1.2 FORMATION OF NICKEL-CITRATE COMPLEXES IN AQUEOUS SOLUTION

A complex may be defined as a species formed by the association of two or more simpler species, each capable of independent existence in solution (31). Each complex has a certain stability which describes the degree of association which occurs in a solution containing the species in equilibrium. Quantitatively, the stability of a complex ML is defined by the equilibrium constant for the reaction.

$$M + L \rightleftharpoons ML$$

where M and L are the free metal and ligand respectively. Then

$$K^{\circ} = \frac{a_{ML}}{a_M a_L}$$

where K° is the thermodynamic equilibrium constant and a_i is the activity of the species. Now $a_i = \gamma_i C_i$, where C_i is the concentration of species i, and γ_i is the activity coefficient of the species relating the concentration to the activity. Therefore

$$K^{\circ} = \frac{C_{ML}}{C_M C_L} \cdot \frac{\gamma_{ML}}{\gamma_M \gamma_L}$$

$$= K_C \cdot \frac{\gamma_{ML}}{\gamma_M \gamma_L}$$

where K_C is the concentration quotient for the reaction. As γ_i is a function of the solution's total ionic strength, K° and K_C are related by a function of ionic strength, I. i.e.

$$K^{\circ} = f(I)\ K_C$$

Concentration quotients are generally determined from studies containing relatively large concentrations of some inert electrolyte, in order to maintain as near constant ionic strength as possible. This background electrolyte must not form insoluble species or complexes with the

reactants under study. The thermodynamic equilibrium constant may then be determined by extrapolation to infinite dilution (I=0) of concentration quotients, determined at a number of ionic strengths. In this work however, the equilibrium constants for all species are those concentration quotients determined in a background of potassium chloride to bring the total ionic strength to 0.1 M.

The formation of complexes between nickel and citric acid is complicated in that citric acid has three acidic protons, and hence, there is scope for the formation of protonated complexes. If citric acid is considered to be a triprotic acid, H_3L, where L^{3-} is the citrate ion (see Section 3.1 for discussion on ionization of the fourth proton), and M the metal (in this case nickel), then the following reaction scheme summarizes the equilibria under consideration in the pH range 3 to 8:

$$p\,M + r\,H_qL \rightleftharpoons M_pH_{rq}L_r$$

Here, and in subsequent equilibrium and mathematical expressions, charges have been omitted for clarity.
The equilibrium constants for this scheme are of the form:

$$K_C = \frac{[M_pH_{rq}L_r]}{[M]^p\,[H_qL]^r}$$

Two examples from the general scheme are:

$$M + HL \rightleftharpoons MHL$$

Then $p = q = r = 1$ and

$$K^M_{MHL} = \frac{[MHL]}{[M]\,[HL]}$$

Similarly, for

$$2\,M + 2\,HL \rightleftharpoons M_2H_2L_2$$

$$K^M_{M_2(HL)_2} = \frac{[M_2(HL)_2]}{[M]^2\,[HL]^2}$$

Other equilibria relating various complex species can be characterized with knowledge of the protonation constants of the free ligand.

For example, for the equilibrium

$$ML + H \rightleftharpoons MHL$$

$$K^{ML}_{MHL} = K^{M}_{MHL} \cdot k^{L}_{HL}$$

Nickel-citric acid complexes of the stoichiometry MH_2L^+, MHL, ML^-, $MH_{-1}L^{2-}$, and ML_2^{4-} have been characterized, and stability constants for some reported (34-43, 53). Note that $MH_{-1}L^{2-}$ is a complex species where either the hydoxy proton, or a proton from a co-ordinated water molecule, has been displaced (46). Most of the studies were done at a temperature of 25°C, with experiments being conducted over a wide range of electrolyte backgrounds, including KNO_3, $NaClO_4$ and NaCl. The reported equilibrium constants are shown in Table 1.2.

Field et al, (34), carried out potentiometric experiments using a glass electrode to determine the hydrogen ion concentration. Mixtures of nickel nitrate and citric acid, at ratios of nickel to citric acid greater than one, were studied. The experimental data was analysed in terms of the complex species ML^- and MHL, and it was reported that no evidence for the existence of MH_2L^+ could be found. However, the point was made that if the equilibrium constant was small, then the species may well be present in too low a concentration for it to be detected under their experimental conditions.

An earlier study (35) reported the species MH_2L^+, along with ML^- and MHL, in solutions over a range of nickel-citric acid ratios. The pH was measured using a glass electrode with calomel reference electrode. However, it was then assumed that the measured pH was the negative logarithm of the hydrogen ion concentration and this would impart a systematic error as described in Section 2.4.

Another study has reported equilibrium constants for ML^- and MHL calculated from titration data where nickel was

Table 1.2 Reported Equilibrium Constants of Complexes of Nickel and Citric Acid at 25 °C

Background Electrolyte	$\log K^{M}_{ML}$	$\log K^{M}_{MHL}$	$\log K^{M}_{MH_2L}$	Reference
NO_3^-, 0.1 M	5.50	3.34		34
$NaClO_4$, 0.1 M [1]	5.54	3.30	1.75	35
NaCl, 0.1 M	5.11	3.19		36
$NaClO_4$, 1 M	4.30	2.90	1.45	91
NO_3^-, -	4.25	2.90	1.55	37
NO_3^-, -	4.54			39

1. At 20°C

in ten-fold excess of citric acid (36). In this work, it was also assumed that the measured pH is the negative logarithm of the hydrogen ion concentration. Calculations were included to show that this probably imparted an error in the log of the equilibrium constant of the order of 1%. With to-day's computational aids and knowledge of the behaviour of electrolyte solutions, this is a relatively high error.

A group of workers in the Soviet Union (37) have studied the complex formation by a cation exchange method. Solutions of nickel nitrate and citric acid were allowed to equilibrate after being shaken with a cation exchange resin. The equilibrium constants were then calculated by consideration of the distribution of the species between the resin and solution. The reported value for $\log K^{M}_{ML} = 4.25$ appears low and could well be a function of the method, or due to differences in ionic strength, which was not reported.

Further spectrophotometric and potentiometric studies have reported evidence for the species MHL, ML^{-}, and $MH_{-1}L^{2-}$ (33, 39, 44, 48, 88, 91). In one of these (39), calculations at pH 6, where it was assumed that all MHL would be neutralized and that the hydroxy proton was still intact, resulted in an equilibrium constant for the formation of ML^{-}. This value is quite low compared to more recent work and may well be due to the presence of acetic acid/sodium acetate buffer.

There is mounting recent evidence to suggest the formation of complexes where the ratio of metal:ligand is not 1:1.

The isolation of the species ML^{-} and $M(HL)_2^{2-}$ from solution has been reported (38). No indication of the ratio of nickel to citric acid mixed initially was given, but if citric acid is present in large excess, then the formation of the latter species would be promoted. Early Russian studies (42, 50) report the evidence of both ML^{-} and ML_2^{4-} in the low pH range, and the formation of $MH_{-1}L^{2-}$ in the alkaline region.

Spectral studies (27) suggest the presence of complexes with nickel:citrate ratios of 1:2, and another reports a complex of stoichiometric ratio 3:2 at pH 7.5 to 8.5 (42).

Although their presence has been indicated spectrophotometrically, no equilibrium constants have been reported for complex species of nickel:citric acid stoichiometry 1:2. Additionally, no equilibrium constants for polymeric species have been reported. Campi (35) reported that no evidence could be found for species of the formula M_2H_nL or $M(H_nL)_m$ where $m > 1$, while a recent spectral study indicates that a species of nickel:citric acid ratio 3:2 may be present (42).

Recent studies of the interaction of copper and citric acid have indicated the presence of both species with a 1:2 nickel:citric acid ratio and dimeric species (33, 45). Bottari, in a very extensive study (45), has reported the stepwise formation constants for nine copper-citric acid complexes. The formation of higher ratio complexes may be facilitated by the fact that the study was carried out with excess citric acid. The reported species include: CuL, CuH_2L, CuL_2, $CuHL_2$, $Cu(HL)_2$, CuH_3L_2, $Cu(H_2L)_2$, $Cu_2H_{-2}L$, and $Cu_2(H_{-1}L)_2$. They found no evidence for the species $CuHL$. This conflicts with the results of other workers (33, 35,46, 48). Other reports of polymeric species include: Cu_2L_2 (46), Cu_2L_{-2}, $Cu_2(H_{-1}L)_2$ (47), and Cu_2L (35).

Evidence has been reported for a cobalt-citric acid complex of the form $Co_2(HL)_2$ (38), while several studies have reported equilibrium constants for CoL, $CoHL$, CoH_2L, $CoH_{-1}L$, (35 ,38,44,49), in addition to complexes of 1:2 cobalt-citric acid ratio (50, 51,52).

The iron (III)-citric acid equilibria have been well documented (46, 81,84-87) and equilibrium constants have been reported for the following species: FeH_2L, $FeHL$, FeL, $FeH_{-1}L$, FeL_2, $Fe(H_{-1}L)_2$, $FeH_{-2}L$, $(FeH_{-1}L)_2$.

In the solid state, complexes of more complicated ratios of nickel to citric acid have been characterized. Complexes with nickel:citric acid ratios 3:2, 1:2, 1:1 have been reported (93). In a recent x-ray characterization

(94) at -156° C, the structure of a complex with a nickel-citric acid ratio of 4:3 has been determined. Carbon-13 NMR studies (95) have produced evidence for a discrete complex of nickel and tetraionized citric-acid with ratio 8:6. In the C-13 NMR study, molecular weight determinations indicate that studies of these complexes in solutions of very high ionic strength (concentrations of both components were 0.100 M) should be interpreted in terms of monomeric transition metal complexes of triionized citrate, and tetrameric complexes of tetraionized citrate.

1.3 THIS WORK

Previous equilibrium studies have resulted in the characterization of two nickel:citric acid complexes MHL, ML^-, (where H_3L = citric acid). There have been occasional papers reporting evidence for MH_2L^+, ML_2^{4-}, $MH_{-1}L^{2-}$. However, those studies have not been able to characterize these species, the reported equilibrium constants varying widely. The majority of studies have been carried out in solutions where nickel is in excess, and this could account for the lack of evidence for species other than those with 1:1 nickel-citric acid ratios.

The object of this study was to reinvestigate nickel-citric acid equilibria, and to determine the equilibrium constants from the data for solutions over the range of nickel concentrations from 1×10^{-3} $moll^{-1}$ to 3×10^{-3} $moll^{-1}$, and the range of nickel:citric acid ratios from 1:0.84 up to 1:3. The background electrolyte used, KCl, is one which is more appropriate to physiological conditions in the nickel-accumulating species.

The range of solutions was subject to extensive study by potentiometric titrations and spectrophotometric techniques. Titration data were analysed with the aid of computer programs (listed in Appendix 2), in order to calculate equilibrium constants from $p[H^+]$ measurements. Visible spectra of solutions with a given ratio were recorded over a wide pH range, allowing interpretation of the spectra based on the distribution of species present, given the equilibrium constants which were determined as outlined.

2

Experimental

2.1 MATERIALS

Wherever possible, AnalaR grade chemicals were used. If the chemicals were not suitable as primary standards, stock solutions were prepared and standardized in an appropriate manner. The source and treatment of each chemical is outlined below.

Nickel Chloride

As nickel chloride ($NiCl_2.6H_2O$) is not a primary standard, a one molar stock solution was prepared using BDH AnalaR nickel chloride (reported assay not less than 98.0%), and the resulting nickel concentration determined gravimetrically as the dimethylglyoximate, as described by Vogel (54). The concentration was known to a precision of 0.2%.

Citric Acid

Throughout this investigation, a sample of Mallinckrodt AR reagent citric acid ($C_6H_8O_7.H_2O$) was used without further purification. Since the chemical is not anhydrous, tests were carried out to determine the best method of handling the chemical. These included analysing samples of the acid which had been dried under a vacuum at room temperature for two hours, dried at 110°C for one hour, and samples without any pretreatment. These samples were analysed both titrimetrically and microanalytically. The sample dried at 110°C decomposed. The results of these tests are recorded in Table 2.1.

Table 2.1 Analysis of Citric Acid After Drying

	Microanalytical Results [1]	Titrimetric Results [2]
Sample used without pretreatment	%C = 34.46 ± 0.06 [3] %H = 4.83 ± 0.03	100.0 ± 0.5 [5]
Sample used after vacuum drying	%C = 35.40 [4] %H = 4.76	102.9 ± 0.3 [6]

1. Expected results based on $C_6H_8O_7 \cdot H_2O$ %C = 34.29
   %H = 4.80

2. % purity = $\frac{\text{moles base used}}{\text{moles base expected}}$

3. Mean and standard deviation of 7 samples.
4. Mean of two samples.
5. Mean and standard deviation of 4 samples.
6. Mean and experimental precision of two samples.

The microanalytical and titrimetric results for the untreated sample indicate that the sample was of 100.0±0.5% purity. The analytical results on the vacuum dried sample suggest that water was lost during the drying process.

Samples of the citric acid were checked titrimetrically and microanalytically throughout the period of study and the results were generally within the precision shown in Table 2.1.

Potassium Chloride

Stock solutions were prepared using either PROlabo "normapur" reagent (reported assay > 99.5%), or May and Baker "R" reagent (reported assay > 99.5%).

Sodium Hydroxide

Sodium hydroxide solutions were prepared by diluting sealed vials of either BDH:CVS or May and Baker "Volucon" concentrated reagent.

Hydrochloric Acid

A stock hydrochloric acid solution was prepared by dilution of a BDH AnalaR concentrated reagent.

Potassium Hydroxide

May and Baker "Proanalysis" reagent pellets were used.

Potassium Dichromate

A sample of Hopkins and Williams AR grade potassium dichromate (reported assay > 99.9%) was used without further purification. It was dried according to Vogel (65).

Reagents for pH Standard

The three pH buffers used throughout the course of this work were phthalate, 1:3.5 phosphate, and borax. The chemicals used were as follows: May and Baker R grade potassium hydrogen phthalate (reported assay 99.9-100%), BDH AR grade potassium dihydrogen phosphate (assay 99.5 to 100.5%), disodium hydrogen phosphate (assay 99.5%) and sodium tetraborate (borax) (assay 99.5%). These chemicals have been shown to give results internally con-

sistent with NBS Standard Reference Materials (56). The chemicals were dried according to Bates (57).

Potassium Hydrogen Phthalate

For the standardization of sodium and potassium hydroxides, NBS Reference Material 185e was used, after drying at 120°C for two hours.

2.2 GLASSWARE

B-grade glassware was used throughout the work, this being all that was available. All pipettes were calibrated by weighing the nominal value of water and calculating the exact volume from published density data (58). Pipettes were initially cleaned by standing in chromic acid overnight, then calibrated, and thereafter cleaned periodically with concentrated nitric acid.

When preparing solutions, volumetric glassware was washed with distilled water and acetone, dried, and then washed with "degassed" water (see Section 2.3).

2.3 PREPARATION OF SOLUTIONS

Water

Water used in the preparation of all solutions was distilled from alkaline potassium permanganate solution (62). To remove dissolved CO_2, it was then boiled for 5 -10 minutes and allowed to cool with nitrogen bubbling through it to ensure no contamination from atmospheric carbon dioxide. Water treated in this manner was used immediately after preparation.

The conductance and pH of this "degassed" water, (also referred to as "CO_2-free"), was checked frequently throughout the period of experimentation. The pH of water so treated was generally within the range 6.3 to 7.2, and the conductance in the range 1.7 to 3.8×10^{-6} reciprocal ohms.

Citric Acid

Citric acid solutions used for purity determinations were prepared by weighing samples to five decimal place precision and then dissolving in "degassed" water.

Sodium Hydroxide

The sodium hydroxide solutions were prepared by adding the contents of the volumetric vials to degassed water. The solution was then standardized just prior to use by potentiometric titration against a solution of potassium hydrogen phthalate. A precision generally less than 0.25% can be obtained this way.

These sodium hydroxide solutions were kept for periods of not more than one week, depending on the frequency of use.

Potassium Hydroxide

Potassium hydroxide solutions were prepared by washing the pellets several times with distilled water before transferring them to a flask where they were dissolved. The concentration of potassium hydroxide was then determined by potentiometric titration against a

solution of standard phthalate. These solutions were kept for about a week at a time.

Potassium Dichromate

Solutions of potassium chromate were used to calibrate the spectrophotometer. These were prepared by adding a weighed sample of potassium dichromate to potassium hydroxide solution. This is discussed in more detail in section 2.5.3.

Buffer Solutions

The buffer solutions used in checking the linearity and slope of the pH measurement system were prepared by weighing out predetermined amounts of the salts and dissolving them in degassed water.

The phthalate buffer was replaced frequently, because it was observed that if kept for any length of time, mould growth developed. This has been reported previously (78). Mould growth in the borax and phosphate buffers was not observed and these standards were replaced less frequently.

Complex Solutions

The term "complex solution" is used to refer to solutions where both nickel chloride and citric acid are present at known total concentrations, and potassium chloride has also been added for ionic strength control.

Aliquots of the stock nickel chloride were added by pipette, potassium chloride by burrette and citric acid weighed out.

The amount of potassium chloride required to bring the solution to an ionic strength of 0.1M was determined by assuming that citric acid behaves as a 1:2 salt i.e. Citric acid is assumed to ionize predominantly to $HL^{2-} + 2H^{+}$, where L^{3-} represents the citrate ion. This assumption appears reasonable based on the distribution of the species at the beginning of the titration, i.e. at a pH of approximately 3 (see Section 3.1, Figure 3.1).

These complex solutions were used immediately after preparation, because mould growth was observed in the solution if left for any length of time.

2.4 pH MEASUREMENTS

2.4.1 The pH Meter and Electrodes

All pH measurements were made using a Radiometer PHM 64 Research pH Meter, coupled with a Beckman Futura E-2 Glass Electrode and a Beckman Futura Calomel Reference Electrode with a quartz junction. One advantage of the E-2 glass electrode is that it shows minimum deviation due to sodium ion concentration, making correction unnecessary at pH values less than 11. The readability of the pH meter was to 0.001 pH units.

2.4.2 pH Titration Cell

The titration cell is shown in Figure 2.1 and was based on a design described by Perrin (59). The cell consisted of two double-walled glass jackets (a and b), through which thermostated water was passed. The temperature was controlled at 25.0 ± 0.10°C by a Thermomix 1440 temperature control unit. The two jackets were joined by a teflon plug (c) which was rigidly fitted to the upper jacket and fitted firmly into the lower jacket. The glass and calomel electrodes were supported in the upper jacket by a teflon plug (d) and enclosed by a teflon lid (e).

Nitrogen, first saturated with water vapour at 25°C, could be passed over the surface of the test solution through the glass tube (f).

A magnetic stirrer and a teflon-covered magnetic "flea" were used to stir the test solution. The moving magnetic field had no observable effect on the stability of the pH of a test solution.

The titrant was added to the test solution from an "Agla" micrometer syringe (Burroughs Wellcome and Co.). This consists of a calibrated all-glass syringe which was attached to a micrometer screw gauge which operates the plunger. The syringe delivers 0.5 cm^3, and the readability of the screw gauge is 0.0002 cm^3. The titrant was passed from the syringe through a 22 gauge stainless steel needle (g) into the test solution. When the tip of

Figure 2.1 The Titration Cell

a upper jacket
b lower jacket
c teflon plug
d teflon support
e teflon lid
f nitrogen line
g stainless steel needle

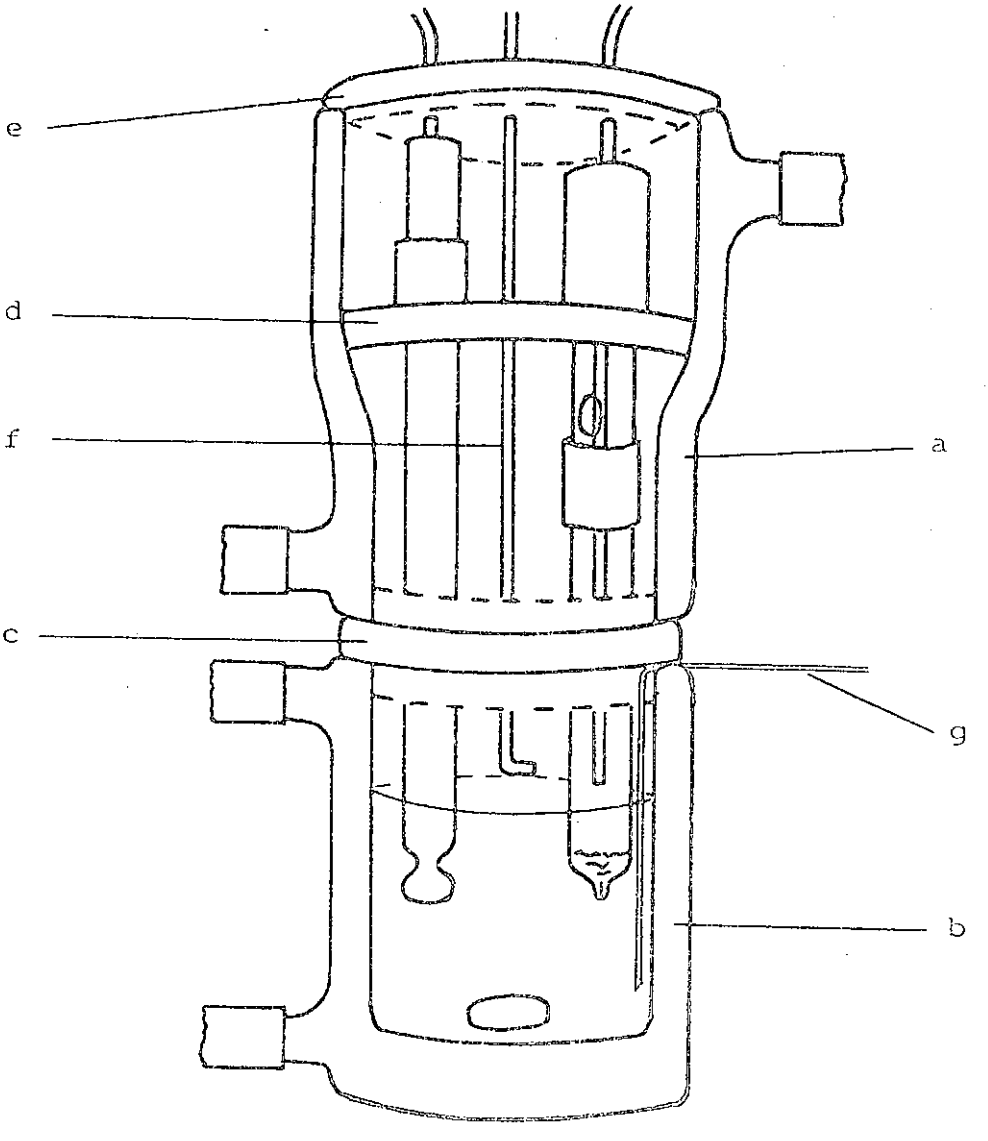

this tube was placed in the test solution, there was no noticeable diffusion of the titrant.

2.4.3 Procedure for pH Measurements

The electrodes and the lower glass jacket were firstly washed with distilled water, and then dried with absorbent tissue. If the test solution was a standard buffer, the electrodes and jacket were washed with this, after which a sample, which had been stored at 25°C, was added to the cell. The measured pH was found to drift initially, becoming stable after about five minutes.

During a titration, after an increment of base had been added, equilibrium was obtained within one minute.

Before a set of pH measurements, the system was standardized using the phthalate buffer (pH(S) = 4.008 at 25°C (65)). The response of at least one of the borax and 1:3.5 phosphate buffers was also checked. After a set of measurements, usually taking about one hour, changes in the reference point were checked by the measurement of the phthalate standard. Generally, the change in the phthalate reading was less than 0.005 pH units, and if the drift was greater than this the data set was discarded.

Throughout the period of experimentation it was observed that drifts in the reference point generally followed a cyclic pattern. Having standardized the pH measurement system initially with phthalate buffer, it was found that after about two to three hours drifts of the order of 0.01 to 0.02 pH units were common. This drifting ceased after about three hours and then always drifted slowly back to the original reference point over a period of about twelve hours.

The titration assembly was in an internal room with a thermostated environment, so that this behaviour cannot be attributed to changes in the physical environment. It seems as though it may be a characteristic of the glass electrode, in that drifting was not experienced when titrations were restricted to acidic pH's.

Aside from inconvenience, this behaviour caused no problems, since it was easily detected by measuring the pH of the standard buffers.

2.4.4 Reproducibility of pH Measurements

The pH of the standard buffers had a reproducibility within ± 0.002 pH units. The reproducibility of the data obtained from the buffer regions during titrations was generally less than ± 0.003 pH units. About the endpoint, deviations greater than this were experienced due to the effects of slight errors in the volume of the titrant added.

2.4.5 The Calibration of the pH Measurement System as a Hydrogen Ion Concentration Probe

The determination of many equilibrium constants involves measuring the pH of a solution in order to calculate the hydrogen ion concentration. The relationship between the measured pH and the hydrogen ion concentration involves assumptions associated with liquid junction potentials and single ion activity coefficients.

The cell used in this work was

glass electrode	test solution	KCl (satd), Hg_2Cl_2 (s); Hg (l)	I

with an emf given by

$$E = E^\circ + E_{as} + E_j - \frac{RT}{F}.\log_e a_{H^+} \qquad 2.1$$

where E_{as} is the asymmetry potential of the glass electrode, E_j is the liquid junction potential, E° is the standard emf for the cell and a_{H^+} is the hydrogen ion activity in the test solution.

Measurements using a cell of type I are often made by comparing the pH of an unknown solution X to the pH of a standard solution S. This sets up the operational definition of pH (60). From equation 2.1 when the test solution is the unknown, the cell emf is given by equation 2.2.

$$E'_X = E^\circ + E_{as} + E'_j + \frac{2.303RT}{F}.pH' \qquad 2.2$$

and for the standard solution

$$E_S = E^\circ + E_{as} + E_j(S) + \frac{2.303RT}{F}.pH(S) \qquad 2.3$$

From equations 2.2 and 2.3

$$pH' = pH(S) - \frac{(E'_j - E_j(S)) + (E_S - E'_X)}{2.303RT/F} \qquad 2.4$$

The assignment of pH(S) values to a set of standard buffers is made on the basis of measurements with hydrogen-silver chloride cells without liquid junction. The methods by which the NBS values of pH(S) were assigned to the reference solutions to define the conventional activity scale are well documented (61).

In equation 2.4, the measured pH of an unknown, pH', will only approach the conventional activity scale if the term $(E'_j - E_j(S))$, the residual liquid junction potential, is small. This will only be so if the standard and the test solution are similar in ionic strength, solution composition, and pH. This is seldom so. For example, many equilibrium constants are often determined with a background electrolyte of ionic strength 1.0 or 0.1 M (53), while the ionic strength of one of the most often used NBS buffers, the phthalate buffer, is only 0.053 M.

An expression for the single ion activity coefficient for hydrogen ions is required to relate the measured pH of the test solution from the operational scale to a hydrogen ion concentration, i.e.

$$pH' = p[H^+] - \log_{10}\gamma_{H^+} \qquad 2.5$$

The $\log_{10}\gamma_{H^+}$ term is often empirically evaluated using an extended form of the Debye-Huckel equation (63).

These assumptions concerning residual liquid junction potentials and single ion activity coefficients can be avoided by calibration of the cell against solutions of

known $[H^+]$ with the same ionic strength and ionic background as the test solutions. The cell I used in this work has previously been extensively calibrated by titrating hydrochloric acid solutions, ethylenediamine/ethylenediammonium and acetic acid/sodium acetate buffers in a NaCl medium at an ionic strength of 0.1 M (56). The method used to carry out this previous calibration has been previously documented (66).

The Response of the NBS Buffers

Three NBS standard buffers were used throughout this work. These buffers and their pH(S) values at 25°C for this system are potassium hydrogen phthalate (4.008), 1:3.5 phosphate (7.413), and borax (9.182) (65). These were used to check the meter and electrode system for linearity and slope based on the conventional activity scale. The procedure was to first standardize the system with the phthalate buffer and then measure the response with the other two standards. Both standards generally gave pH' values within ± 0.002 pH units of the pH(S) values.

The HCl/NaOH Calibration

Using dilute hydrochloric acid solutions in a potassium chloride medium the cell I was calibrated in the pH range 2 to 3. Data from the titration of sodium hydroxide against a hydrochloric acid/potassium chloride solution at ionic strength 0.1 M are given in Table 2.2. Values of $p[H^+]$ were calculated from the analytical concentrations of the acid and alkali assuming complete dissociation.

Data were collected in the pH range 2 to 4. However, a plot of pH' against $p[H^+]$ was linear in the pH' range 2 to 3, and became curved at higher pH' values. This tendency toward larger $pH'/p[H^+]$ as the pH' approaches 3.5 has been observed previously (64). A linear least squares regression on the data from the linear portion of the $p[H^+]$ versus pH' curve gave the following result.

$$p[H^+] = 1.0005\ pH' - 0.062 \qquad 2.6$$

If the same NBS buffer is used to standardize the system

Table 2.2 pH' and $p[H^+]$ Values From HCl/NaOH Titration in KCl Media at I = 0.10 M

pH' [1]	$p[H^+]$	Δ [2]
2.071	2.007	0.064
2.079	2.016	0.063
2.088	2.025	0.063
2.097	2.034	0.063
2.116	2.054	0.062
2.136	2.074	0.062
2.158	2.096	0.062
2.180	2.118	0.062
2.203	2.142	0.061
2.229	2.167	0.062
2.255	2.193	0.062
2.283	2.221	0.062
2.313	2.251	0.062
2.345	2.284	0.061
2.380	2.319	0.061
2.417	2.356	0.061
2.459	2.398	0.061
2.505	2.444	0.061
2.555	2.495	0.060
2.614	2.553	0.061
2.678	2.620	0.058
2.757	2.699	0.058
2.976	2.921	0.055

1. pH' = pH(measured).
2. Δ = pH' - $p[H^+]$.

for both the calibration titrations and for the test solution measurement then the residual liquid junction potentials for the two solutions will be almost identical. Additionally, if the test solution and the calibration solution have the same ionic strength (in this case 0.1 M), then γ_{H^+}(standard) = γ_{H^+}(test), and hence, standard and test solutions with the same pH' have the same value of $p[H^+]$

Conclusions

The HCl/NaOH calibration as expressed in equation 2.6 is in excellent agreement with the previous calibration in NaCl medium (56). For this previous calibration, the calibration equation, valid over the pH range 2 to 10.5, was $p[H^+] = 1.000\ pH' - 0.062$. It was assumed therefore that the calibration function given by equation 2.6 was valid throughout the pH range of interest.

Any change in the slope or linearity of the calibration curve since the previous calibration (56) could be discounted, on the basis of the excellent agreement for the NBS standard buffers over the period since that calibration.

2.5 SPECTROPHOTOMETRIC MEASUREMENTS

2.5.1 The Spectrophotometer and Sample Cells

All visible and near-infrared spectra were recorded using a Shimadzu MPS-5000 Multipurpose Spectrophotometer. Spectra were recorded over the visible wavelength range (340 to 740 nm) with a photomultiplier detector, and over the near-infrared wavelength range (650 to 1300 nm) using a PbS photoconductive cell.

A matched pair of "Spectrosil" Precision Cells with path length 10 mm were used during the calibration of the spectrophotometer. For the nickel-citric acid solution spectra, a pair of cells, nominally 10 cm pathlength, were constructed.

These cells were made from a length of glass tubing, 1.8 cm internal diameter, with quartz windows glued to each end. The cell had a smaller piece of glass tubing attached close to one end to facilitate filling. The cells and the perspex holders made to mount them in the sample and reference compartments are illustrated in Figure 2.2.

2.5.2 Procedure For Spectrophotometric Measurements

Sample cells were washed with distilled water, and then rinsed with acetone, before drying with compressed air.

When recording spectra, a base line was always recorded, as the base line of the instrument was not linear over the desired wavelength range (300 to 1400 nm). This base line was recorded by recording the spectra of a sample blank (distilled water), with distilled water as the reference standard. When several spectra were recorded as a group the base line was checked frequently.

All solution spectra were recorded using distilled water as the reference standard, and between recording the spectra of each solution the sample cell was treated in the manner noted above.

Complex solutions were prepared by titrating aliquots of a stock solution with sodium hydroxide. In this manner, it was possible to prepare several samples of the same nickel

Figure 2.2 Sample Cells and Mounting Plate

1. Sample Cell

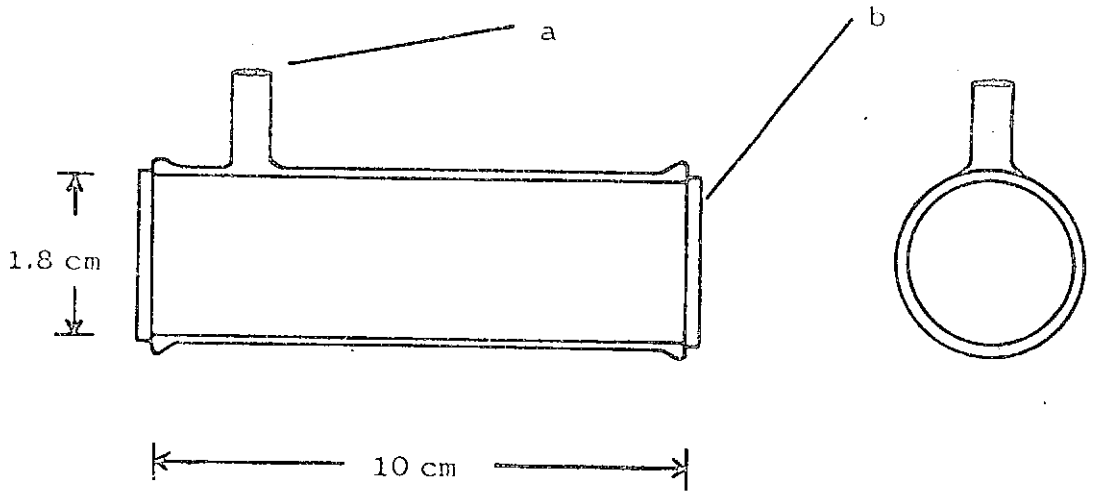

side view end view

a. Filling hole

b. Quartz window

2. Mounting Plate

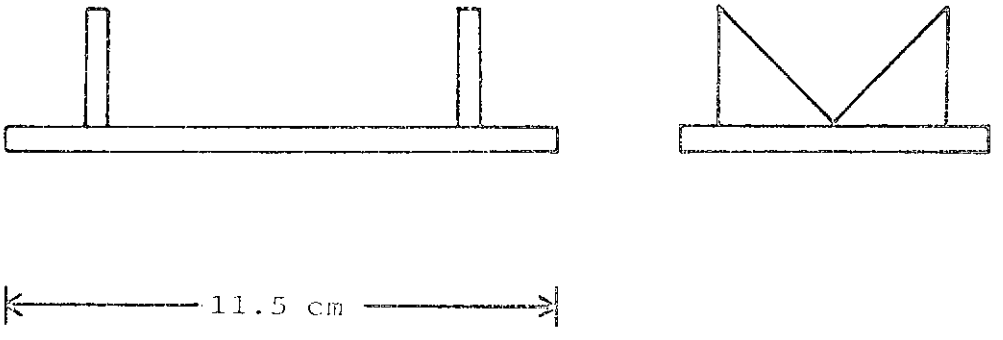

side view end view

and citric acid ratios to any desired pH. Generally, a 500 cm^3 stock solution was prepared, allowing ten samples, each of approximately 50 cm^3, to be prepared over a range of pH's.

The spectrophotometer had two wavelength ranges which were used, 340 to 740 nm and 650 to 2500 nm. The cells had a capacity of approximately 20 cm^3, hence a 50 cm^3 sample allowed separate spectra to be recorded for both wavelength ranges. This enabled a check to be made on the experimental precision, in that the absorbance over the range 650 to 740 nm from both wavelength ranges could be compared. Generally, the agreement between the two scales was within 1-2%.

2.5.3 Calibration of the Spectrophotometer and 10 cm Cells

The wavelength and absorbance accuracy of the spectrophotometer was checked by recording spectra of potassium chromate and comparing the results with the literature values. The path length of the long cells (nominally 10 cm) was determined by dilution of potassium chromate standards and comparing the absorbance of solutions in 10 mm and the long cells.

The Spectrophotometer

Calibration of the spectrophotometer with alkaline solutions of potassium chromate was decided upon after consideration of the available literature (67 - 72). R N Rand (67) in his review discusses the relative advantages of many methods, including the use of mercury lamps for wavelength calibration, and standard solutions and solid glass plates for checking both wavelength and absorbance accuracy. Owing to the difficulty of using mercury lamps in dual beam instruments (67), and the unavailability of holmium oxide and didymium glass, the only alternative was the preparation of an appropriate standard solution. Of the generally accepted solution standards, alkaline potassium chromate was used. Acidic potassium dichromate was not used because of the need for accurate control of the pH (68).

The potassium chromate solutions were prepared by weighing out potassium dichromate and dissolving this in potassium hydroxide in the proportions recommended by Haupt (70). Haupt reported that no difference could be determined between a solution prepared as above and one prepared directly by using potassium chromate. The use of the dichromate has the advantage that potassium dichromate is generally available in a more pure state than potassium chromate. Haupt lists the absorbance and transmittance of a solution containing 0.0400 g of potassium chromate in 1 litre of 0.05M KOH as a function of wavelength, and this meant that the spectrophotometer could be checked at any wavelength in the range 210 to 500 nm.

Potassium chromate displays two absorption maxima at 273 and 373 nm and two minima at 229 nm and 312 nm, providing four well-spaced points for control. Comparison of the experimental spectra and the table given by Haupt (70) showed that the wavelength accuracy was satisfactory, being within 1 or 2 nm of the literature value. The absorbance agreement in the ultraviolet region was excellent, but in the visible region, the experimental absorbance was 2% less than the literature value.

Characteristics of the Long Cells

For the long sample cells, a path length of exactly 10 cm could not be guaranteed because the quartz windows were glued to the glass tube. For all spectra, the same cell was used as the sample cell, hence any discrepancies in pathlength and optical properties between the cells would be constant.

The pathlength of the sample cell was determined by comparing the absorbance of a diluted sample of alkaline potassium chromate using the long cells with the absorbance of the stock solution using 1 cm cells. In this manner the path length of the long sample cell was determined to be 9.858 cm $\pm$ 0.3%.

The spectral characteristics of the long cells in the visible region displayed no peculiarities. However, in the

near-infrared region, the spectra showed a sudden decrease in transmittance at approximately 1350 nm. This is shown in Figure 2.3. This can only be a function of the type of quartz used for the windows, but since the nickel-citric acid absorption spectra have peaks in the range 390 to 1150nm, the sudden absorbance at about 1350 nm was not investigated further.

Figure 2.3 Transmittance Spectrum of Long Cells

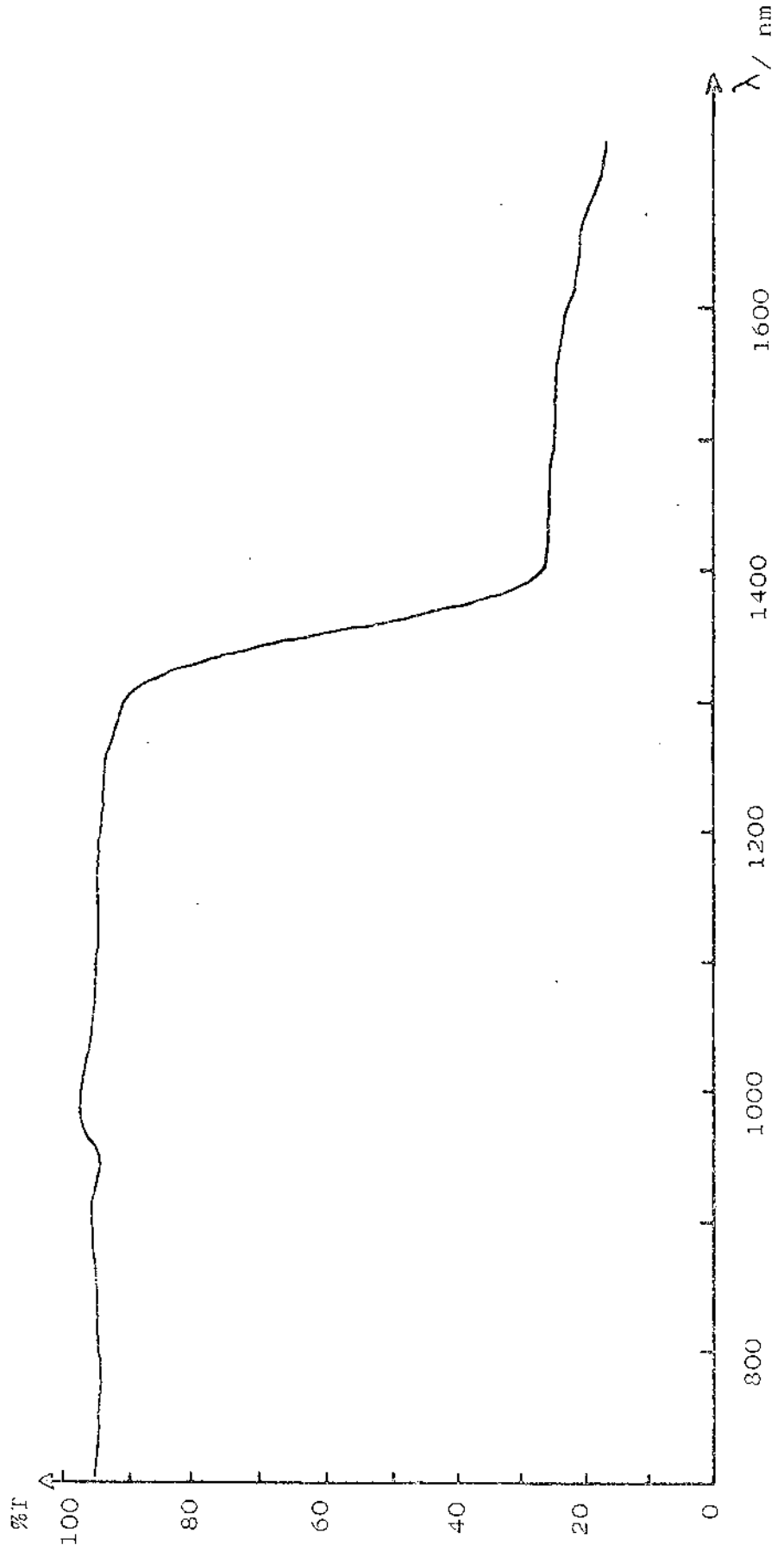

2.6 DETERMINATION OF ENDPOINTS

The endpoint of a potentiometric acid-base titration is characterized by an increase in the slope of a plot of pH or emf against titre as the titration approaches the endpoint. The endpoint is that volume for which the slope is greatest, and thereafter the slope will decrease. Equations 2.7 and 2.8 define the endpoint for a titration of an acid by a base, the titre at any point being v_B.

$$\frac{dpH}{dv_B} = \text{maximum} \qquad 2.7$$

$$\frac{d^2pH}{dv_B^2} = 0 \qquad 2.8$$

The relationships defined above are illustrated in Figure 2.4.

Since equations 2.7 and 2.8 are only exact for infinitely small increments in the volume of base, the accuracy of any derivative method for determining the endpoint will depend on the magnitude of the change in the volume and consequently the magnitude of the change in pH in the region of the endpoint.

Three methods of determining the endpoint of potentiometric titrations were investigated during this work, in order to find a quick, reliable method to verify that titration data were stoichiometrically correct. One was a simple graphical approach to the derivative method, another was a tabular derivative method, and the third a graphical approach first developed by Gran (75, 76).

The application of each of these methods is described below, and then each is applied to several titrations in order to determine which can best satisfy the criteria of simplicity and reliability.

1. Graphical Analysis of Derivatives

This method is perhaps the simplest of the three. As the titration progresses, pH is plotted against the volume of base and a smooth curve fitted through the points, which

Figure 2.4 The Relationships Between Titrimetric Data and Their Derivatives

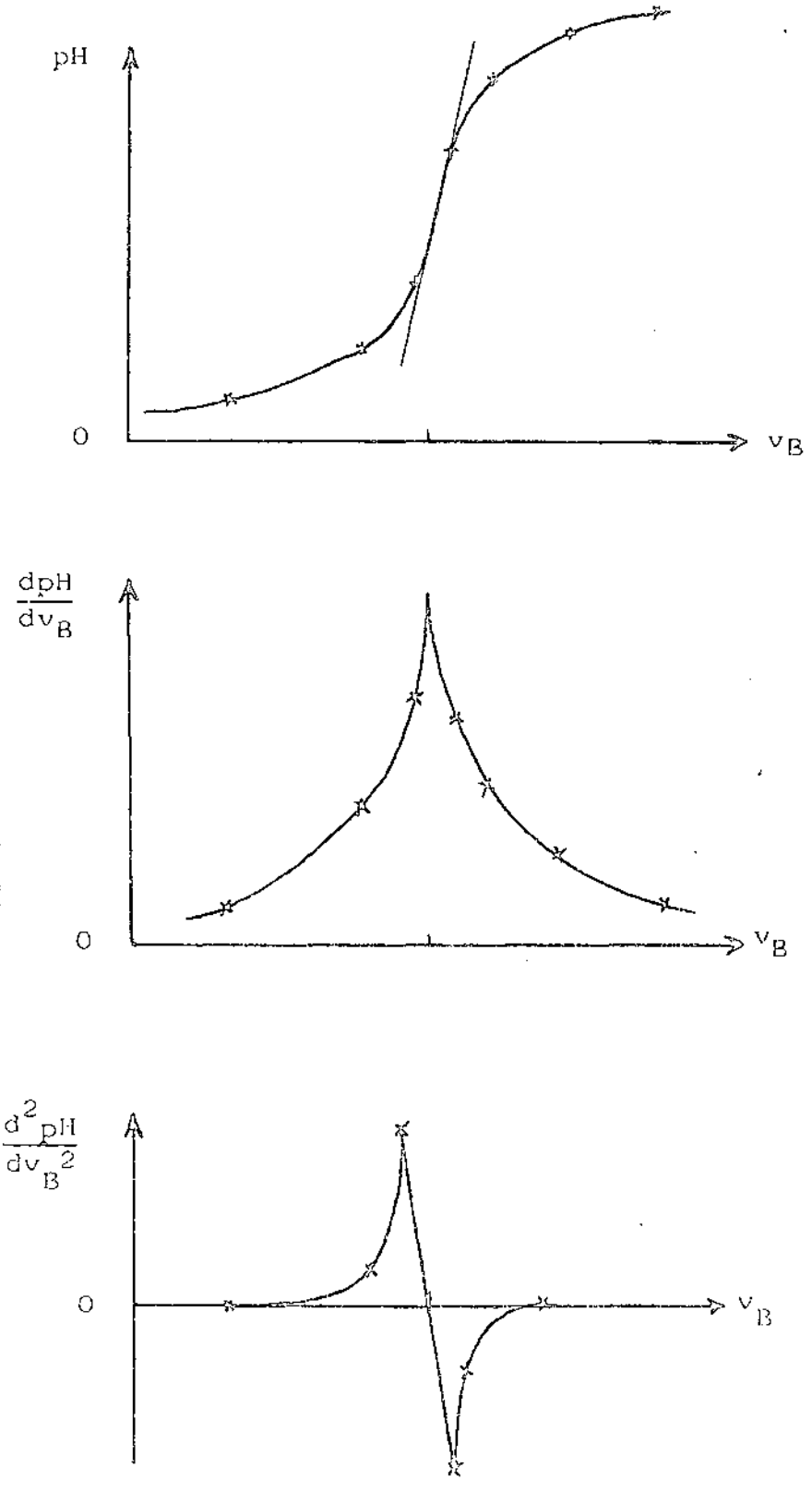

need only be those in the vicinity of the endpoint. By inspection, a straight line is drawn through the titration curve to intersect the curve at the point of greatest slope. The endpoint will then be the midpoint of that region of the straight line which is coincident with the titration curve.

This method is illustrated by Figure 2.5 for the data given in Table 2.3. The region of coincidence is given by the distance AB, and its midpoint, C, corresponds to an endpoint volume of 0.2578 cm^3.

Inaccuracies in the use of this method can arise from the drawing of the curve of best fit through the experimental observations, and this, along with locating the point of maximum slope, may be a matter of personal judgement. As an illustration, the titration curve for a single titration was plotted four times, with the variation in the endpoints being less than the readability of the micrometer.

2. Tabulation of Derivatives

Detailed theoretical discussion of the determination of titrimetric endpoints is given in Dick's "Analytical Chemistry" (73). The tabular derivative method uses the approximate expressions for derivatives as given below.

$$\frac{dpH}{dv_B} \doteq \frac{\Delta pH}{\Delta v_B} \qquad 2.9$$

$$\frac{d^2pH}{dv_B^2} \doteq \frac{\Delta^2 pH}{\Delta v_B^2} \qquad 2.10$$

where ΔpH is the change in pH as a result of an increment in the volume, Δv_B.

Equations 2.9 and 2.10 are exact only for infinitely small increments in base. However, a point will be reached where taking smaller increments in base results in a change in the endpoint titre less than the experimental precision of the titre. In general, the larger the rate of change of the pH about the endpoint, the smaller the volume increment required to bring about the desired precision in the

Table 2.3 Experimental Data For a Titration of Potassium Hydrogen Phthalate versus Sodium Hydroxide

Concentration of pot. hyd. phthalate = 0.0103 ± 0.0005 M
Volume of pot.hyd. phthalate = 24.98 ± 0.02 cm^3

Vol of Base[1]	pH
0.240	6.564
0.242	6.620
0.244	6.684
0.246	6.754
0.248	6.848
0.250	6.950
0.251	7.008
0.252	7.086
0.253	7.167
0.254	7.268
0.255	7.405
0.256	7.580
0.257	6.852
0.258	8.370
0.259	8.750
0.260	9.032
0.261	9.270
0.262	9.414

1. Volume of base readable to 0.0002 cm^3

Figure 2.5 Graphical Determination of the Endpoint of a Potentiometric Acid-Base Titration

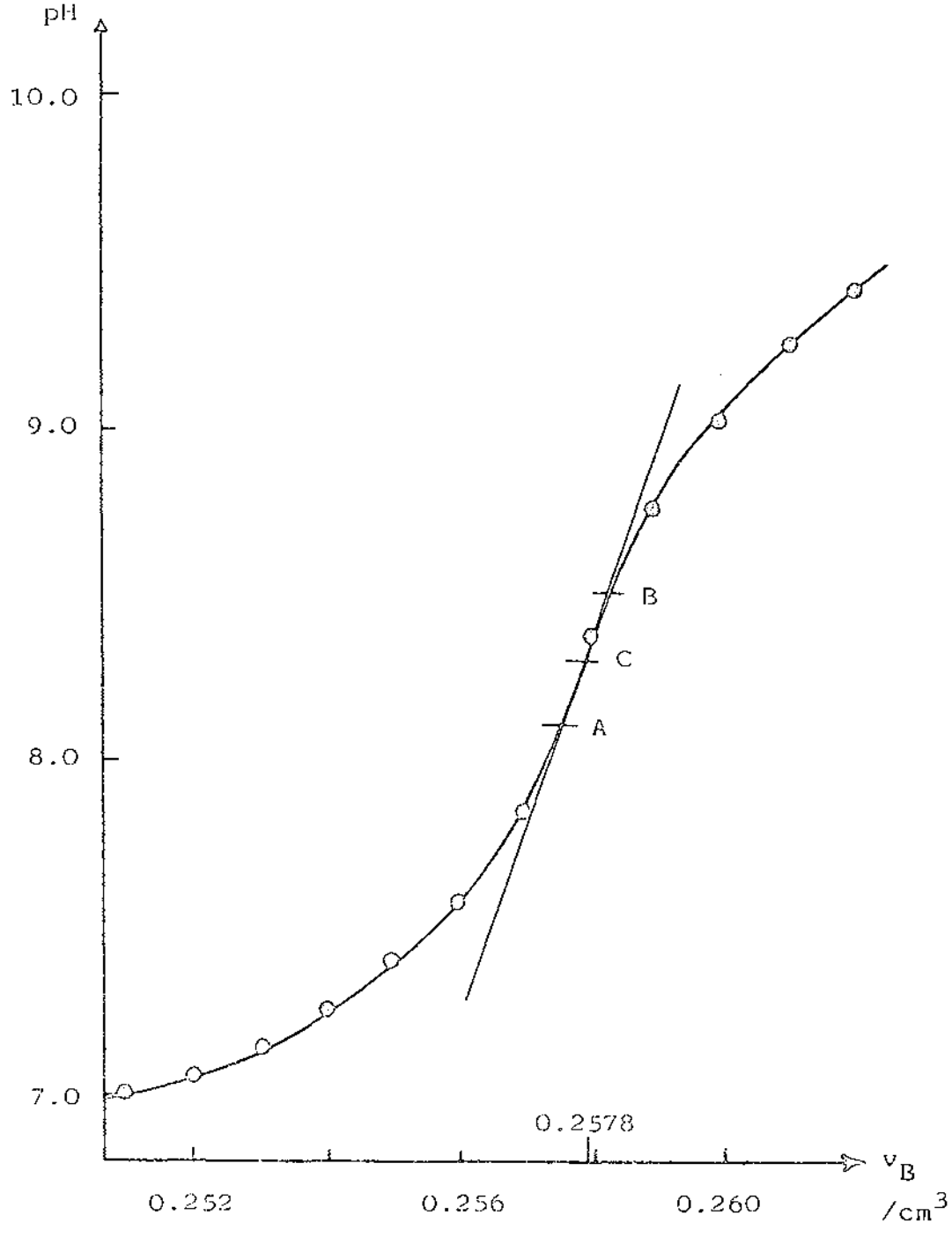

determination of the endpoint (74). The selection of Δv_B is a matter of personal judgement.

A tabulation method for the determination of endpoints is preferred over the graphical method previously described due to the possible errors of curve fitting.

The tabulation required to determine the endpoint of the data given in Table 2.3 is given in Table 2.4.

Table 2.4 Tabulation Required to Determine the Endpoint of a Titration by Tabulation of Derivatives

Volume of Base v_B	pH	$\frac{\Delta pH}{\Delta v_B}$ $\Delta v_B = 0.001$ cm^3	$\left(\frac{\Delta^2 pH}{\Delta v_B^2}\right) \times 10^{-3}$
0.2540	7.268		
		137	
0.2550	7.405		38
		175	
0.2560	7.580		97
		272	
0.2570	7.852		246
		518	
0.2580	8.370		-138
		380	
0.2590	8.750		-98
		282	
0.2600	9.032		-44
		238	
0.2610	9.270		

On the basis of the criteria given by equations 2.7 and 2.8 (i.e. the slope is a maximum and the second derivative changes sign) the endpoint is clearly between 0.257 and 0.258 cm^3. The endpoint volume can be determined from the tabulated values of $\Delta^2 pH/\Delta v_B^2$ in the manner on the following page.

Hence, using this derivative-tabulation technique with a volume increment of 0.001 cm^3, the endpoint is located at 0.2576 cm^3

The same process carried out for increments of

0.002 and 0.004 cm^3 resulted in endpoints of 0.2576 and 0.2577 cm^3 respectively. This shows that an increment as large as 0.004 cm^3 would have been acceptable.

Determination of Endpoint from Second Derivatives

Refer to Table 2.4.

magnitude of last positive value = 246 corresponds to $v_B = 0.2570$ cm^3

magnitude of first negative value = 138 corresponds to $v_B = 0.2580$ cm^3

$$\text{then endpoint volume} = 0.2570 + \frac{246}{246 + 138} \times (0.2580 - 0.2570)$$

$$= 0.2570 + 0.0006$$

$$= 0.2576 \text{ cm}^3$$

3. The Gran Plot

A method of determination of the endpoint of a potentiometric acid-base titration that has not received wide recognition is that developed by Gran (75, 76) and reviewed by Rossotti (77). An extension of the method is applicable to potentiometric precipitation titrations, some complex formation titrations, and oxidation-reduction titrations.

The theoretical treatment for a titration involving a weak acid with a strong base, as applicable to titrations of potassium hydrogen phthalate, and citric acid with sodium hydroxide, is outlined below. The method is not applicable to the titration of the nickel and citrate complex solutions due to the complexity of the equilibria involved.

A volume V of acid of initial concentration H, is titrated with a volume v of strong base of concentration B. If the acid, HA, is not fully dissociated in solution then the concentration of the hydrogen ion is given by equation 2.12.

$$[H^+] = k_a[HA][A^-] \qquad 2.12$$

where k_a is the stoichiometric acid dissociation constant

of HA, and A^- is the conjugate base, If the titrant is monobasic, BOH, then

$$[A^-] = [B^+] + [H^+] - [OH^-]$$

$$[A^-] = \frac{v.B}{V + v} + [H^+] - [OH^-] \qquad 2.13$$

and $[HA] = C_A - [A^-]$

where C_A is the total concentration of HA in the solution. Hence.

$$[HA] = \frac{VH - vB}{V + v} - [H^+] + [OH^-] \qquad 2.14$$

For a weak acid

$$\frac{vB}{V + v} >> [H^+] - [OH^-] \qquad 2.15$$

and

$$\frac{VH - vB}{V + v} >> [H^+] - [OH^-] \qquad 2.16$$

Therefore, it follows that

$$[H^+] = \frac{k_a(VH - vB)}{vB}$$

Now if v_e is the volume at the endpoint then $VH = v_eB$, and hence for volumes less than the endpoint

$$[H^+] = \frac{k_a(v_e - v)}{v} \qquad 2.17$$

By multiplying both sides of equation 2.17 by the activity coefficient for the hydrogen ion, γ_{H^+}, and defining a function, $\tau(v)$, such that

$$\tau(v) \equiv [H^+].\gamma_{H^+} = \frac{k_a(v_e - v).\gamma_{H^+}}{v} \qquad 2.18$$

then

$$\tau(v) \equiv v.10^{-pH} = k_a(v_e - v).\gamma_{H^+} \qquad 2.19$$

If the initial concentration of HA is low, the ionic strength will not vary greatly through the titration, and the terms k_a and γ_{H^+} will remain approximately constant. This results in a linear relationship between τ and v, such that $\tau(v)$ intersects the abscissa at the point $v = v_e$.

Deviations from linearity may occur if any of the following factors is present:

1. at the very beginning of the titration, condition 2.15 may not be fulfilled if the acid is only moderately weak. In this case, only the linear portion of $\tau(v)$ should be used.
2. as v approaches v_e, condition 2.16 may not be satisfied if the acid is very weak, in which case only the linear portion of $\tau(v)$ is used.
3. other complications which may cause deviations from linearity are the presence of metal ions in the acid, or carbonate in the base.

Polymeric Acids

In the case of citric acid, where it was desirable to know the endpoint for the third acidic proton, a slightly different formula is used. Immediately after this endpoint

$$[H^+] = \frac{K_W}{[OH^-]}$$

$$[H^+] = \frac{K_W(V + v)}{B(v - v_e)} \qquad 2.20$$

where K_W is the stoichiometric ionic product of water. Then a function $\theta(v)$ is defined by rearrangement of equation 2.20.

$$\theta(v) \equiv \frac{(V + v)}{[H^+].\gamma_{H^+}} = \frac{(v - v_e).B}{K_W.\gamma_{H^+}} \qquad 2.21$$

Now

$$\theta(v) = (V + v).10^{pH} \qquad 2.22$$

If γ_{H^+} and K_W remain constant throughout the titration, $\theta(v)$ will be linear in v and will intersect the abscissa at $v = v_e$

Deviation from linearity may again be caused by

metal ion and carbonate contaminants.

Application of the Gran Plot

Table 2.5 lists the τ values necessary for the determination of the endpoint of the titrimetric data in Table 2.3.

Table 2.5 Calculations Required for Gran Plot

Vol of base v_B/cm^3	Total Volume $V + v\ /cm^3$	pH	$\tau\ /10^{-7}$
0.252	25.232	7.086	20.70
0.253	25.233	7.167	17.18
0.254	25.234	7.268	13.61
0.255	25.235	7.405	9.93
0.256	25.236	7.580	6.63
0.257	25.237	7.852	3.55

The endpoint is located at 0.2580 cm^3, determined from Figure 2.6.

The advantages of Gran plots are primarily their simplicity of calculation, and the precision which is inherent in linear plots, especially if the titration curve is not symmetrical.

Summary

The endpoint of the data given in Table 2.3 has been determined in three ways, and the results are

Graphical derivative	0.2578 cm^3
Tabulation derivative	0.2576 cm^3
Gran Plot	0.2580 cm^3

The three methods give results that agree well, the spread of values being only 0.15% of the mean.

Several other sets of data were analysed by all three methods and the results are presented in Table 2.6. The results indicate that there was no significant difference between the methods for the system being studied, so only

Figure 2.6 The Gran Plot

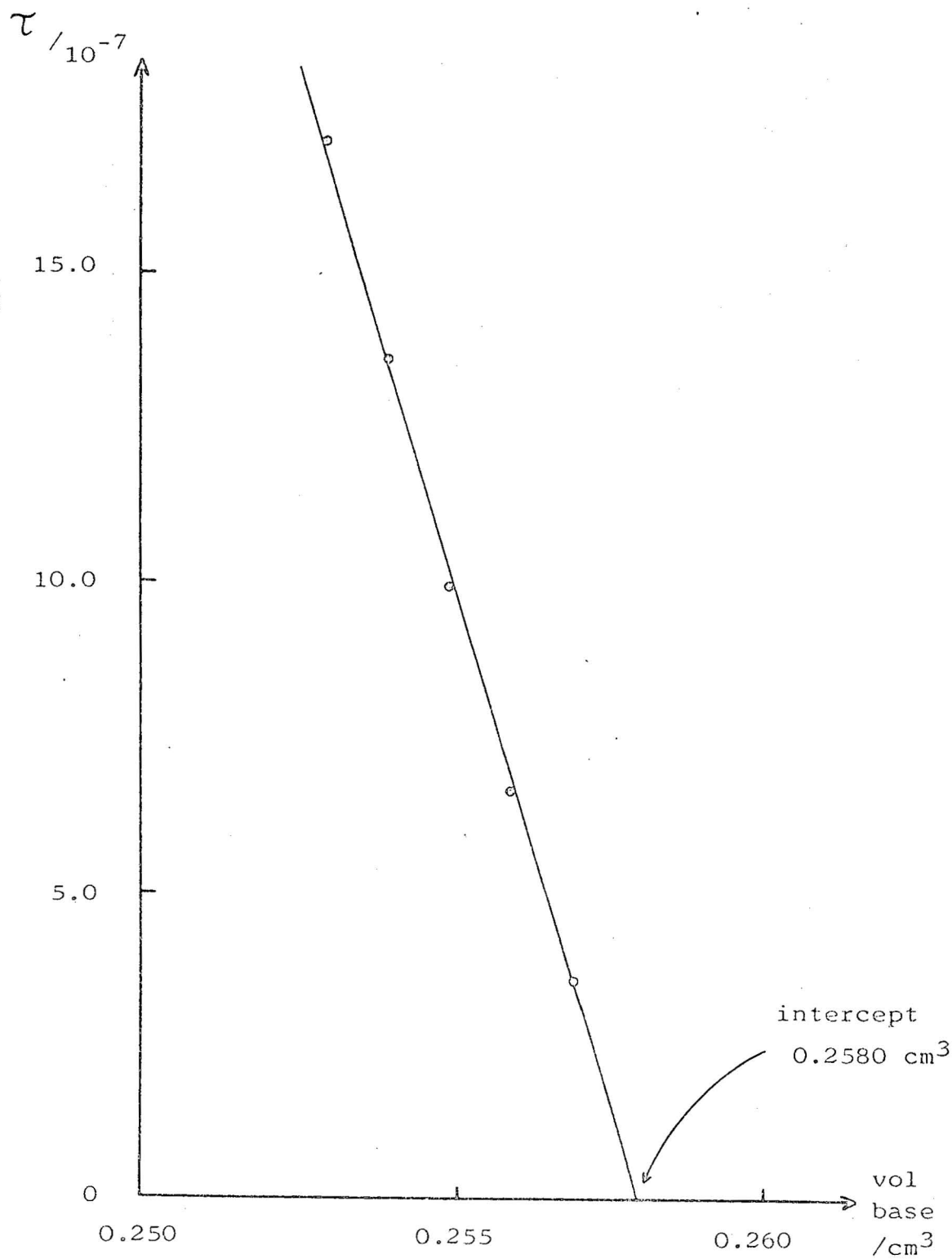

Table 2.6 Summary of Comparison Between Various Methods of Determining Titrimetric Endpoints [1]

Reagents	Titration Number	Graphical Derivative	Tabular Derivative	Gran plot
Sod. hydroxide	1	0.2562	0.2563	0.2562
Pot. hyd. phthal.	2	0.2579	0.2576	0.2580
	3	0.2562	0.2564	0.2564
	4	0.2572	0.2572	0.2572
Sod. hydroxide	1	0.4020	0.4018	0.4020
Citric Acid	2	0.4015	0.4015	0.4016
	3	0.4012	0.4011	0.4013
	4	0.4009	0.4007	0.4018
Sod. hydroxide	1	0.1433	0.1434	
Nickel-citrate	2	0.1431	0.1432	
solution	3	0.1432	0.1434	

1. All volumes cm^3

the graphical derivative method was used to check the stoichiometry of all titrations. The Gran plot cannot be applied to metal complex equilibria such as those under investigation, but the results in Table 2.6 show that there is no significant difference between the graphical derivative and the Gran plot methods for determining the endpoint of acid-base titrations, and that there is no significant difference between the graphical and tabular derivative methods for determining the endpoint of the complex solutions.

2.7 MICROANALYSES

Carbon and hydrogen analyses were determined in the Microanalytical Laboratory, University of Otago.

3

Titrimetric Results

3.1 THE PROTONATION CONSTANTS OF CITRIC ACID

The protonation constants of citric acid are well documented (34, 35, 36, 53, 79 - 82), and have been determined over a wide range of experimental conditions (temperature, background electrolyte and ionic strength). Table 3.1 lists some of these constants determined under conditions which enable a useful comparison with the values obtained in this work.

If citric acid is regarded as a triprotic acid, H_3L, then the equilibria under consideration are

$$H + L \rightleftharpoons HL \qquad k_1$$

$$H + HL \rightleftharpoons H_2L \qquad k_2$$

$$H + H_2L \rightleftharpoons H_3L \qquad k_3$$

where

$$k_1 = \frac{[HL]}{[H][L]}$$

$$k_2 = \frac{[H_2L]}{[H][HL]}$$

$$k_3 = \frac{[H_3L]}{[H][H_2L]}$$

The charges have been omitted for clarity.

Table 3.1 The Reported Protonation Constants of Citric Acid at 25°C

Background Electrolyte 0.1 M	Logarithm of Protonation Constant k_1	k_2	k_3	Reference
KCl	5.72	4.37	2.94	this work
KCl	5.69	4.36	2.89	80
KCl	5.83	4.34	2.89	79
$NaClO_4$	5.68	4.35	2.87	35
KNO_3	5.72	4.39	2.92	82
KNO_3	5.70	4.36	2.81	34
NaCl	5.95	4.34	2.94	36
KCl (20°C)	5.67	4.39	2.96	81

1. k_1 : $H + L \rightleftharpoons HL$

   k_2 : $H + HL \rightleftharpoons H_2L$

   k_3 : $H + H_2L \rightleftharpoons H_3L$

In the pH range of interest (3.0 to 9.0), citric acid was considered triprotic because the fourth proton is part of a hydroxy group, and the pK for the displacement of the proton is about 12.0 (33). The distribution plot of Figure 3.1 confirms that, with a pK of 12.0, this equilibrium plays no part in the citric acid equilibria below about pH 10.

3.1.1 Determination of the Protonation Constants of Citric Acid

The mass balance equations for T_L, the total concentration of citric acid, and T_H, the total concentration of dissociable hydrogen ions, are given by

$$T_L = [L] + [HL] + [H_2L] + [H_3L] \qquad 3.1$$

and

$$T_H = [H] + [HL] + 2[H_2L] + 3[H_3L] - [OH]_{hyd} \qquad 3.2$$

where [H] and [L] are the concentrations of hydrogen ions and free citrate respectively. The term $[OH]_{hyd}$ is the concentration of hydroxide ions, which arise from hydrolysis reactions of the type

$$H_nL + H_2O \rightleftharpoons H_{n+1}L + OH^-$$

A secondary concentration variable, $\bar{n}_H$, is defined as the degree of protonation of the system, i.e. the average number of protons attached per citrate.

$$\bar{n}_H = \frac{T_H - [H] + [OH]}{T_L} \qquad 3.3$$

By using equations 3.1 , 3.2 and 3.3

$$\bar{n}_H = \frac{[HL] + 2[H_2L] + 3[H_3L]}{[L] + [HL] + [H_2L] + [H_3L]} \qquad 3.4$$

Figure 3.1 Distribution Curves of Citric Acid

Citric Acid conc. = 1×10^{-3} M [2]

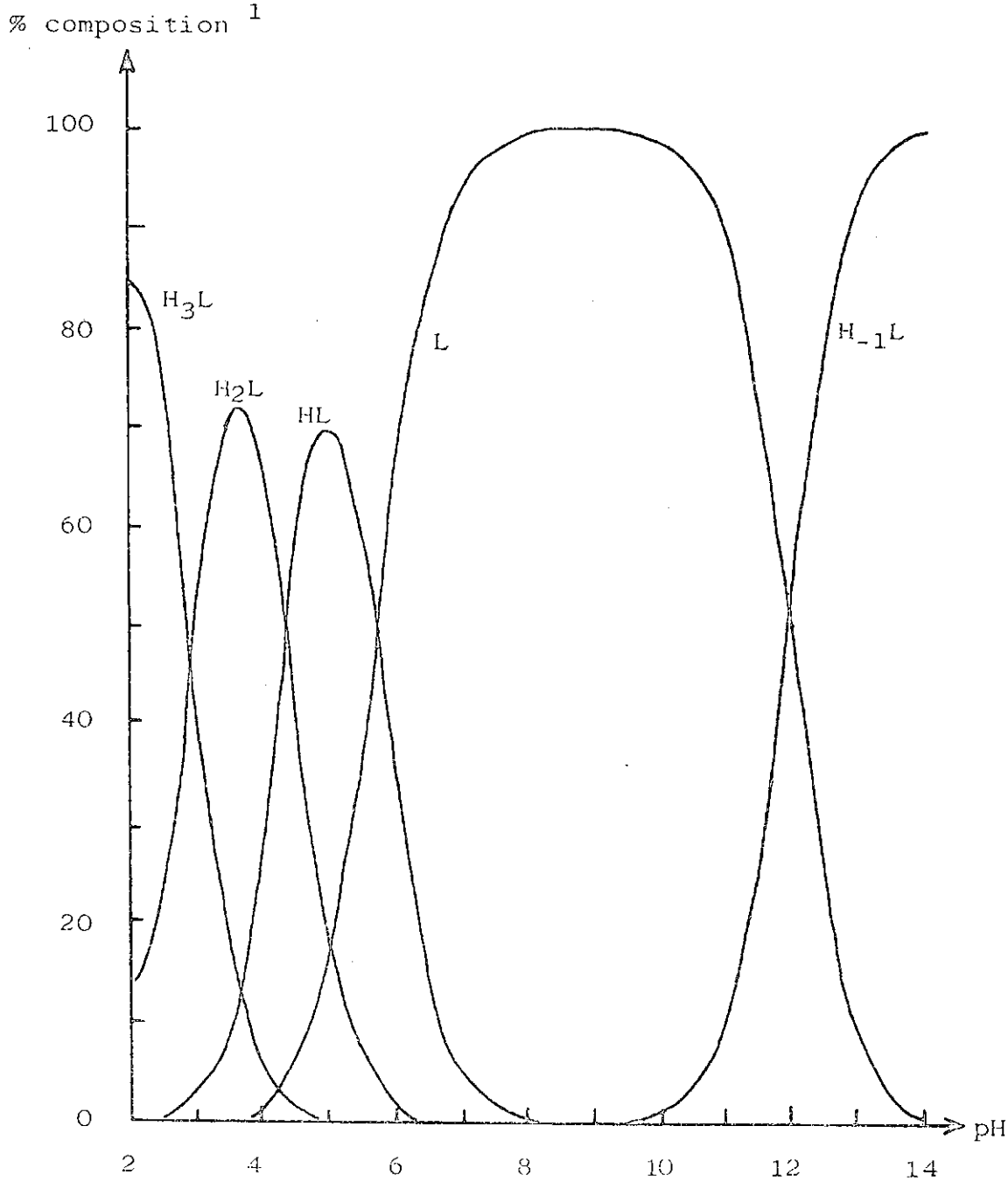

1. As a percentage of total citrate concentration
2. Citric Acid = H_3L

Equation 3.4 may be expanded, using the equilibrium expressions, into a function of hydrogen ion concentration:

$$\bar{n}_H = \frac{k_1[H] + 2k_1k_2[H]^2 + 3k_1k_2k_3[H]^3}{1 + k_1[H] + k_1k_2[H]^2 + k_1k_2k_3[H]^3} \qquad 3.5$$

In general, equation 3.5 may be expressed as

$$\bar{n}_H = \frac{\sum_1^N n\beta_n[H]^n}{\sum_0^N \beta_n[H]^n} \qquad 3.6$$

where $\beta_i = \prod_{j=1}^{i} k_j$ is the overall stability constant of the species.

Equation 3.5 was used to calculate the protonation constants of citric acid. The left hand side, (termed Yobs), is readily calculated from the analytical concentrations and the hydrogen ion concentration using equation 3.3. The right hand side, (termed Ycalc), is a function of the hydrogen ion concentration and the unknown parameters k_1, k_2 and k_3. The least squares method was used to vary the unknown parameters so as to minimize the function M, expressed in equation 3.7. The algebra involved in the least squares process is given in Appendix 1.

$$M = \sum_j^n w_i ((F_o)_i - (F_c)_i)^2 \qquad 3.7$$

where F_o and F_c are the observed and calculated functions respectively, and the weighting factor, $w_i = 1/\sigma_i^2$. σ_i is the standard deviation of the i-th observation, and the weighting of data for a least squares analysis is incorporated to allow for the variation of σ_i. In the calculation of the protonation constants of citric acid, the least squares process minimizes

$$M = \sum (\bar{n}_H(obs) - \bar{n}_H(calc))^2 \qquad 3.8$$

An estimation of $\sigma(\bar{n}_H(obs))$ can be calculated from the terms contributing to the expression for $\bar{n}_H$.

$$\bar{n}_H = \frac{T_H - [H] + K_W/[H]}{T_L} \qquad 3.9$$

where the component $K_W/[H] = [OH]_{hyd}$, and K_W is the ionic product of water in 0.1 M KCl. The uncertainties in T_H and T_L will be constant throughout a titration. The term [H] is small compared with T_H; therefore the uncertainty in [H] has a negligible effect on $\sigma(\bar{n}_H)$, and may be disregarded. In the pH range of interest (pH < 10), the term $K_W/[H]$ makes a negligible contribution to $\bar{n}_H$ and may be disregarded. Under these conditions, $\sigma(\bar{n}_H(obs))$ will be approximately constant and hence, the data may be weighted at unity.

A computer program, ORGLS, was available to perform the least squares process and was used with minor modification. This program is described in Appendix 2.

3.1.2 The Protonation Constants of Citric Acid

Three citric acid solutions were prepared with potassium chloride as the background electrolyte to bring the ionic strength up to 0.1 M. The concentration of citric acid in these solutions was approximately 1.5, 2.0 and 2.7×10^{-3} $moll^{-1}$. Representative titration data for these solutions is given in Table 3.2. The protonation constants calculated from the data for each of these solutions are given in the first part of Table 3.3. The mean and standard deviation of the logs of the protonation constants determined from the three titrations of the 2.0×10^{-3} M solution are

$$\log k_1 = 5.718 \quad (0.005)$$

$$\log k_2 = 4.369 \quad (0.003)$$

$$\log k_3 = 2.947 \quad (0.007)$$

The results from the three titrations show excellent internal consistency, in that the relative standard deviations are less than 0.2%.

The averages and standard deviations for all six titration sets are given in part B of Table 3.3. These values were used in all subsequent analyses of the nickel-citric acid titrations. By reference to Table 3.1, it can be seen that the values for the protonation constants are in excellent agreement with those determined under closely similar conditions. This confirms that there are no systematic errors in the experimental and computational procedures adopted during this work.

The effect of errors in the concentration of hydroxide on the protonation constants was established by calculation of the constants with the alkali concentration changed by the experimental uncertainty of the alkali concentration. The results, presented in Table 3.4, show that variations of the alkali concentration within the experimental uncertainty result in changes in the log of the protonation constants generally less than 0.1%. The largest change

Table 3.2 Titration Data for Citric Acid Solutions

A. Initial $[H_3L]$ 1.499×10^{-3} M
[NaOH] 0.9988 M
Aliquot Vol 49.88 cm^3

Vol Alkali / cm^3	$p[H^+]$	Vol Alkali / cm^3	$p[H^+]$
0.000	3.049	0.170	5.456
0.005	3.080	0.175	5.551
0.010	3.116	0.180	5.647
0.015	3.153	0.185	5.746
0.020	3.192	0.190	5.847
0.025	3.233	0.195	5.957
0.030	3.278	0.200	6.078
0.035	3.324	0.205	6.214
0.040	3.374	0.210	6.383
0.045	3.427	0.215	6.611
0.050	3.484	0.200	7.006
0.055	3.544	0.221	7.134
0.060	3.607	0.222	7.313
0.065	3.674	0.223	7.605
0.075	3.818	0.224	8.221
0.080	3.893	0.225	8.761
0.085	3.970	0.226	9.135
0.090	4.048	0.230	9.745
0.095	4.128	0.235	10.061
0.100	4.207	0.240	10.252
0.105	4.287	0.245	10.386
0.110	4.368	0.250	10.489
0.115	4.450	0.255	10.573
0.120	4.533	0.260	10.643
0.125	4.619	0.265	10.704
0.130	4.707	0.270	10.758
0.135	4.796	0.275	10.805
0.140	4.888	0.280	10.849
0.145	4.982	0.285	10.887
0.150	5.076	0.290	10.923
0.155	5.172	0.295	10.956
0.160	5.266	0.300	10.985
0.165	5.361	0.305	11.016

Table 3.2 Titration Data for Citric Acid Solutions

B. Intial H_3L 1.998×10^{-3} M
[NaOH] . 0.9943 M
Aliquot Vol 49.97 cm^3

Vol Alkali / cm^3	p[H^+]	Vol Alkali / cm^3	p[H^+]	Vol Alkali / cm^3	p[H^+]
0.000	2.964	0.125	4.075	0.250	5.754
0.005	2.990	0.130	4.135	0.255	5.831
0.010	3.018	0.135	4.196	0.260	5.911
0.015	3.047	0.140	4.256	0.265	5.996
0.020	3.076	0.145	4.319	0.270	6.089
0.025	3.107	0.150	4.379	0.275	6.190
0.030	3.139	0.155	4.441	0.280	6.312
0.035	3.173	0.160	4.504	0.285	6.453
0.040	3.208	0.165	4.567	0.290	6.644
0.046	3.254	0.170	4.632	0.295	6.942
0.050	3.283	0.175	4.697	0.300	7.848
0.055	3.323	0.180	4.765	0.305	9.658
0.060	3.365	0.185	4.832	0.310	10.030
0.065	3.410	0.190	4.900	0.315	10.233
0.070	3.455	0.195	4.971	0.320	10.374
0.075	3.503	0.200	5.042	0.325	10.480
0.080	3.553	0.205	5.112	0.330	10.568
0.085	3.606	0.210	5.184	0.335	10.639
0.090	3.659	0.215	5.255	0.340	10.702
0.095	3.717	0.220	5.326	0.345	10.757
0.100	3.773	0.225	5.396	0.350	10.805
0.105	3.832	0.230	5.466	0.355	10.848
0.110	3.892	0.235	5.536	0.360	10.887
0.115	3.952	0.240	5.608	0.365	10.923
0.120	4.013	0.245	5.679	0.370	10.957

Table 3.2 Titration Data for Citric Acid Solutions

C. Intial H_3L 2.666×10^{-3} M
[NaOH] 1.0009 M
Aliquot Vol 49.92 cm^3

Vol Alkali / cm^3	p[H^+]	Vol Alkali / cm^3	p[H^+]	Vol Alkali / cm^3	p[H^+]
0.000	2.879	0.165	4.042	0.330	5.721
0.005	2.899	0.170	4.090	0.335	5.778
0.010	2.920	0.175	4.137	0.340	5.834
0.015	2.942	0.180	4.184	0.345	5.893
0.020	2.965	0.185	4.232	0.350	5.956
0.025	2.989	0.190	4.279	0.355	6.023
0.030	3.014	0.195	4.326	0.360	6.092
0.035	3.039	0.200	4.373	0.365	6.167
0.040	3.065	0.205	4.421	0.370	6.253
0.045	3.092	0.210	4.469	0.375	6.349
0.050	3.120	0.215	4.517	0.380	6.458
0.055	3.149	0.220	4.565	0.385	6.592
0.060	3.178	0.225	4.614	0.390	6.767
0.065	3.209	0.230	4.663	0.395	7.038
0.070	3.241	0.235	4.713	0.398	7.348
0.075	3.274	0.240	4.764	0.399	7.498
0.080	3.307	0.245	4.815	0.400	7.744
0.085	3.342	0.251	4.877	0.401	8.116
0.090	3.378	0.255	4.919	0.402	8.791
0.095	3.416	0.260	4.972	0.403	9.157
0.100	3.455	0.265	5.025	0.405	9.558
0.105	3.495	0.270	5.078	0.410	9.985
0.110	3.536	0.275	5.131	0.415	10.207
0.115	3.578	0.280	5.186	0.420	10.355
0.120	3.621	0.285	5.239	0.425	10.468
0.125	3.676	0.290	5.292	0.430	10.556
0.130	3.711	0.295	5.345	0.435	10.632
0.135	3.757	0.300	5.399	0.440	10.695
0.140	3.804	0.305	5.451	0.445	10.750
0.145	3.852	0.310	5.505	0.450	10.799
0.150	3.899	0.315	5.558	0.455	10.841
0.156	3.956	0.320	5.611	0.460	10.882
0.160	3.994	0.325	5.666	0.465	10.918

Table 3.3 Protonation Constants of Citric Acid as Calculated by the Program ORGLS

A. Protonation Constants From Each Data Set [1]

Concentration of Citric Acid (approx.) /M		Titration 1	2	3	Average
1.5×10^{-3}	k_1	5.738			
	k_2	4.378			
	k_3	2.941			
2.0×10^{-3}	k_1	5.719	5.723	5.712	5.718
	k_2	4.367	4.373	4.367	4.369
	k_3	2.939	2.953	2.950	2.947
2.7×10^{-3}	k_1	5.696	5.702		5.699
	k_2	4.355	4.358		4.357
	k_3	2.920	2.925		2.923

1. Protonation Constants Recorded as logs.

B. The Mean and Standard Deviation of all Six Data Sets

log k_1	5.71_5	$\pm$	0.02
log k_2	4.366	$\pm$	0.008
log k_3	2.93_8	$\pm$	0.01

Table 3.4 Calculation of the Protonation Constants of Citric Acid, With Alkali Concentration Varied by the Uncertainty in the Concentration

Citric Acid Concentration and the Change in Alkali Concentration		Logarithms of Protonation Constants		
		No Change in Alkali conc.	Inc. Alkali Conc by ΔOH	Dec. Alkali Conc by ΔOH
$[H_3C] = 2.0 \times 10^{-3}$	k_1	5.719	5.714	5.725
titration 2	k_2	4.367	4.364	4.369
ΔOH = 0.13%	k_3	2.939	2.939	2.939
$[H_3C] = 1.5 \times 10^{-3}$	k_1	5.738	5.728	5.746
titration 1	k_2	4.378	4.372	4.383
ΔOH = 0.25%	k_3	2.941	2.940	2.941

occurs in the value for k_1, ($H + L \rightleftharpoons HL$), but this may be expected, because this equilibrium is dominant in the region of the titration closest to the endpoint, where the effect of uncertainties in the concentration of sodium hydroxide is greatest.

3.1.3 The Distribution of Equilibrium Species

The concentration of each citric acid species as a function of pH can be determined if given the protonation constants and the total concentration of citric acid. These calculations were performed using the computer program COMICS (Appendix 2). This program is also able to draw the distribution curves of the equilibrium species, expressing for any given pH the concentration of each species as a percentage of the total concentration of citric acid. Such a distribution plot is given in Figure 3.1 for a citric acid solution where the total concentration of citric acid is 1×10^{-3} M. These curves have been calculated using the protonation constants of Table 3.3, Part B, and for the removal of the fourth proton, a pK of 12.0 has been used (33).

3.2 ALGEBRAIC ANALYSIS OF NICKEL-CITRATE EQUILIBRIA

Analysis of the nickel-citric acid titration data was carried out in a similar manner to the calculation of the protonation constants of citric acid. In this section, the formation constants of the nickel-citric acid species are referred to as parameters, and given the symbol P, in order to avoid any confusion with the citric acid protonation constants, k.

3.2.1 The Equilibria Considered

The following set of equilibria define the species which were considered likely to be present in the pH range 3.0 to 6.0.

1.	M	+ L	$\rightleftharpoons$	ML	P_1
2.	M	+ HL	$\rightleftharpoons$	MHL	P_2
3.	MHL	+ HL	$\rightleftharpoons$	$M(HL)_2$	P_3
4.	ML	+ L	$\rightleftharpoons$	ML_2	P_4
5.	M	+ H_2L	$\rightleftharpoons$	MH_2L	P_5
6.	MHL	+ L	$\rightleftharpoons$	MHL_2	P_6
7.	2M	+ 2L	$\rightleftharpoons$	$(ML)_2$	P_7
8.	H	+ L	$\rightleftharpoons$	HL	k_1
9.	H	+ HL	$\rightleftharpoons$	H_2L	k_2
10.	H	+ H_2L	$\rightleftharpoons$	H_3L	k_3

M represents nickel, L is tri-ionized citrate, and charges have been omitted for clarity.

3.2.2 Algebraic Manipulation of the Proposed Equilibria

For the equilibria proposed in the above section, the mass balance equations for T_M, the total concentration of metal, T_L, the total concentration of ligand, and T_H, the total concentration of hydrogen ions, are given by:

$$T_M = M + ML + MHL + M(HL)_2 + ML_2 + MH_2L + MHL_2 + 2(ML)_2 \quad 3.10$$

$$T_L = L + HL + H_2L + H_3L + ML + MHL + 2M(HL)_2 + 2ML_2 + MH_2L + 2MHL_2 + 2(ML)_2 \quad 3.11$$

$$T_H = H + HL + 2H_2L + 3H_3L + MHL + 2M(HL)_2 + 2MH_2L + MHL_2 - K_w/H \quad 3.12$$

The square brackets representing concentration have been omitted in these, and subsequent equations, for clarity.

If the concentration of co-ordinated acid, T'_H, is defined as the concentration of hydrogen ions which are co-ordinated to a ligand in any form,

i.e. $$T'_H = T_H - H + K_w/H \quad 3.13$$

then from equation 3.12

$$T'_H = HL + 2H_2L + 3H_3L + MHL + 2M(HL)_2 + 2MH_2L + MHL_2 \quad 3.14$$

The expressions for T_M, T_L, and T'_H may be simplified by expressing the concentration of each species in terms of the free metal concentration, M, the free ligand concentration, L, the hydrogen ion concentration, H, the formation constants of the complex species, and the protonation constants of citric acid.

$$T_M = M + P_1 M L + k_1 P_2 M L H + k_1^2 P_2 P_3 M L^2 H^2 + P_1 P_4 M L^2 + k_1 k_2 P_5 M L H^2 + k_1 P_2 P_6 M L^2 H + 2 P_7 M^2 L^2 \quad 3.15$$

$$T_L = L + k_1 L H + k_1 k_2 L H^2 + k_1 k_2 k_3 L H^3 + P_1 M L + k_1 P_2 M L H + 2 k_1^2 P_2 P_3 M L^2 H^2 + 2 P_1 P_4 M L^2 + k_1 k_2 P_5 M L H^2 + 2 k_1 P_2 P_6 M L^2 H + 2 P_7 M^2 L^2 \quad 3.16$$

$$T'_H = k_1 L H + 2 k_1 k_2 L H^2 + 3 k_1 k_2 k_3 L H^3 + k_1 P_2 M L H + 2 k_1^2 P_2 P_3 M L^2 H^2 + 2 k_1 k_2 P_5 M L H^2 + k_1 P_2 P_6 M L^2 H \quad 3.17$$

Equations 3.15, 3.16, and 3.17 are made easier to handle by further rearrangement and substitution.

$$2 P_7 L^2 M^2 + M (1 + L^2 (AA + P_1 P_4 + CC) + L (P_1 + BB + DD)) - T_M = 0 \quad 3.18$$

$$L^2 (2 P_7 M^2 + 2 M (AA + P_1 P_4 + CC)) + L (A + M (P_1 + BB + DD)) - T_L = 0 \quad 3.19$$

$$T'_H = L (B + M (2 DD + BB + L (2 AA + CC))) \quad 3.20$$

where $A = 1 + k_1 H + k_1 k_2 H^2 + k_1 k_2 k_3 H^3$

$B = k_1 H + 2 k_1 k_2 H^2 + 3 k_1 k_2 k_3 H^3$

$AA = k_1^2 P_2 P_3 H^2$

$BB = k_1 P_2 H$

$CC = k_1 P_2 P_6 H$

$DD = k_1 k_2 P_5 H^2$

3.2.3 The Determination of Ycalc and Yobs

To calculate the formation constants of the nickel-citric acid complexes, the co-ordinated acid, T'_H, was used as the observed function in the non-linear least squares process. This observed quantity, ($Yobs = T'_H(obs)$), was calculated using equation 3.13. The total acid at any given titration point is the initial concentration of acid corrected for volume changes, less the amount of base added. Hence, for the i-th titration point:

$$Yobs_i = T_H(i) - OH_i - H_i + K_W/H_i \quad 3.21$$

where OH_i is the concentration of the added base, corrected for dilution.

The calculated quantity used in the least squares process, (Ycalc = T_H'(calc)), is given by equation 3.20 and its determination requires the calculation of the concentrations of free metal and free ligand at each titration point. These were calculated in the following manner.

Equations 3.18 and 3.19 are polynomials in both the free metal concentration, M, and the free ligand concentration, L. The concentration of hydrogen ions, H, and T_M and T_L are known for each titration point. The parameters, P_i, are fixed for the given least squares cycle, and the values of k_1, k_2, and k_3 are constant. Hence, the only unknown in equations 3.18 and 3.19 are M and L. Given an initial estimate of M and L, equation 3.18 may be solved using the Newton-Raphson method of successive approximation (96, 97) to give an estimate of M, which may be used to calculate a better estimate of L by solving equation 3.19 employing the same method. This in turn, may be used to get a better estimate of M, and so on, until the value of L has converged to the desired level. This process is summarized by Algorithm 3.1.

For the first titration point of a titration, the initial estimates of M and L are determined by assuming that there is no complex formation. In this case, the concentration of the free metal is equal to the total metal concentration, and the free ligand concentration may be calculated from the total ligand concentration and the protonation constants of citric acid. For all other points, the initial estimates of M and L are assigned the refined values of M and L from the previous titration point. The number of times that this Newton-Raphson routine could be entered was restricted, and if the maximum number of iterations was reached without convergence, this would have been obvious on inspection of the output of the computer program ORGLS. This was never observed, and tests on the titration data showed that the routine was seldom entered more than twenty times for any titration point.

Algorithm 3.1 CALC for Nickel-Citric Acid Complexes

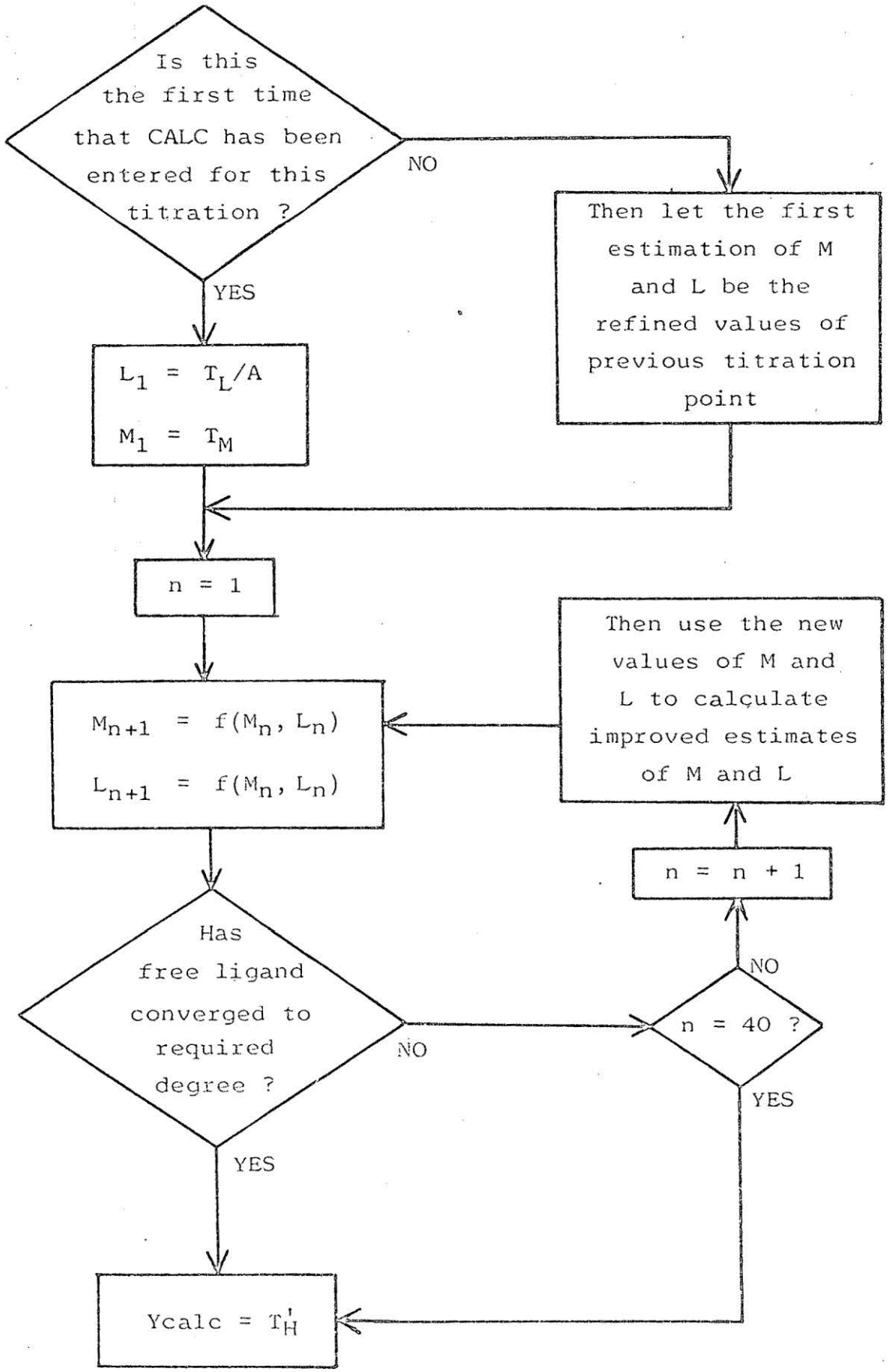

3.2.4 Using ORGLS to Test the Equilibrium Models

Each set of titration data could be analysed using any combination of the equilibria of Section 3.2.1. Different models, (i.e. sets of proposed complexes), could be tested by setting the parameters of the excluded species at zero. For example: to test the model where the only metal complex species are ML and MHL,

$$M + L \rightleftharpoons ML \qquad P_1$$

$$M + HL \rightleftharpoons MHL \qquad P_2$$

Then P_3 through to P_7 are set to zero. This results in equations 3.10 and 3.11 reducing to equations 3.22 and 3.23 respectively:

$$T_M = M + ML + MHL \qquad 3.22$$

$$T_L = L + HL + H_2L + H_3L + ML + MHL \qquad 3.23$$

and equations 3.18, 3.19 and 3.20 become equations 3.24, 3.25 and 3.26 respectively.

$$M (1 + L (P_1 + BB)) - T_M = 0 \qquad 3.24$$

$$L (A + M (P_1 + BB)) - T_L = 0 \qquad 3.25$$

$$T'_H = L (B + M BB) \qquad 3.26$$

In this way, any combination of the species defined in Section 3.2.1 could be tested by setting the appropriate parameters to zero.

3.2.5 Criteria for the Selection of a Satisfactory Model

In the calculation of stability constants using the least squares method, a set of chemical species is first proposed and the fit of this model to the titration data is then noted. A method is required to assess the agreement of fit of the model to the data. In this study, a quantitative measure of fit, the agreement factor or Rfactor, Rf, was used (105).

$$Rf = \sqrt{\frac{\sum_{1}^{N} w_i (Yobs_i - Ycalc_i)^2}{\sum_{1}^{N} w_i (Yobs_i)^2}}$$

where N is the total number of experimental observations, and w_i is the weighting factor discussed previously.

Another quantity, the limiting agreement factor Rlim, is defined

$$Rlim = \sqrt{\frac{\sum_{1}^{N} w_i \epsilon_i^2}{\sum_{1}^{N} w_i (Yobs_i)^2}} \qquad 3.28$$

where ϵ_i^2 is the total maximum uncertainty in the i-th residual $(Yobs_i - Ycalc_i)$, calculated from estimates of the errors in all the experimental quantities. Rlim may be regarded as a significance limit for the function Rf, and if

$$Rf < Rlim \qquad 3.29$$

the hypothesis that the model fits the experimental data is accepted. If the reverse relationship holds, then the model is discarded.

To calculate Rlim, the uncertainty in Yobs - Ycalc must be calculated.

The maximum possible uncertainty in Yobs can be calculated using the formula for propagation of errors (111, 112;).

$$\epsilon_y^2 = \sum_i \left[\frac{\partial y}{\partial x_i}^2 \cdot \epsilon_{x_i}^2 \right] \qquad 3.30$$

where $y = F(x_i)$ and the x_i are a set of experimental quantities having uncertainty ϵ_{x_i}. Considering equation 3.31 for Yobs:

$$Yobs = T_H \text{ (initial)} - [OH]\text{(added)} + Kw/[H] - [H] \qquad 3.31$$

where all terms have been previously defined.
Then, from equation 3.30

$$\epsilon_{Yo}^2 = \epsilon_{T_H}^2 + \epsilon_{OH}^2 + \epsilon_H^2 \qquad 3.32$$

Calculations showed that variations in pH of the order of the experimental uncertainty ($\pm$ 0.002) resulted in variations in Ycalc of about 0.1%. Hence, $\epsilon_{Y_c}^2 = 0.1\%$.

Using equations 3.28, 3.32 and the value of $\epsilon_{Y_c}^2$, an Rlim of $0.4_3\%$ was calculated. Any model that has an agreement factor less than $0.4_3\%$ is regarded as an acceptable model for the given data set.

However, as Rlim is a quantity averaged over the entire titration set, if the model does not fit part of the titration data particularly well, this may be masked by a good fit elsewhere in the titration set. It is therefore important to consider the table of residuals in conjunction with the use of Rlim in accepting a given model.

If the inclusion of an additional species into an "Rlim-acceptable" model results in an improvement in the fit to some part of the titration curve, then the inclusion of the extra species is warranted.

3.3 ANALYSIS OF TITRATION DATA WHEN $T_M \doteq T_L$ IN THE pH RANGE 3 TO 5

Titration data were obtained for solutions where the nickel chloride:citric acid ratios were 1:0.845, 1:1 and 1:1.2, and the concentration of nickel chloride was 1×10^{-3} M. Two further solutions of ratio 1:1 were titrated, one with a nickel chloride concentration of 2×10^{-3} M and the other 3×10^{-3} M. To distinguish each set of titration data, a shorthand notation will be used. Data with a total nickel concentration of 1×10^{-3} M will be referred to as single sets (S), those with a total nickel concentration of 2×10^{-3} M as double sets (D), and 3×10^{-3} M total nickel concentration as triple sets (T).

3.3.1 The Simplest Equilibrium Model

The titration data for solutions with total nickel at 1×10^{-3} M and near equal total nickel and citric acid concentrations were first analysed in terms of the formation of two complexes, ML^- and MHL. As outlined earlier (Section 1.2) these complexes have been characterized by previous workers. The refined values for the logs of the formation constants of these species and the agreement factors are recorded in Table 3.10.

The agreement among the three sets of constants is quite satisfactory, the means and standard deviations for $\log K^M_{ML}$ and $\log K^M_{MHL}$ being 5.448 (0.002) and 3.30_7 (0.013) respectively. These values agree well with those previously reported by Field and Campi, (34, 35), bearing in mind the differences in background electrolyte. These values and the means of those determined in the course of this work are recorded in Table 3.11.

The agreement factors (R factor) for the 1:1 and 1:1.2 data sets are quite satisfactory, being less than Rlim (0.4_3%).

There are no regions of the titration curve where deviations between Yobs and Ycalc show any trends, or are excessively large. The values for Yobs, Ycalc and the residuals of the 1:1 titration data are given in Table 3.12.

Table 3.5 Titration Data for Nickel-Citric Acid Solution With Nickel:Citric Acid = 1:0.845

Ni:Cit ratio 1:0.8450
Initial [Ni] 9.506×10^{-4} M
Initial [Cit] 8.033×10^{-4} M
[NaOH] 0.9988 M
Aliquot Vol 49.88 cm^3

Vol Alkali	p[H^+]	Vol Alkali	p[H^+]
0.000	3.184	0.100	4.429
0.005	3.223	0.105	4.568
0.010	3.265	0.110	4.756
0.015	3.310	0.115	5.061
0.020	3.358	0.119	5.641
0.025	3.406	0.120	5.971
0.030	3.457	0.121	6.623
0.035	3.509	0.122	7.990
0.040	3.562	0.123	8.316
0.045	3.617	0.125	8.490
0.050	3.673	0.130	8.681
0.055	3.731	0.135	8.802
0.060	3.790	0.140	8.910
0.065	3.852	0.145	9.025
0.070	3.916	0.150	9.150
0.075	3.984	0.156	9.313
0.080	4.057	0.160	9.439
0.085	4.134	0.170	9.808
0.090	4.220	0.175	9.995
0.095	4.316	0.180	10.154

Table 3.6 Titration Data for Nickel-Citric Acid Solution With Nickel:Citric Acid = 1:1

Ni:Cit ratio 1:1.0003
Initial[Ni] 9.554×10^{-4} M
Initial[Cit] 9.556×10^{-4} M
[NaOH] 0.9860 M
Aliquot Vol 49.97 cm^3

Vol Alkali	p[H^+]	Vol Alkali	p[H^+]
0.000	3.134	0.135	4.960
0.010	3.206	0.140	5.324
0.015	3.246	0.145	6.287
0.020	3.286	0.150	8.572
0.025	3.329	0.155	8.778
0.030	3.373	0.160	8.914
0.035	3.438	0.165	9.042
0.040	3.464	0.170	9.153
0.045	3.512	0.175	9.273
0.050	3.560	0.180	9.405
0.055	3.609	0.185	9.550
0.060	3.659	0.190	9.709
0.065	3.711	0.195	9.878
0.070	3.763	0.200	10.045
0.075	3.816	0.205	10.193
0.080	3.871	0.210	10.321
0.085	3.928	0.215	10.422
0.090	3.988	0.220	10.509
0.095	4.052	0.225	10.582
0.100	4.118	0.230	10.645
0.105	4.191	0.235	10.699
0.110	4.270	0.240	10.748
0.115	4.359	0.245	10.790
0.120	4.462	0.250	10.827
0.125	4.585	0.255	10.862
0.130	4.741	0.260	10.893

Table 3.7 Titration Data for Nickel-Citric Acid Solution With Nickel:Citric Acid = 1:1.2

Ni:Cit ratio 1:1.2058
Initial [Ni] 9.506×10^{-4} M
Initial [Cit] 1.146×10^{-3} M
[NaOH] 0.9988 M
Aliquot Vol 49.88 cm^3

Vol alkali	$p[H^+]$	Vol Alkali	$p[H^+]$
0.000	3.081	0.120	4.180
0.005	3.113	0.125	4.252
0.010	3.147	0.130	5.330
0.015	3.183	0.135	4.419
0.020	3.220	0.140	4.521
0.025	3.257	0.145	4.643
0.030	3.297	0.150	4.796
0.035	3.337	0.155	4.997
0.040	3.378	0.160	5.284
0.045	3.420	0.165	5.711
0.050	3.464	0.168	6.120
0.055	3.507	0.169	6.315
0.060	3.551	0.170	6.605
0.065	3.597	0.171	7.284
0.070	3.643	0.172	8.192
0.075	3.689	0.173	8.478
0.080	3.736	0.175	8.683
0.085	3.785	0.180	8.891
0.090	3.834	0.185	9.025
0.095	3.886	0.190	9.141
0.100	3.939	0.195	9.258
0.105	3.994	0.200	9.369
0.110	4.052	0.205	9.498
0.115	4.114	0.210	9.628
		0.215	9.776
		0.220	9.932
		0.225	10.085

Table 3.8 Titration Data for Nickel-Citric Acid Solution With Nickel:Citric Acid = 1:1 D

Ni:Cit ratio	1:1.0016
Initial [Ni]	1.901×10^{-3} M
Initial [Cit]	1.904×10^{-3} M
[NaOH]	1.0012 M
Aliquot Vol	49.92 cm^3

Vol Alkali	$p[H^+]$	Vol Alkali	$p[H^+]$	Vol Alkali	$p[H^+]$
0.000	2.907	0.135	3.594	0.270	5.012
0.005	2.929	0.140	3.623	0.275	5.264
0.010	2.952	0.145	3.651	0.280	5.728
0.015	2.975	0.150	3.681	0.282	6.088
0.020	2.997	0.155	3.710	0.283	6.404
0.025	3.021	0.160	3.741	0.284	6.950
0.030	3.044	0.165	3.771	0.285	7.843
0.035	3.068	0.170	3.802	0.386	8.074
0.040	3.091	0.175	3.834	0.287	8.203
0.045	3.116	0.180	3.867	0.290	8.368
0.050	3.140	0.185	3.900	0.295	8.505
0.055	3.166	0.190	3.934	0.300	8.598
0.060	3.190	0.195	3.969	0.305	8.679
0.065	3.216	0.200	4.007	0.310	8.752
0.070	3.243	0.205	4.045	0.315	8.818
0.075	3.268	0.210	4.086	0.320	8.885
0.080	3.294	0.215	4.128	0.325	8.950
0.085	3.320	0.220	4.171	0.330	9.016
0.090	3.347	0.225	4.219	0.335	9.088
0.095	3.373	0.230	4.270	0.340	9.158
0.100	3.400	0.235	4.324	0.345	9.232
0.105	3.428	0.240	4.386	0.350	9.312
0.110	3.455	0.245	4.451	0.355	9.398
0.115	3.482	0.250	4.526	0.360	9.496
0.120	3.510	0.255	4.612	0.365	9.599
0.125	3.538	0.260	4.717	0.370	9.718
0.130	3.566	0.265	4.845		

Table 3.9 Titration Data for Nickel-Citric Acid Solution With Nickel:Citric Acid = 1:1T

Ni:Cit ratio	1:1.0034
Initial [Ni]	2.853×10^{-3} M
Initial [Cit]	2.859×10^{-3} M
[NaOH]	1.0012 M
Aliquot vol	49.92 cm^3

Vol Alkali	p[H^+]	Vol Alkali	p[H^+]	Vol Alkali	p[H^+]
0.000	2.796	0.180	3.420	0.360	4.294
0.005	2.809	0.185	3.348	0.365	4.336
0.010	2.825	0.190	3.458	0.370	4.382
0.015	2.840	0.195	3.477	0.375	4.430
0.020	2.855	0.200	3.495	0.380	4.485
0.025	2.871	0.205	3.515	0.385	4.544
0.030	2.887	0.210	3.534	0.390	4.610
0.035	2.903	0.215	3.554	0.395	4.686
0.040	2.919	0.220	3.573	0.400	4.775
0.045	2.936	0.225	3.593	0.405	4.883
0.050	2.953	0.230	3.613	0.410	5.017
0.055	2.969	0.235	3.638	0.415	5.201
0.060	2.986	0.240	3.654	0.420	5.478
0.065	3.003	0.245	3.674	0.424	5.882
0.070	3.021	0.250	3.695	0.425	6.042
0.075	3.039	0.255	3.716	0.426	6.238
0.080	3.056	0.260	3.738	0.427	6.558
0.085	3.074	0.265	3.759	0.428	7.054
0.090	3.091	0.270	3.781	0.429	7.648
0.095	3.109	0.275	3.804	0.430	7.863
0.100	3.126	0.280	3.826	0.431	7.993
0.105	3.144	0.285	3.850	0.435	8.209
0.110	3.162	0.290	3.874	0.440	8.331
0.115	3.180	0.295	3.898	0.445	8.415
0.120	3.198	0.300	3.922	0.450	8.478
0.125	3.216	0.305	3.947	0.455	8.536
0.130	3.234	0.310	3.974	0.460	8.593
0.135	3.253	0.315	4.000	0.465	8.638
0.140	3.271	0.320	4.028	0.470	8.691
0.145	3.289	0.325	4.056	0.476	8.745
0.150	3.308	0.330	4.086	0.480	8.783
0.155	3.326	0.335	4.117	0.485	8.828
0.160	3.344	0.340	4.149	0.490	8.874
0.165	3.363	0.345	4.182	0.495	8.921
0.170	3.382	0.350	4.217	0.500	8.966
0.175	3.401	0.355	4.254	0.505	9.018

Figure 3.2 Titration Curves for Nickel-Citric Acid Solutions With Nickel:Citric Acid = 1:1

o [Ni] = [Cit] = 1×10^{-3} M

× [Ni] = [Cit] = 3×10^{-3} M

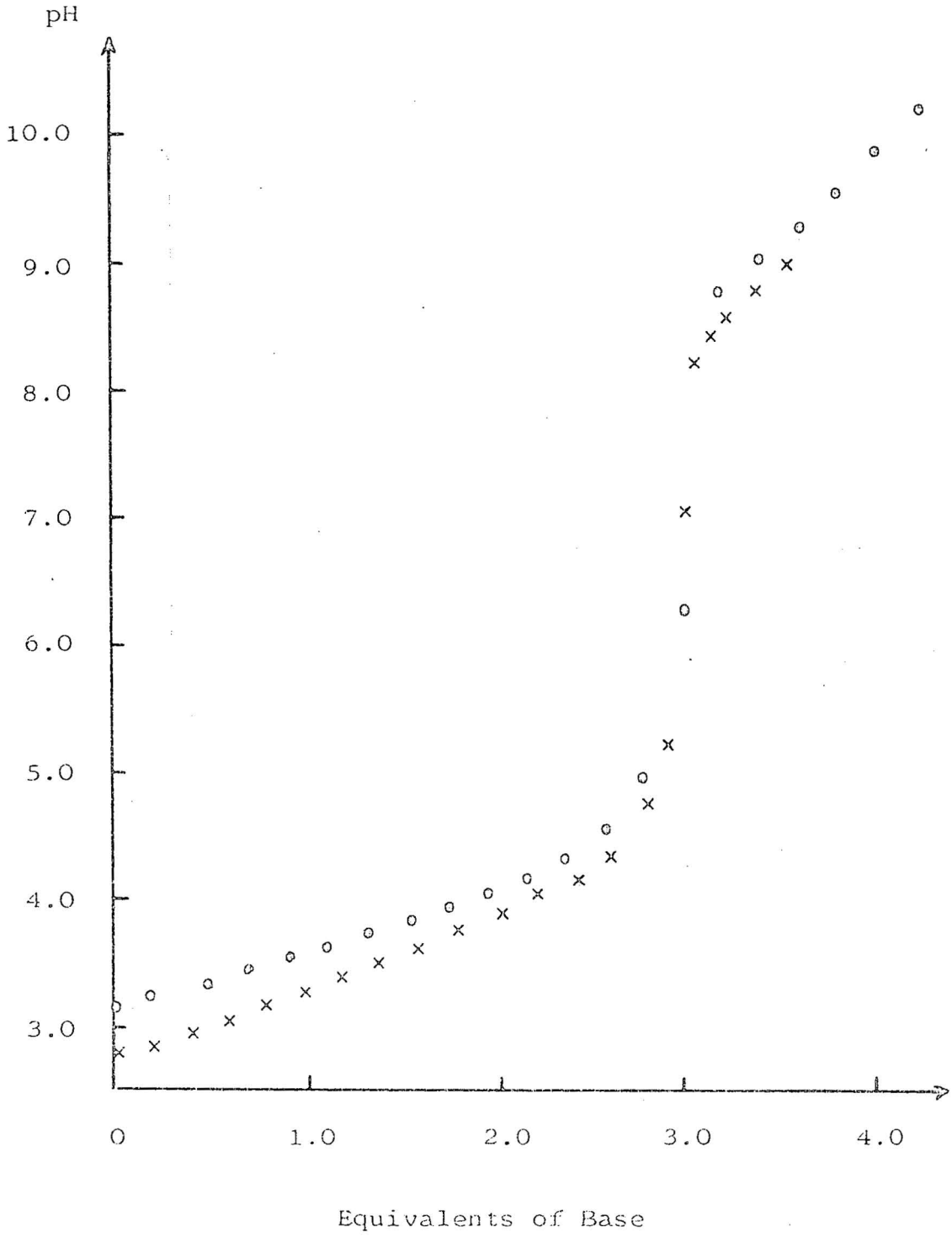

Table 3.10 Equilibrium Constants Obtained From Titration Data of Near-Equimolar Nickel-Citric Acid Solutions With Low Nickel Concentration [1]

The Equilibria	Equilibrium Constant
$M + L \rightleftharpoons ML$	K^{M}_{ML}
$M + HL \rightleftharpoons MHL$	K^{M}_{MHL}

Solution Ratio	$\log K^{M}_{ML}$	$\log K^{M}_{MHL}$	Agreement Factor %
1:0.84	5.450	3.300	0.40
1:1	5.449	3.299	0.23
1:1.2	5.446	3.322	0.17

1. Nickel concentration = 1×10^{-3} M.

With the exception of the first couple and the last few data points, the residuals are generally less than 0.2% of Yobs.

Table 3.11 Formation Constants of ML^- and MHL

Background Electrolyte	$\log K^M_{ML}$	$\log K^M_{MHL}$	Reference
KNO_3	5.50	3.34	Field et al (34)
$NaClO_4$	5.54	3.30	Campi et al (35)
KCl	5.44_8	3.30_7	this work

The Rfactor for the 1:0.845 titration data is somewhat higher than that for the 1:1 and 1:1.2 data, but smaller than Rlim. There is no obvious reason for this. However, with the lower acid concentration, fewer data points were collected and this could have contributed to the higher agreement factor.

A further 1:1 solution of total nickel concentration 1×10^{-3} M was titrated. However, a large drift in the reference point (0.02 pH units) was recorded after the titration. This set was analysed to show the effects of systematic variations in the pH. While the values of the equilibrium constants, $\log K^M_{ML} = 5.439$, and $\log K^M_{MHL} = 3.312$, do not differ greatly from those for the other 1:1 data sets, the Rfactor, (0.46%), is much higher than that of the other 1:1S data set (see Table 3.10). Calculations involving an arbitrary linear correction of the titration data as the endpoint was approached resulted in improvement in the Rfactor and the equilibrium constants. The correction however, was quite arbitrary and merely shows that if changes are made to counter the effects of the reference point drift, improvements may be obtained.

The titration data for the 1:1D and 1:1T solutions did not analyse as well assuming the formation of ML^- and MHL.

Table 3.12 Comparison of Yobs and Ycalc for the 1:1S Nickel- Citric Acid Solution as Calculated by the Computer Program ORGLS

$p[H^+]$	Yobs $/10^{-3}$	Ycalc $/10^{-3}$	Yobs - Ycalc $/10^{-6}$
3.134	2.132	2.119	13.490
3.206	2.047	2.044	3.090
3.246	2.003	2.000	2.738
3.268	1.954	1.955	-0.961
3.329	1.904	1.904	-0.666
3.373	1.850	1.851	-0.992
3.348	1.771	1.769	1.667
3.364	1.733	1.735	-2.502
3.512	1.670	1.671	-1.183
3.560	1.603	1.605	-1.830
3.609	1.534	1.536	-2.200
3.659	1.462	1.464	-2.364
3.711	1.388	1.388	-0.546
3.763	1.311	1.312	-0.908
3.816	1.232	1.234	-1.777
3.871	1.152	1.154	-1.858
3.928	1.070	1.072	-1.913
3.988	0.986	0.987	-1.061
4.052	0.902	0.901	1.005
4.118	0.816	0.816	-0.068
4.191	0.729	0.722	1.327
4.270	0.641	0.640	1.324
4.359	0.553	0.551	1.805
4.462	0.464	0.461	2.521
4.585	0.374	0.371	2.635
4.741	0.283	0.281	2.352
4.960	0.192	0.190	2.236

The equilibrium constants for ML^- and MHL calculated from the 1:1D and 1:1T titration data are recorded in Table 3.13(a). It will be noted that they differ somewhat from those calculated from the single data sets (Table 3.10). When the formation constants for ML^- and MHL are calculated from all five equimolar nickel and citric acid solutions, the means and standard deviations of the formation constants of ML^- and MHL are 5.46 ($\pm$ 0.02), and 3.33 ($\pm$ 0.04) respectively.

While the agreement factors for the 1:1D and 1:1T titration data are of the same order as those for the single data, reference to Table 3.14 shows that the agreement is not good in the low pH region of the titration curve for the 1:1T titration data.

It has previously been suggested that the species MH_2L^+ may be present (35, 37,83). Evidence for the existence of copper, cobalt and iron complexes of this stoichiometry has been mentioned in Section 1.2. Inclusion of this species in the analysis of the 1:1D and 1:1T titration data results in an improvement of the agreement between Yobs and Ycalc in the low pH part of the titration curve (except for the first couple of points), see Table 3.14.

While the Rfactor for the analysis of the 1:1D and 1:1T data by the model ML^- and MHL suggests that that model should be accepted, it will be noted that the inclusion of the species MH_2L^+ results in an improvement in the fit of the model to the data of low pH (Table 3.14). Its inclusion is therefore justified.

The mean value for the formation constant of MH_2L^+ is 1.42 and this agrees reasonably well with the other reported values of 1.75 (35), 1.55 (37), and 1.45 (91). The agreement between the formation constants for MH_2L^+ obtained from the 1:1D and the 1:1T titration data is not good. However, the distribution plot (Figure 3.3) for a 1:1T solution shows that, with a $\log K^M_{MH_2L} = 1.42$, the concentration of the species MH_2L^+ is never greater than three percent of the total metal concentration. With such a low concentration it will be very difficult to characterize such a species. Field et al (34) have report-

Table 3.13 Equilibrium Constants Obtained From the Titration Data of the 1:1D and the 1:1T Nickel-Citric Acid Solutions

A. Constants for the Model ML, and MHL

Solution Ratio	$\log K^{M}_{ML}$	$\log K^{M}_{MHL}$	Agreement Factor %
1:1D	5.469	3.380	0.33
1:1T	5.485	3.358	0.25

B. Constants for the Model ML, MHL, and MH_2L

$$M + H_2L \rightleftharpoons MH_2L \qquad K^{M}_{MH_2L}$$

Solution Ratio	$\log K^{M}_{ML}$	$\log K^{M}_{MHL}$	$\log K^{M}_{MH_2L}$	Agreement Factor %
1:1D	5.486	3.389	1.535	0.21
1:1T	5.498	3.363	1.298	0.10

1. Nickel concentrations 1:1D = 2×10^{-3} M

1:1T = 3×10^{-3} M.

Table 3.14 Changes in the Residual (Yobs - Ycalc) With the Introduction of MH_2L to the Model for the Analysis of the 1:1T Titration Data

p[H^+]	Yobs / 10^{-3}	Yobs - Ycalc / 10^{-5}	
		Model ML, MHL	Model ML, MHL, MH_2L
2.796	6.978	-0.190	2.496
2.825	6.880	-1.030	1.141
2.855	6.777	-1.963	0.051
2.887	6.674	-1.978	-0.149
2.919	6.564	-2.317	-0.690
2.953	6.453	-1.730	-0.473
2.986	6.333	-2.015	-0.859
3.021	6.211	-1.350	-0.447
3.056	6.083	-0.909	-0.042
3.091	5.950	-0.666	0.032
3.126	5.811	-0.603	-0.476
3.162	5.669	-0.139	-0.259
3.198	5.523	0.160	-0.188
3.234	5.372	0.298	0.255
3.271	5.218	0.829	0.094
3.308	5.061	1.186	0.304
3.344	4.899	0.821	0.084
3.382	4.736	1.353	0.281
3.420	4.570	1.671	0.557

Figure 3.3 Distribution Curves for Nickel-Citric Acid Solution With Nickel:Citric Acid = 1:1

Nickel conc. = 3×10^{-3} M

Citric Acid conc = 3×10^{-3} M

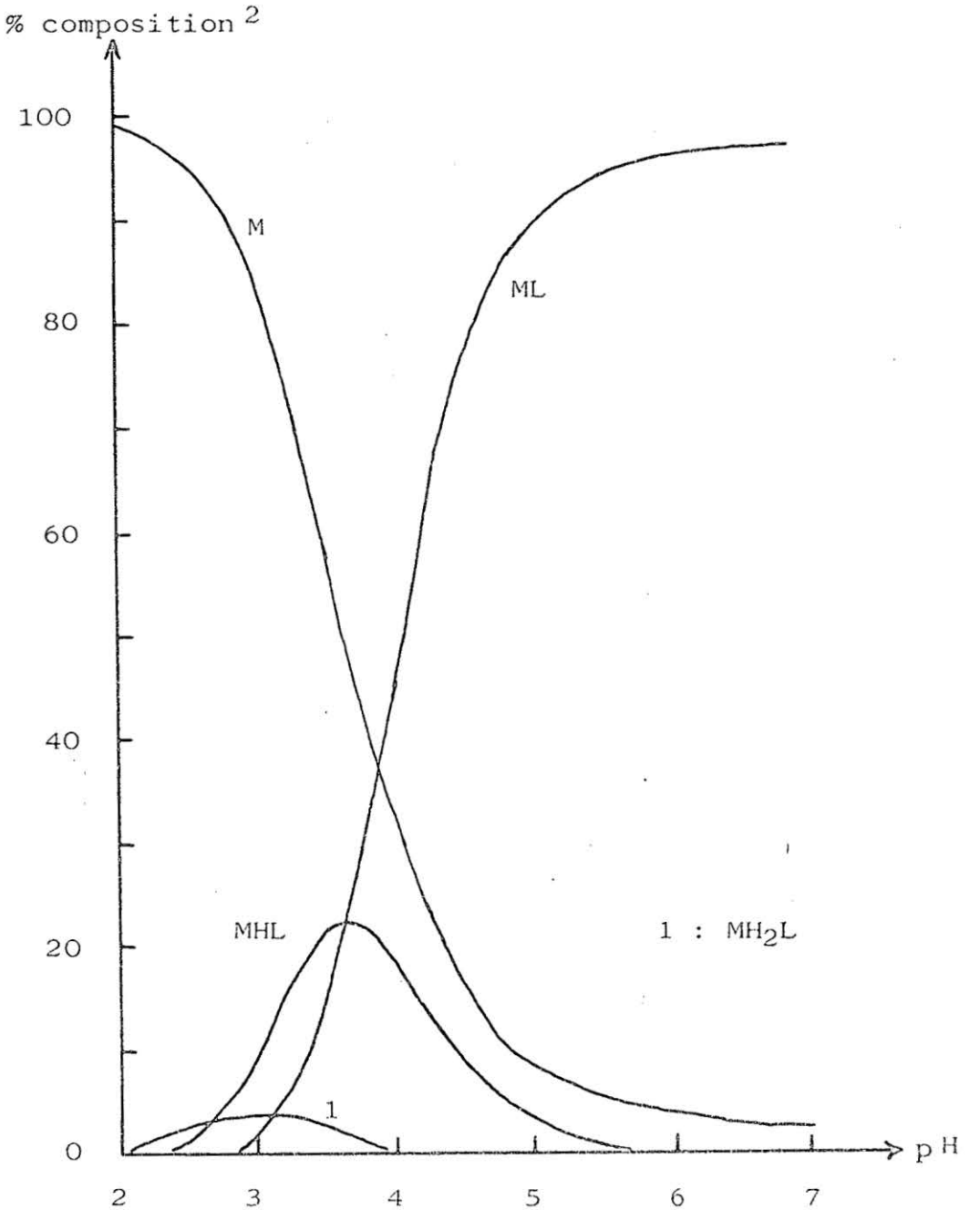

2. As a percentage of total nickel

ed calculations that support this observation.

Although it is difficult to characterize a precise equilibrium constant, MH_2L^+ is still an important complex species in this low pH range. As indicated in Figure 3.3, at pH 2.5 it accounts for about 50% of the total complexed species, and at pH 3.0 accounts for 23%.

Since the inclusion of MH_2L^+ in the analysis of the 1:1D and 1:1T data improved the fit, the single titration data was also analysed including MH_2L^+. For the 1:1S data, an equilibrium constant could not be refined. A possible reason for this is that, as indicated by the distribution plot for the 1:1T solution (Figure 3.3), MH_2L^+ dominates at pH's less than about 3.3. The titration data for the 1:1T solution begins at pH 2.8, whereas for the 1:1S titration data the pH data are available down to only 3.1 (see Figure 3.2, Tables 3.5 to 3.9). It is likely that because of the lower total acid concentrations in the single solutions, the pH is never low enough for MH_2L^+ to be present in reasonable concentrations. The distribution plot for a 1:1S solution (Figure 3.4) with MH_2L^+ included failed to record a significant concentration of the species.

Summary

The titration data of solutions with near-equimolar nickel chloride and citric acid at low concentrations, (1×10^{-3} M), may be analysed in terms of two complexes of 1:1 nickel:citric acid stoichiometry, ML^- and MHL. At higher concentrations ($2\text{-}3 \times 10^{-3}$ M), if a third species MH_2L^+ is introduced the fit of the model to the experimental data in the $p[H^+]$ range 2.8 to 3.3 is improved.

While the agreement between the parameters obtained from the three titration sets of low concentration is excellent, the formation constants obtained from the higher concentration data sets do not agree that well with those from the lower concentration sets.

The next section attempts to assess the effect of errors on the magnitude of the equilibrium constants, in the hope that the differences between the data sets may be explained.

Figure 3.4 Distribution Curves for Nickel-Citric Acid Solution With Nickel:Citric Acid = 1:1

Nickel conc. = 1×10^{-3} M

Citric acid conc = 1×10^{-3} M

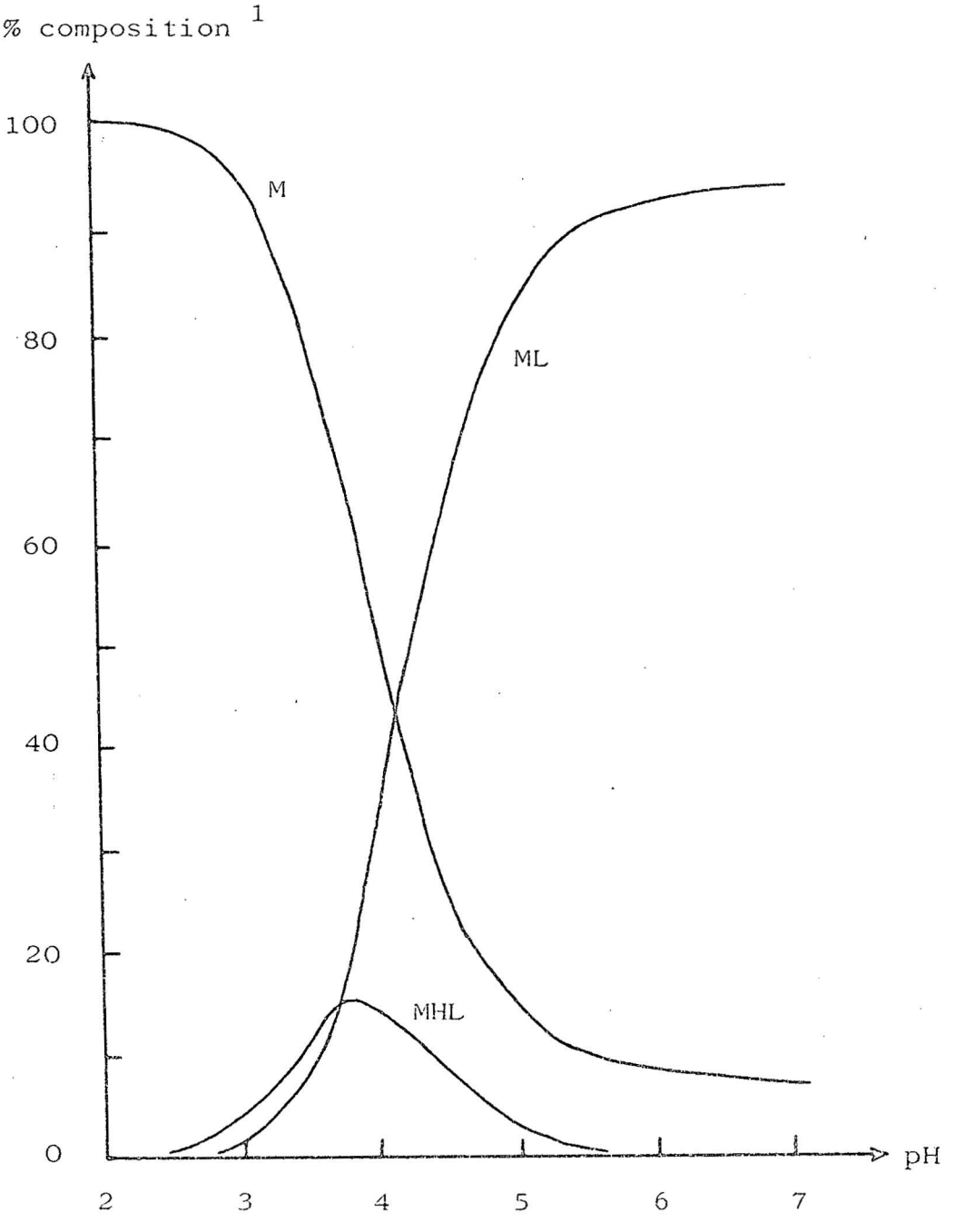

1. As a percentage of total nickel.

3.3.2 Effects of Experimental Errors on the Magnitude of the Equilibrium Constants

In order to assess the effects of experimental errors on (i) the magnitude of the equilibrium constants, and (ii) the fit of any given model to the titration data, several calculations were carried out with changes made to the experimental data. These included: changes in concentrations of reagents, changing the $p[H^+]$ at points through the titration, and altering the protonation constants of citric acid.

The Effects of Errors in the pH

The hydrogen ion concentration plays an important part in determining the free metal and ligand concentrations and the total co-ordinated acid equation, which is the function minimized by the leastsquares process (see Section 3.2.2). Therefore, it is important that the hydrogen ion concentration, and hence the measured pH, is known accurately. The errors inherent in calculating the hydrogen ion concentration from the measured pH have already been discussed in section 2.4.5. This section reports the effect that changes in the pH have on the results from the leastsquares process.

The pH of several data points was altered by the maximum uncertainty in the pH, and the results are presented in Table 3.15. Changes in the $p[H^+]$ of between 0.002 to 0.004 pH units have little effect on the values of Yobs and Ycalc. The change is generally less than 0.1% of the original quantity. However, since $p[H^+]$ is used to calculate both quantities, it is possible that the combined effects result in large changes in the residual, Yobs-Ycalc, and this can be seen in the appropriate columns of Table 3.15. Comparison of the values of Yobs, before and after changing the pH, shows that the changes are restricted to the fourth significant digit, and errors in the measured pH of this magnitude, (0.002 to 0.004 of a pH unit), will have little effect on the refinement process.

It was found that for the 1:1S data set, the changes

Table 3.15 Effects of Changes in the pH on the Values of Yobs and Ycalc for the 1:1S Data Set

$p[H^+]$	Yobs $/ 10^{-3}$	Ycalc $/ 10^{-3}$	Residual[1] $/ 10^{-5}$	$\Delta p[H^+]$	Yobs* $/ 10^{-3}$	Ycalc* $/ 10^{-3}$	Residual* $/ 10^{-5}$
3.134	2.132	2.117	1.349	-0.002	2.129	2.121	0.810
3.206	2.047	2.041	0.309	+0.002	2.050	2.042	0.810
3.560	1.603	1.602	-0.183	-0.002	1.602	1.608	-0.585
3.609	1.534	1.534	-0.220	+0.002	1.535	1.533	0.181
4.118	0.816	0.818	-0.006	-0.003	0.815	0.820	-0.430
4.191	0.729	0.730	0,133	+0.003	0.730	0.724	0.530
4.741	0.283	0.282	0.235	-0.004	0.283	0.283	0.019
4.966	0.192	0.191	0.224	+0.004	0.192	0.188	0.372

* Data after the change in $p[H^+]$

1. Residual = Yobs - Ycalc

in the measured pH for eight data points (from the total of 23) as indicated in Table 3.15, had no effect on the values of the equilibrium constants and only a slight effect in the agreement factor (R increased from 0.23% to 0.24%).

The problem of uncertainties in the measured pH is not to be confused with the systematic errors arising from drifting of the pH meter and electrode system, where the resultant errors in the pH can be very much larger and will cause distortions in the refinement process.

Errors in the Analytical Concentrations

The uncertainties of T_M, T_L, T_H and the alkali concentration were typically ±0.5%, ± 0.1%, ±0.1%, and ± 0.2% respectively. The potassium chloride concentration was known to within ±0.3%, but an error in the concentration of the background electrolyte of this magnitude was not considered important.

Calculations were carried out where the analytical concentration of each of the reagents was varied within its experimental uncertainty. The total concentrations of acid and ligand were varied together because the acid present arises from the protonated ligand and hence, the uncertainty in the acid concentration is identical to that of the ligand. The results are presented in Table 3.16.

In general, the effects on both the equilibrium constants and the fit were small. Changes in the analytical concentrations by the maximum uncertainty results in changes in the logs of the equilibrium constants only in the third decimal place, and the agreement factors are virtually unchanged.

These calculations show that changes in the analytical concentrations of reagents within the experimental uncertainty have little effect on the refinement or the values of the equilibrium constants.

Table 3.16 Effects of Variations in the Analytical Concentrations on the Formation Constants Obtained From the 1:1S Titration Data

Operation	$\log K^{M}_{ML}$	$\log K^{M}_{MHL}$	Agreement Factor %
No Changes	5.449	3.299	0.23
$[OH^-]$ inc 0.2%	5.455	3.293	0.22
$[OH^-]$ dec 0.2%	5.442	3.305	0.26
T_M inc 0.5%	5.444	3.301	0.24
T_M dec 0.5%	5.453	3.300	0.22
T_L and T_H inc 0.1%	5.445	3.299	0.25
T_L and T_H dec 0.1%	5.452	3.299	0.21

Uncertainties in the Citric Acid Protonation Constants

The protonation constants play a very important part in the calculation of free metal and ligand concentrations and total co-ordinated acid concentrations. They, therefore, make an important contribution to Ycalc. (see equations 3.15 to 3.17). The protonation constants, and the uncertainties in them, are given in Part B of Table 3.3.

This test consisted of increasing the protonation constants by the uncertainty and then calculating the equilibrium constants for ML^- and MHL. The results are recorded in Table 3.17.

Variations in the protonation constants can have large effects on the values of the complex species formation constants, as much as one percent in the case when all three protonation constants are increased.

Summary

Variations in the experimental quantities of the order of their experimental uncertainties have small effects on the equilibrium constants of ML^- and MHL, and little effect on the agreement factors. Errors in the analytical concentrations and measured pH equal to the experimental uncertainties of these quantities cannot account for the differences between the equilibrium constants obtained from the titration data of solutions with low and high total nickel concentrations.

Variations in the protonation constants of citric acid will not be the cause of the differences, as the same set of protonation constants was used for the analysis of all nickel-citric acid titration data.

Table 3.17 The Effects of Altering the Citric Acid Protonation Constants on the Formation Constants Obtained From the 1:1S Data

Operation	$\log K^{M}_{ML}$	$\log K^{M}_{MHL}$
No changes	5.449	3.299
Increase $\log k_1$ by 0.015	5.464	3.299
Increase $\log k_2$ by 0.009	5.458	3.312
Increase $\log k_3$ by 0.013	5.454	3.328
Increase all three constants as above	5.479	3.340

3.3.3 Attempts to Fit Other Models to the 1:1 Data

The 1:1 nickel:citric acid solution titration data have been analysed in terms of two complexes, ML^- and MHL, in the case of the lower concentration level data, and a further complex has been characterized in the case of higher total nickel and citric acid concentrations, probably due to the availability of data at a slightly lower pH. However, the agreement between the equilibrium constants obtained from the higher concentration solution data and that of the lower concentration data is not good. This difference cannot be explained in terms of errors, as discussed in the previous section, so it is necessary to consider other equilibria that may be present.

Dimeric complexes of citric acid with copper (45,46,47), cobalt (38), and iron (84, 86), have been reported. It is possible that a dimeric nickel species may also be formed. An analysis of the titration data with a dimeric species, $(ML)_2^{2-}$, was attempted.

The equilibrium is defined as

$$2M^{2+} + 2L^{3-} \rightleftharpoons (ML)_2^{2-}$$

and the equilibrium constant for the formation of $(ML)_2^{2-}$ is given by

$$K_7 = \frac{[(ML)_2]}{[M]^2 [L]^2}$$

Model ML^-, MHL, $(ML)_2^{2-}$

The 1:1D and 1:1T data could not be analysed adequately on the basis of the above three complexes. Values of $\log K_7$ of the order of 12.0 were obtained for the formation of the dimer. The agreement between the lower and higher concentration data sets did not improve; in fact for K^M_{MHL} the range of values increased. The agreement factor for the 1:1T titration data was improved over the ML^- and MHL model (a decrease from 0.23 to 0.16%). However, it was not better than that for the ML^-, MHL and MH_2L model.

Table 3.18 records the agreement factors obtained for each of the three models mentioned above.

Table 3.18 Agreement Factors % for Higher Concentration Data For Various Models of Analysis

Solution	Model		
	ML^-, MHL	ML^-, MHL, MH_2L^+	ML^-, MHL, $(ML)_2^{2-}$
1:1D	0.33	0.21	0.32
1:1T	0.25	0.10	0.16

Model ML^-, MHL, MH_2L^+, $(ML)_2^{2-}$

The titration data did not analyse well when the above combination of complexes was used. While the agreement factor for the 1:1T solution data was similar (0.11%) to that for the model ML^-, MHL, MH_2L^+, since no improvement in the fit to the titration data was obtained there appears no justification for the acceptance of this model. The analysis of the 1:1D solution data resulted in a negative value for the equilibrium constant of the dimer.

Model MHL, $(ML)_2^{2-}$

Field et al (46) has reported that in the case of copper-citrate complexes the acidic titration data was best analysed in terms of CuHL and $(CuL)_2^{2-}$, and the fit was better for this model than the model CuL^- and CuHL. It was found that for the nickel-citrate system this was not the case. Analysis of the titration data in terms of the complexes MHL and $(ML)_2^{2-}$ resulted in agreement factors far worse than those obtained when analysis was in terms of ML^- and MHL. For the 1:1S and 1:1T titration data, agreement factors of 2.12% and 1.87%, respectively, were obtained. These are to be compared with agreement factors

of 0.23% for the 1:1S data, (model ML^- , MHL), and 0.10% for the 1:1T data, (model ML^-, MHL, MH_2L^+).

Summary

There is no improvement in the agreement factors of the higher concentration data sets when the dimer, $(ML)_2^{2-}$, is included in the analysis, compared to the model ML^-, MHL and MH_2L^+. In the case of the single solutions, no equilibrium constant for the dimer was able to be refined.

Inclusion of the dimer in the analysis of the 1:1 nickel:citrate titration data did not improve the agreement between the single sets and the 1:1D and 1:1T sets. It appears that inadequate definition of equilibrium species is not the cause of this poor agreement.

On the basis of the calculations of this section, there appears to be no justification for the inclusion of the dimer in the analysis of solutions of near equimolar nickel chloride and citric acid, given the data and methods of analysis used in this work.

3.3.4 Conclusions

Titration data of solutions with nickel:citrate ratios near 1:1 can be analysed in the pH range 3 to 5 in terms of two complexes, ML^- and MHL, in the case of low nickel chloride and citric acid concentrations. In the case of higher nickel and acid concentrations, a third complex species, MH_2L^+, can be characterized because data are available to a slightly lower pH. No evidence for the existence of a dimeric species, $(ML)_2^{2-}$, could be found on the basis of the data and methods of analysis of this work.

The agreement between the equilibrium constants for ML^- and MHL obtained from the low nickel-citric acid concentration (1×10^{-3}M) titration data, and those from the data of higher concentration ($2\text{-}3 \times 10^{-3}$M) solutions is not as good as one would like. This disagreement cannot be explained in terms of either experimental errors, or by the inclusion of other equilibrium species.

The logs of the equilibrium constants for the

formation of ML^- and MHL as defined by the following equilibria

$$M^{2+} + L^{3-} \rightleftharpoons ML^-$$

$$M^{2+} + HL^{2-} \rightleftharpoons MHL$$

are 5.45 ± 0.05 and 3.31 ± 0.05 respectively. The uncertainty of ±0.05 log units in each constant is based on the effects of experimental errors and uncertainties in the protonation constants discussed in Section 3.3.2.

The equilibrium constant for the formation of MH_2L^+

$$M^{2+} + H_2L^- \rightleftharpoons MH_2L^+$$

is difficult to characterize, probably because in the pH range under study its concentration is very low. The log of the constant appears to be 1.4 ± 0.1. Further values for this equilibrium constant are reported in Section 3.4.

3.4. ANALYSIS OF TITRATION DATA WITH $T_M < T_L$ IN THE pH RANGE 3 TO 6

Many of the previous analyses (34-37,39) of nickel-citric acid complex equilibria have been on the basis of experimental data collected from solutions where total metal is in excess of citric acid. Work on the copper-citric acid system (45) when citric acid is in excess of copper has resulted in the characterization of several complexes of copper:citric acid ratio 1:2. Therefore, it is of interest to study the nickel:citric acid system when citric acid is in excess over total nickel.

Titration data were obtained for solutions with a total nickel concentration of 1×10^{-3}M and nickel chloride: citric acid ratios of 1:1.5, 1:2 and 1:3. Titration data were also collected for 1:2D, 1:2T and 1:3D solutions. Representative titration data for each solution are given in Tables 3.19 to 3.24 and the corresponding titration curves are shown in Figures 3.5 and 3.6. With the exception of the 1:1.5 titration data set, each titration data set was analysed up to about pH 6.

3.4.1 Selection of an Acceptable Model

The titration data for all the higher ratio solutions were first analysed in terms of the two major complexes of the previous section, i.e. ML^- and MHL. This analysis was far from satisfactory, with very poor agreement factors, especially for those solutions with the greatest nickel to citric acid ratios. These agreement factors are shown in Table 3.25. The Rfactor for each data set, with the exception of the 1:1.5 data set, is greater than 0.4% and in the case of the 1:2T and 1:3D data sets, is as high as 1.4%, much larger than Rlim. Use of the model ML^- and MHL to analyse these data sets is clearly unsatisfactory, and an alternative should be considered.

The table of residuals of Yobs and Ycalc obtained in the analysis of the 1:2T titration data (Table 3.26) shows that the fit is very much worse at each end of the acidic titration data.

Table 3.19 Titration Data for Nickel-Citric Acid Solution With Nickel:Citric Acid = 1:1.5

Ni:Cit ratio	1:1.5020
Initial [Ni]	9.506×10^{-4} M
Initial [Cit]	1.428×10^{-3} M
[NaOH]	1.0012 M
Aliquot Vol	49.92 cm^3

Vol Alkali	p[H^+]	Vol Alkali	p[H^+]
0.000	3.021	0.150	4.243
0.005	3.048	0.155	4.311
0.010	3.076	0.160	4.388
0.015	3.106	0.165	4.471
0.020	3.137	0.170	4.569
0.025	3.168	0.175	4.682
0.030	3.201	0.180	4.814
0.035	3.235	0.185	4.970
0.040	3.269	0.190	5.154
0.045	3.305	0.195	5.368
0.050	3.341	0.200	5.616
0.055	3.378	0.205	5.913
0.060	3.415	0.210	6.361
0.065	3.454	0.211	6.497
0.070	3.492	0.212	6.688
0.075	3.531	0.213	6.958
0.080	3.570	0.214	7.494
0.085	3.610	0.215	8.375
0.090	3.651	0.216	8.583
0.095	3.692	0.220	8.890
0.100	3.734	0.225	9.058
0.105	3.786	0.230	9.172
0.110	3.821	0.235	9.288
0.115	3.867	0.240	9.396
0.120	3.913	0.245	9.518
0.125	3.962	0.250	9.633
0.130	4.012	0.255	9.764
0.135	4.064	0.260	9.908
0.140	4.119	0.265	10.050
0.145	4.178	0.270	10.188

Table 3.20 Titration Data for Nickel-Citric Acid Solution With Nickel:Citric Acid = 1:2

Ni:Cit ratio	1:2.0006
Initial [Ni]	9.506×10^{-4} M
Initial [Cit]	1.902×10^{-3} M
[NaOH]	0.9920 M
Aliquot vol	49.92 cm^3

Vol Alkali	p[H^+]	Vol Alkali	p[H^+]	Vol Alkali	p[H^+]
0.000	2.939	0.130	3.723	0.260	5.639
0.005	2.962	0.135	3.756	0.265	5.790
0.010	2.986	0.140	3.799	0.270	5.968
0.015	3.010	0.145	3.833	0.275	6.185
0.020	3.036	0.150	3.876	0.280	6.504
0.025	3.062	0.155	3.917	0.282	6.698
0.030	3.088	0.160	3.957	0.284	6.997
0.035	3.116	0.165	4.002	0.285	7.308
0.040	3.143	0.170	4.048	0.286	7.858
0.045	3.171	0.175	4.096	0.287	8.438
0.050	3.201	0.180	4.146	0.288	8.669
0.055	3.230	0.185	4.198	0.289	8.793
0.060	3.260	0.190	4.252	0.290	8.871
0.065	3.290	0.195	4.310	0.295	9.105
0.070	3.321	0.200	4.378	0.300	9.238
0.075	3.353	0.205	4.446	0.305	9.353
0.080	3.384	0.210	4.519	0.310	9.458
0.085	3.416	0.215	4.600	0.315	9.563
0.090	3.448	0.220	4.698	0.320	9.680
0.095	3.481	0.225	4.783	0.325	9.800
0.100	3.514	0.230	4.885	0.330	9.927
0.105	3.549	0.235	4.996	0.335	10.051
0.110	3.583	0.240	5.113	0.340	10.176
0.115	3.617	0.245	5.236	0.345	10.294
0.120	3.652	0.250	5.361	0.350	10.392
0.125	3.685	0.255	5.496		

Table 3.21 Titration Data for Nickel-Citric Acid Solution With Nickel-Citric Acid = 1:3

Ni:Cit ratio	1:3.0022
Initial [Ni]	9.506×10^{-4} M
Initial [Cit]	2.854×10^{-3} M
[NaOH]	1.0012 M
Aliquot vol	49.92 cm^3

Vol Alkali	p[H^+]	Vol Alkali	p[H^+]	Vol Alkali	p[H^+]
0.000	2.840	0.180	3.686	0.360	5.424
0.005	2.857	0.185	3.716	0.365	5.490
0.010	2.875	0.190	3.748	0.370	5.561
0.015	2.892	0.195	3.778	0.375	5.638
0.020	2.911	0.200	3.809	0.380	5.716
0.025	2.931	0.205	3.843	0.385	5.798
0.030	2.949	0.210	3.874	0.390	5.883
0.035	2.969	0.215	3.906	0.395	5.977
0.040	2.990	0.220	3.941	0.400	6.079
0.045	3.011	0.225	3.976	0.405	6.198
0.050	3.032	0.230	4.012	0.410	6.337
0.055	3.053	0.235	4.050	0.415	6.518
0.060	3.075	0.240	4.086	0.420	6.787
0.065	3.098	0.245	4.126	0.422	6.946
0.070	3.120	0.250	4.167	0.423	7.041
0.075	3.143	0.255	4.208	0.424	7.188
0.080	3.165	0.260	4.251	0.425	7.358
0.085	3.189	0.265	4.295	0.426	7.648
0.090	3.212	0.270	4.341	0.427	8.111
0.095	3.236	0.275	4.390	0.428	8.568
0.100	3.260	0.280	4.438	0.429	8.736
0.105	3.284	0.285	4.487	0.430	8.878
0.110	3.309	0.290	4.539	0.435	9.196
0.115	3.334	0.295	4.591	0.440	9.368
0.120	3.360	0.300	4.651	0.445	9.485
0.125	3.385	0.305	4.704	0.450	9.598
0.130	3.411	0.310	4.764	0.455	9.682
0.135	3.437	0.315	4.822	0.460	9.787
0.140	3.464	0.320	4.884	0.465	9.893
0.145	3.490	0.325	4.949	0.470	10.001
0.150	3.517	0.330	5.012	0.475	10.106
0.155	3.545	0.335	5.078		
0.160	3.571	0.340	5.141		
0.165	3.602	0.345	5.213		
0.170	3.628	0.350	5.276		
0.175	3.658	0.355	5.348		

Table 3.22 Titration Data for Nickel-Citric Acid Solution With Nickel:Citric Acid = 1:2D

Ni:Cit ratio 1:2.0016
Initial [Ni] 1.901×10^{-3} M
Initial [Cit] 3.805×10^{-3} M
[NaOH] 0.9988 M
Aliquot vol 49.88 cm^3

Vol Alkali	p[H^+]	Vol Alkali	p[H^+]	Vol Alkali	p[H^+]
0.000	2.730	0.240	3.530	0.480	5.094
0.005	2.752	0.245	3.549	0.485	5.156
0.010	2.766	0.250	3.568	0.490	5.218
0.015	2.780	0.255	3.587	0.495	5.280
0.020	2.796	0.260	3.606	0.500	5.348
0.025	2.809	0.265	3.627	0.505	5.421
0.030	2.823	0.270	3.646	0.510	5.490
0.035	2.839	0.275	3.666	0.515	5.560
0.040	2.853	0.280	3.687	0.520	5.635
0.045	2.868	0.285	3.707	0.525	5.712
0.050	2.883	0.290	3.729	0.530	5.795
0.056	2.901	0.295	3.750	0.535	5.884
0.060	2.914	0.300	3.771	0.540	5.983
0.065	2.929	0.305	3.793	0.545	6.095
0.070	2.945	0.310	3.816	0.550	6.228
0.075	2.960	0.315	3.838	0.555	6.395
0.080	2.976	0.320	3.862	0.560	6.630
0.085	2.992	0.325	3.885	0.564	6.936
0.090	3.008	0.330	3.910	0.565	7.051
0.095	3.024	0.336	3.939	0.566	7.244
0.100	3.041	0.340	3.959	0.567	7.428
0.104	3.057	0.345	3.985	0.568	7.784
0.110	3.073	0.350	4.012	0.569	8.187
0.115	3.090	0.355	4.039	0.570	8.386
0.120	3.106	0.360	4.067	0.571	8.778
0.125	3.124	0.365	4.095	0.575	8.919
0.130	3.140	0.370	4.125	0.580	9.018
0.135	3.157	0.375	4.156	0.585	9.092
0.140	3.174	0.380	4.187	0.590	9.162
0.145	3.191	0.385	4.209	0.595	9.231
0.150	3.208	0.390	4.253	0.600	9.278
0.155	3.225	0.395	4.288	0.610	9.334
0.160	3.243	0.400	4.324	0.615	9.398
0.165	3.260	0.405	4.361	0.620	9.461
0.170	3.277	0.410	3.398	0.625	9.519
0.175	3.295	0.415	4.439	0.630	9.586
0.180	3.312	0.420	4.480	0.635	9.653
0.185	3.330	0.425	4.521	0.640	9.720
0.190	3.347	0.430	4.565	0.645	9.794
0.195	3.365	0.435	4.611	0.650	9.875
0.200	3.383	0.440	4.659	0.655	9.961
0.205	3.401	0.445	4.707	0.660	10.045
0.210	3.419	0.450	4.757	0.665	10.138
0.215	3.437	0.455	4.810	0.670	10.224
0.220	3.453	0.460	4.864	0.675	10.310
0.225	3.473	0.465	4.918	0.680	10.392
0.230	3.492	0.470	4.975	0.685	10.468
0.235	3.511	0.475	5.034		

Table 3.23 Titration Data for Nickel-Citric Acid Solution With Nickel-Citric Acid = 1:2T

Ni:Cit ratio	1:2.0007
Initial [Ni]	2.853×10^{-3} M
Initial [Cit]	5.709×10^{-3} M
[NaOH]	1.9492 M
Aliquot vol	49.92 cm^3

Vol Alkali	p[H^+]	Vol Alkali	p[H^+]	Vol Alkali	p[H^+]
0.000	2.631	o.185	3.461	0.360	4.905
0.005	2.648	0.190	3.486	0.365	4.977
0.010	2.668	0.195	3.512	0.370	5.054
0.015	2.688	0.200	3.538	0.375	5.131
0.020	2.708	0.205	3.565	0.380	5.212
0.025	2.729	0.210	3.592	0.385	5.294
0.030	2.750	0.215	3.619	0.390	5.382
0.035	2.771	0.220	3.647	0.395	5.470
0.040	2.793	0.225	3.675	0.400	5.564
0.045	2.814	0.230	3.704	0.405	5.665
0.055	2.857	0.235	3.734	0.410	5.773
0.060	2.879	0.240	3.764	0.415	5.894
0.065	2.901	0.245	3.795	0.420	6.035
0.070	2.923	0.250	3.828	0.425	6.206
0.075	2.945	0.255	3.860	0.430	6.448
0.080	2.968	0.260	3.894	0.434	6.760
0.085	2.990	0.265	3.928	0.435	6.882
0.090	3.013	0.270	3.965	0.436	7.030
0.095	3.035	0.275	4.001	0.437	7.274
0.100	3.058	0.280	4.040	0.438	7.685
0.105	3.081	0.285	4.081	0.439	8.192
0.110	3.103	0.290	4.122	0.440	8.451
0.115	3.127	0.295	4.163	0.445	8.827
0.120	3.150	0.300	4.209	0.450	8.977
0.125	3.173	0.305	4.256	0.455	9.078
0.130	3.196	0.310	4.303	0.460	9.168
0.135	3.219	0.315	4.353	0.465	9.252
0.140	3.243	0.320	4.406	0.470	9.334
0.145	3.267	0.325	4.460	0.475	9.416
0.150	3.290	0.330	4.516	0.480	9.505
0.155	3.314	0.335	4.576	0.485	9.598
0.160	3.338	0.340	4.637	0.490	9.688
0.165	3.363	0.345	4.699	0.495	9.799
0.170	3.386	0.350	4.766	0.500	9.921
0.175	3.411	0.355	4.834	0.505	10.048
0.180	3.436				

Table 3.24 Titration Data for Nickel-Citric Acid Solution With Nickel:Citric Acid = 1:3D

Ni :Cit ratio	1:3.0012
Initial [Ni]	1.903×10^{-3} M
Initial [Cit]	5.706×10^{-3} M
[NaOH]	1.9492 M
Aliquot vol	49.92 cm^3

Vol Alkali	p[H^+]	Vol Alkali	p[H^+]	Vol Alkali	p[H^+]
0.000	2.644	0.170	3.484	0.340	4.974
0.005	2.663	0.175	3.514	0.345	5.035
0.010	2.683	0.180	3.544	0.350	5.099
0.015	2.704	0.185	3.574	0.355	5.161
0.020	2.725	0.190	3.606	0.360	5.229
0.025	2.747	0.195	3.637	0.365	5.294
0.030	2.769	0.200	3.670	0.370	5.362
0.035	2.792	0.205	3.704	0.375	5.431
0.040	2.815	0.210	3.737	0.380	5.502
0.045	2.838	0.215	3.772	0.385	5.574
0.050	2.862	0.220	3.807	0.390	5.649
0.055	2.885	0.225	3.843	0.395	5.727
0.060	2.909	0.230	3.881	0.400	5.810
0.065	2.933	0.235	3.920	0.405	5.898
0.070	2.958	0.240	3.960	0.410	5.998
0.075	2.983	0.245	4.001	0.415	6.106
0.080	3.007	0.250	4.043	0.420	6.236
0.085	3.032	0.255	4.086	0.425	6.394
0.090	3.057	0.261	4.138	0.430	6.616
0.095	3.082	0.266	4.183	0.435	6.992
0.100	3.107	0.270	4.217	0.436	7.111
0.105	3.131	0.275	4.268	0.437	7.272
0.110	3.158	0.280	4.314	0.438	7.486
0.115	3.184	0.285	4.363	0.439	8.075
0.120	3.210	0.290	4.413	0.440	8.551
0.125	3.236	0.295	4.465	0.441	8.783
0.130	3.262	0.300	4.517	0.445	9.106
0.135	3.288	0.305	4.570	0.450	9.288
0.140	3.316	0.310	4.624	0.455	9.417
0.145	3.343	0.315	4.679	0.460	9.533
0.150	3.371	0.320	4.736	0.465	9.636
0.155	3.398	0.325	4.794	0.470	9.751
0.160	3.427	0.330	4.854	0.475	9.874
0.165	3.455	0.335	4.912		

Figure 3.5 Titration Curves for Nickel-Citric Acid Solutions With Nickel:Citric Acid = 1:1.5 and 1:2

o Ni:Cit = 1:1.5 [Ni] = 1×10^{-3} M

× Ni:Cit = 1:2 [Ni] = 2×10^{-3} M

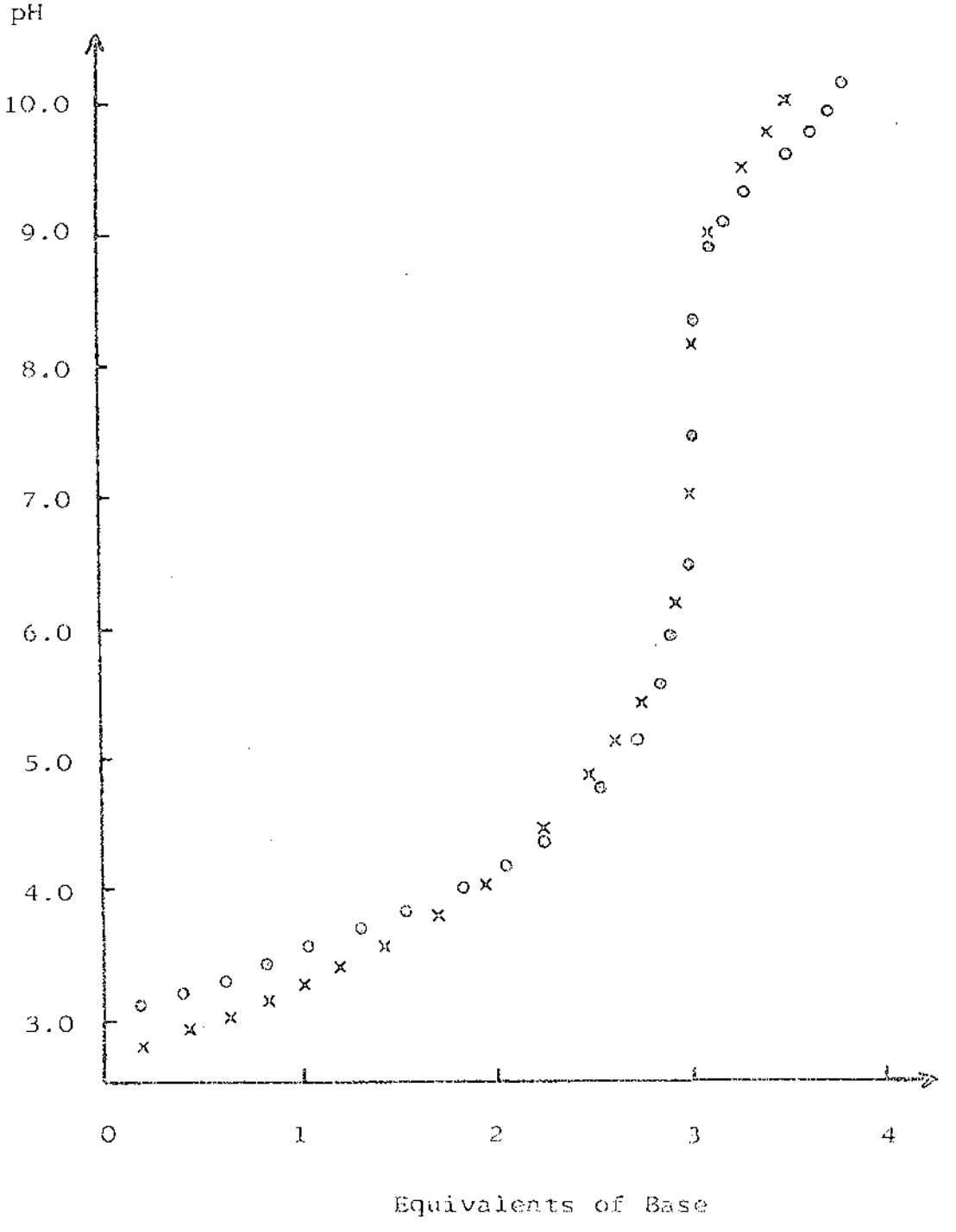

Figure 3.6A Titration Curves for Nickel-Citric Acid Solutions With Nickel:Citric Acid = 1:2

o [Ni] = 1×10^{-3} M

x [Ni] = 3×10^{-3} M

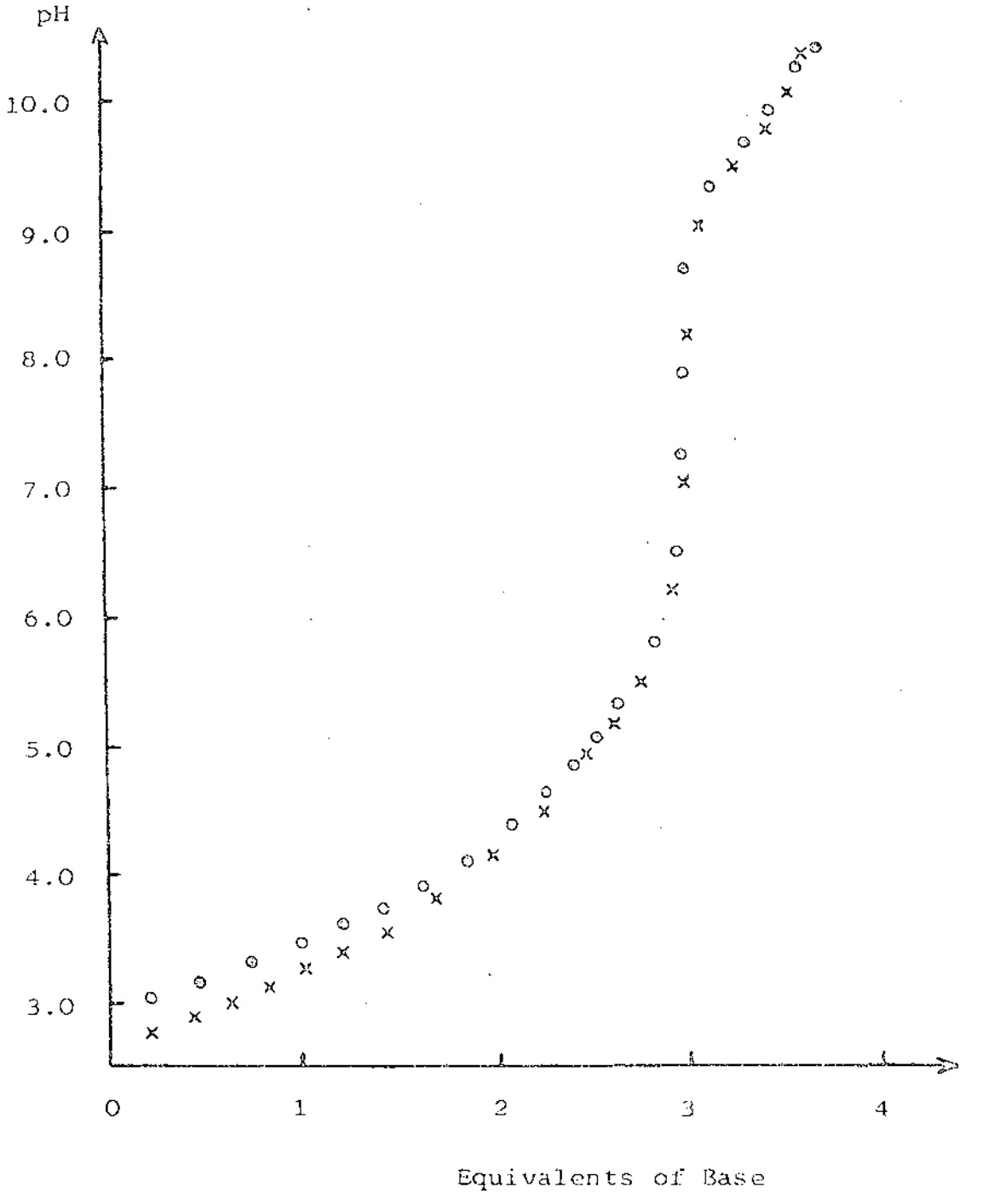

Figure 3.6B Titration Curves for Nickel-Citric Acid Solutions With Nickel:Citric Acid = 1:3

o [Ni] = 1×10^{-3} M

× [Ni] = 2×10^{-3} M

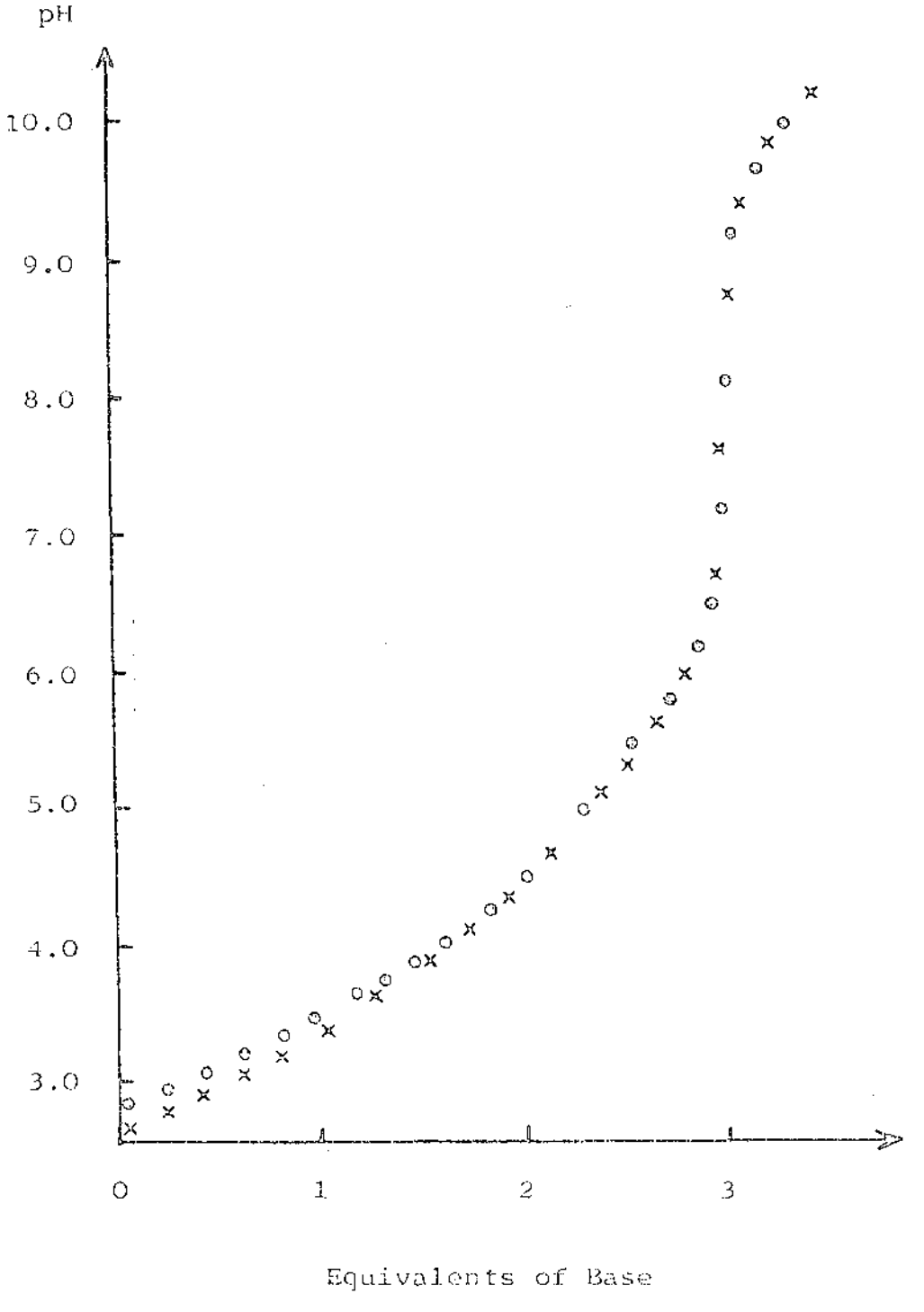

Table 3.25 Agreement Factors (%) for Analysis of High Nickel:Citric Acid Ratio Titration Data by Several Models

Solution	Model		
	ML, MHL	ML, MHL, MH_2L	ML, MHL, MH_2L, ML_2
1:1.5	0.26	0.24	0.12 [1]
1:2	0.44	0.38	0.13
1:2D	0.88	0.81	0.10
1:2T	1.42	1.35	0.13
1:3	0.76	0.74	0.12
1:3D	1.44	1.39	0.11

1. Data set analysed in terms of ML, MHL and ML_2 only.

Table 3.26 Residuals from the Analysis of the 1:2T Titration Data by Various Models

$p[H^+]$	Residuals / 10^{-6}		
	ML, MHL	ML, MHL, MH_2L	ML, MHL, MH_2L, ML_2
2.631	-27.75	75.18	53.89
2.688	-64.88	31.19	14.19
2.750	-69.63	15.43	4.51
2.857	-68.21	-8.13	-7.98
2.945	-59.26	-23.73	-14.09
3.035	-41.30	-30.92	-13.15
3.127	-15.47	-27.16	-4.41
3.219	4.92	-29.34	-6.39
3.314	13.77	-16.43	1.58
3.411	19.82	-4.25	3.35
3.512	21.19	11.60	5.52
3.619	19.69	30.55	9.73
3.734	13.14	45.10	11.86
3.828	8.29	53.51	15.00
3.928	-11.41	42.60	4.19
4.040	-24.96	32.94	1.19
4.163	-50.70	5.23	-11.14
4.303	-74.18	-25.01	-15.08
4.460	-108.20	-68.62	-19.69
4.637	-152.30	-123.10	-19.30
4.834	-212.70	-192.80	-18.49
5.131	-301.30	-290.20	-10.56
5.382	-343.30	-337.20	0.93
5.665	-337.70	-334.50	5.64
6.035	-246.50	-244.70	9.74

The model ML^- and MHL was extended by including the species MH_2L^+. It was expected that this could well improve the fit of the data around pH = 3 as was observed for the 1:1D and 1:1T data sets (see Section 3.1.1). The agreement factors for this model are also given in Table 3.25. There is no significant improvement in the agreement factor over the simple model ML^- and MHL. The residuals of Table 3.26 show that while the introduction of MH_2L^+ makes a slight improvement in the fit to the data below about pH 3, the agreement at the end of the acidic data is still poor. As this agreement is so poor, a new species (or species) must be considered. Several workers have reported copper and cobalt complexes with citric acid where the metal:citrate ratio is 1:2 (see Section 1.2). With this in mind, two additional complex species were considered, $M(HL)_2^{2-}$ and ML_2^{4-}.

Using the model ML^-, MHL, MH_2L^+ and ML_2^{4-}, the analysis of the higher ratio titration data resulted in considerable lowering of the agreement factors from those obtained for the model ML^-, MHL and MH_2L^+. These agreement factors are recorded in Table 3.25. The changes for the 1:2T and 1:3D titration data are from 1.35 to 0.13 and 1.39 to 0.11% respectively, both less than Rlim. The reasons for the drop in the agreement factors can be seen from the residuals in Table 3.26. In each case, there has been considerable improvement in the fit above pH 4.

Analysis of the titration data using the model ML^-, MHL, MH_2L^+ and $M(HL)_2^{2-}$ resulted in no improvement over that of ML^-, MHL and MH_2L^+, so there appears to be no justification for the inclusion of $M(HL)_2^{2-}$.

Analysis of the 1:1.5 data in terms of ML^-, MHL, MH_2L^+ and ML_2^{4-} resulted in a negative value for the equilibrium constant for MH_2L^+. It will be noted that this also occurred for the 1:1S solution (see Section 3.3.1). The effect probably results from the lack of titration data below pH 3. The 1:1.5 data were analysed satisfactorily in terms of the three complexes ML^-, MHL and ML_2^{4-},

the agreement factor being 0.12%. The 1:1.5 data differs from the 1:1S data in that citric acid is in slight excess, and so the bis complex species is formed, although only in small amounts (see Figure 3.7).

Reference to Table 3.25 shows that the Rfactor for the 1:1.5 data is less than Rlim when analysed in terms of ML^- and MHL only. However, inclusion of the species ML_2^{4-} resulted in a large improvement of the fit above pH 4, and the analysis of the 1:1.5 titration data in terms of ML^-, MHL and ML_2^{4-} is acceptable on those grounds.

The equilibrium constants obtained from the analysis of the higher ratio titration data are recorded in Table 3.27. The means and standard deviations of the logs of the equilibrium constants for the formation of ML^-, MHL, MH_2L^+ and ML_2^{4-} are 5.50 (0.03), 3.36 (0.02), 1.5_4 (0.13) and 2.3_8 (0.16) respectively. The agreement between the values for K^M_{ML} and K^M_{MHL} obtained from each titration data set is good. The relatively high standard deviation for the equilibrium constant of MH_2L^+ is probably due to the low concentration of this species with respect to total metal.

The distribution curves for solutions of ratio 1:1.5, 1:3, 1:2T (Figures 3.7 to 3.9 respectively) show the importance of MH_2L^+ and ML_2^{4-} in the low and high acidic pH range respectively. For example, in the case of the 1:2T solution (Figure 3.9), while MH_2L^+ accounts for only 8% of the total nickel at pH 3, it accounts for 26% of complexed nickel. At lower pH's MH_2L^+ is even more important; at pH 2.5 it accounts for 50% of complexed nickel.

ML_2^{4-} becomes an important species as the pH increases. For the 1:2T solution, the distribution curves of Figure 3.9 show that at pH 5, ML_2^{4-} accounts for 15% of complexed metal, while at pH 7 the percentage is 51%.

For the 1:1.5 solution ML_2^{4-} is not an important species. Figure 3.7 shows that at pH 7 ML_2^{4-} accounts for only 9% of complexed nickel. This results from the smaller excess of citric acid over nickel.

Table 3.27 Equilibrium Constants Obtained From Titration Data Where Total Citric Acid > Total Nickel

The Equilibria	Equilibrium Constant
$M + L \rightleftharpoons ML$	K^{M}_{ML}
$M + HL \rightleftharpoons MHL$	K^{M}_{MHL}
$M + H_2L \rightleftharpoons MH_2L$	$K^{M}_{MH_2L}$
$ML + L \rightleftharpoons ML_2$	$K^{ML}_{ML_2}$

Solution	$\log K^{M}_{ML}$	$\log K^{M}_{MHL}$	$\log K^{M}_{MH_2L}$	$\log K^{ML}_{ML_2}$	Rfactor %
1:1.5	5.485	3.346		2.624	0.12
1:2	5.493	3.376	1.745	2.155	0.13
1:2D	5.496	3.366	1.444	2.297	0.10
1:2T	5.523	3.361	1.475	2.420	0.13
1:3	5.467	3.329	1.440	2.351	0.12
1:3D	5.555	3.372	1.578	2.435	0.11
Mean	5.50	3.36	1.54	2.38	
Standard Deviation	0.03	0.02	0.13	0.16	

Figure 3.7 Distribution Curves for Nickel-Citric Acid Solution With Nickel:Citric Acid = 1:1.5

Nickel conc. = 1×10^{-3} M

Citric acid conc. = 1.5×10^{-3} M

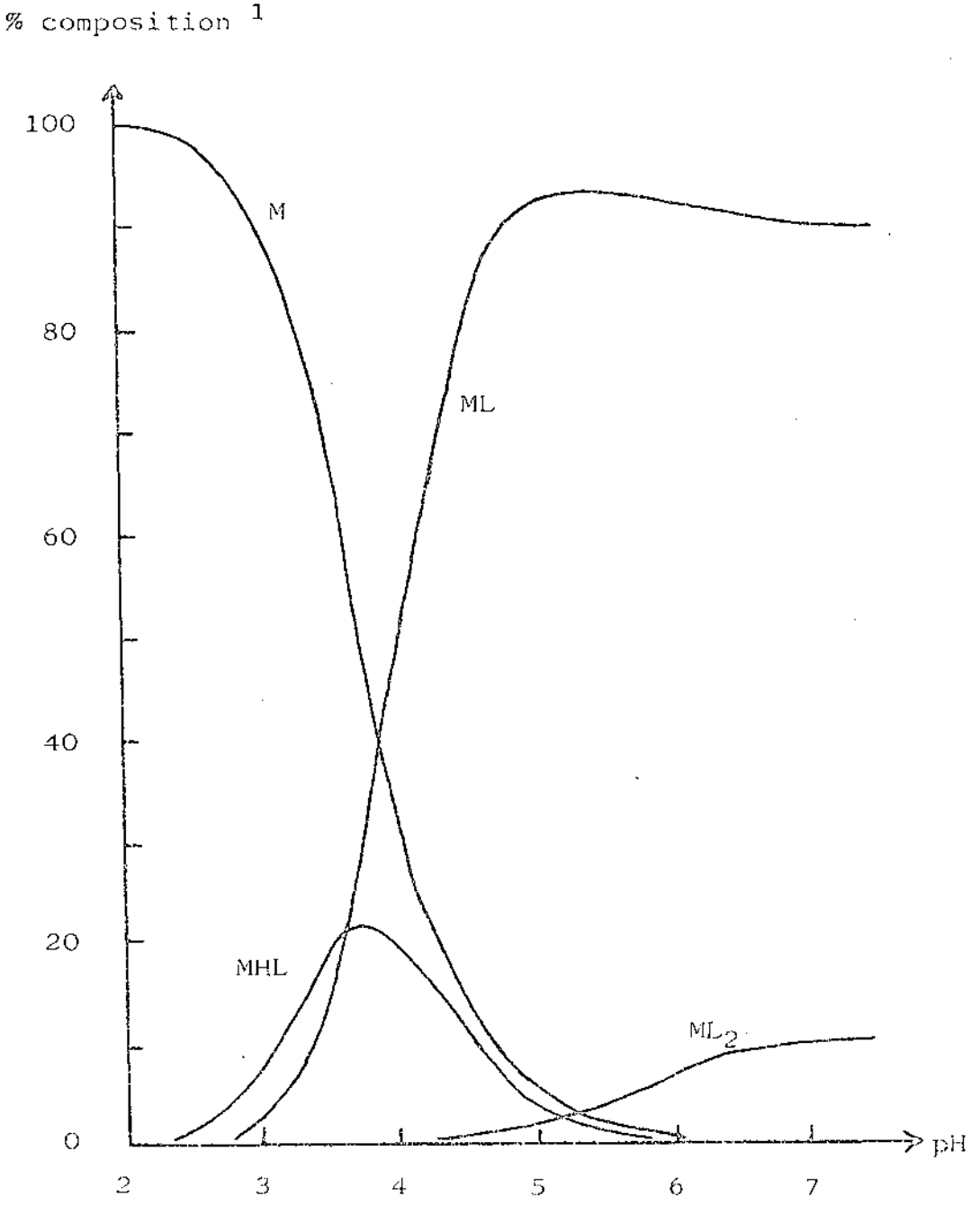

1. As a percentage of total nickel

Figure 3.8 Distribution Curves for Nickel-Citric Acid Solution With Nickel:Citric Acid = 1:3

Nickel conc. = 1×10^{-3} M

Citric acid conc. = 3×10^{-3} M

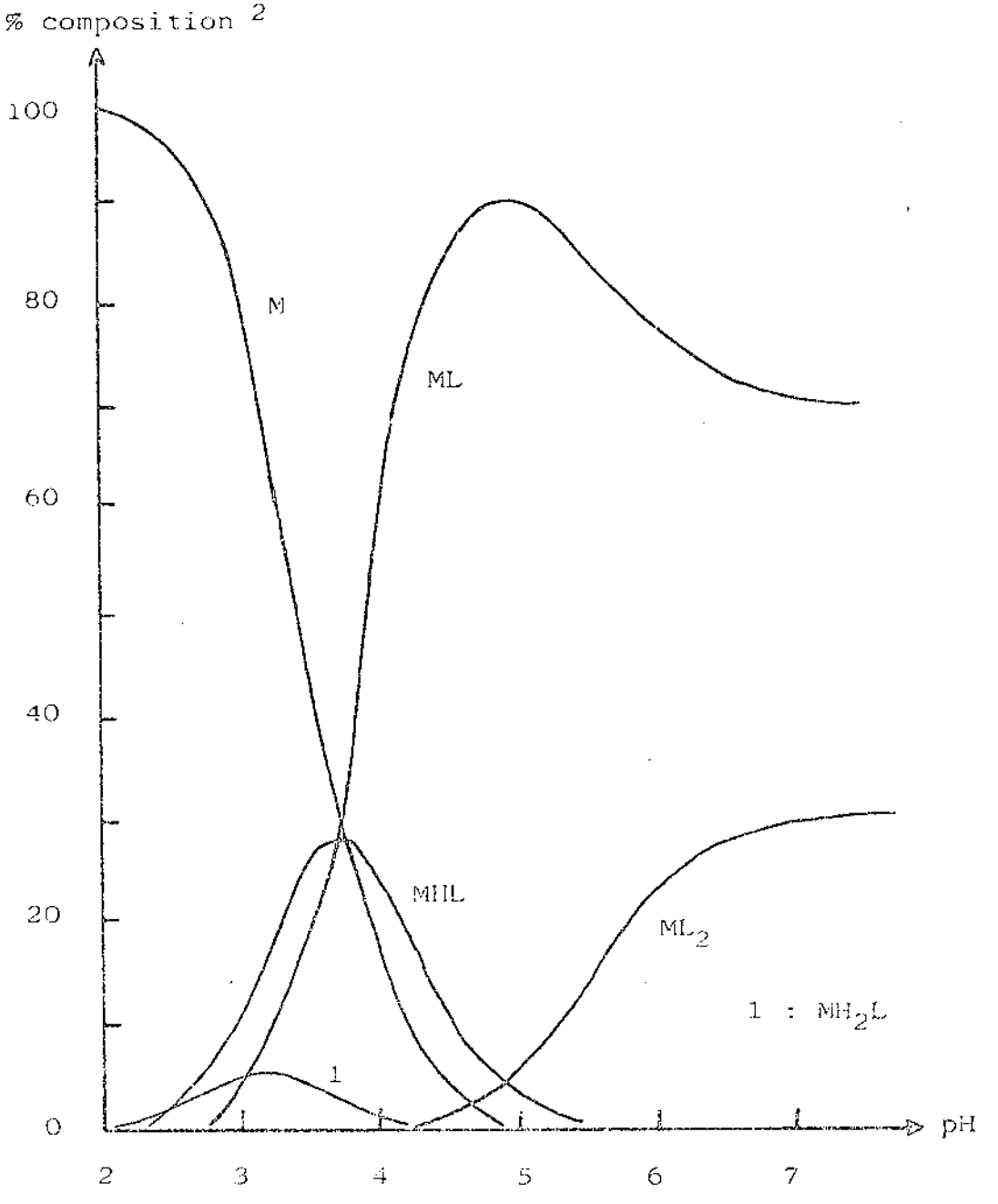

2. As a percentage of total nickel

Figure 3.9 Distribution Curves for Nickel-Citric Acid Solution With Nickel:Citric Acid = 1:2

Nickel conc. = 3×10^{-3} M

Citric Acid conc. = 6×10^{-3} M

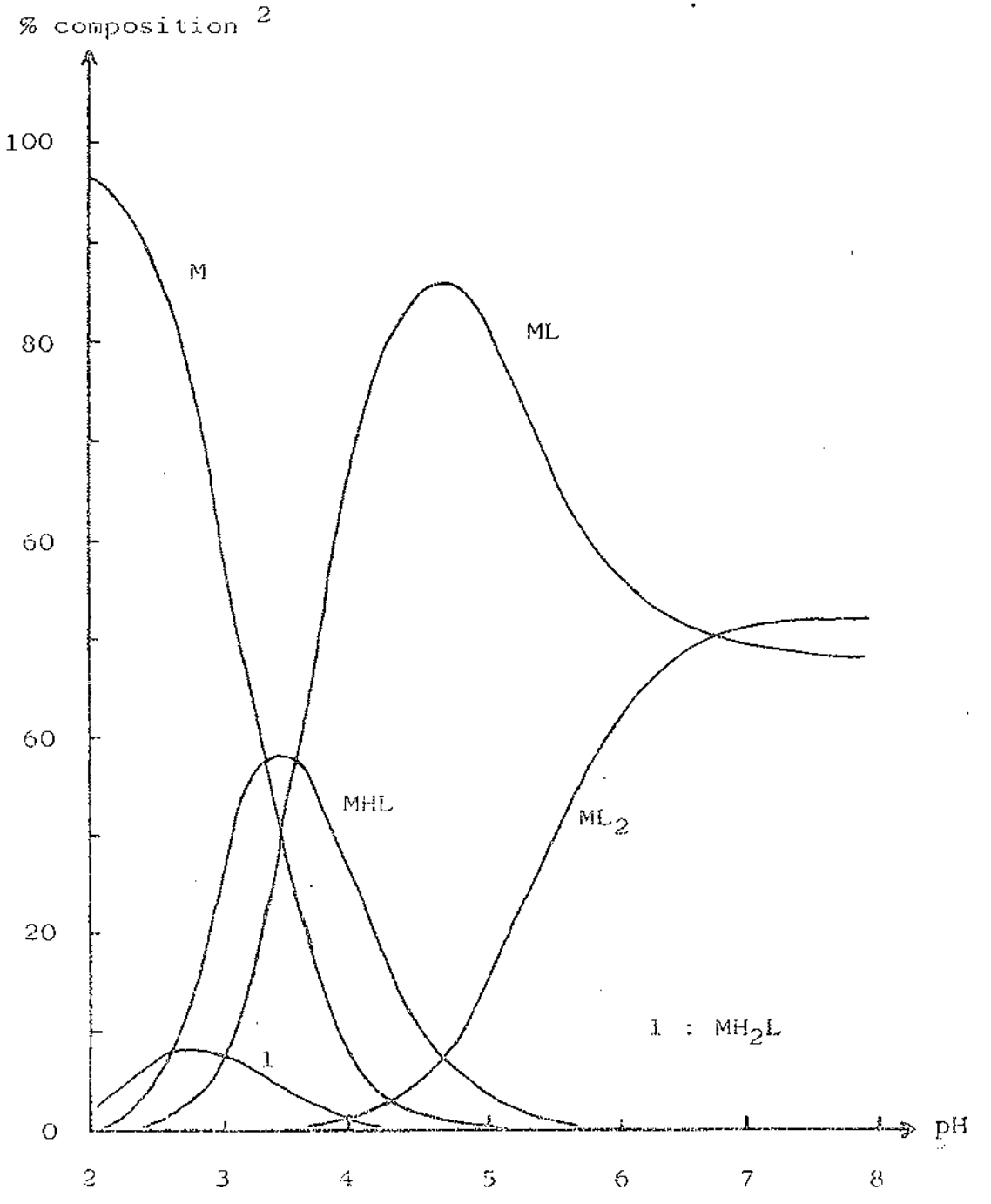

2. As a percentage of total nickel

The values for the logs of the equilibrium constants for the formation of ML^-, MHL and MH_2L^+ obtained from the higher ratio data sets agree well with those obtained from the 1:1D and 1:1T data sets. When these latter two data sets are included, the means and standard deviations of the formation constants for ML^-, MHL and MH_2L^+ do not change significantly, as Table 3.28 shows.

Comparison of the values of the constants obtained from the 1:1S titration data with those from the higher ratio data sets shows that the agreement is not too good (see Table 3.28). No reason could be found to explain this disagreement. It did not appear to result from experimental errors. Calculations on the 1:2T data set after changing the experimental quantities (e.g. T_M, T_L, [OH] and pH) by their uncertainties resulted in changes in the magnitude of the equilibrium constants of the same order as described earlier for the 1:1 data (see Section 3.3.2).

3.4.2 Other Models

Analysis of the higher ratio data in terms of the dimer, $(ML)_2^{2-}$, was also attempted. Table 3.29 records the agreement factors obtained when the 1:2T data were analysed by several models which included $(ML)_2^{2-}$. Also listed in Table 3.29 are the agreement factors for the 1:2T data set when analysed by the other models discussed in the previous section. Although the results in Table 3.29 show that the agreement factors are much the same when $(ML)_2^{2-}$ is included, this inclusion of $(ML)_2^{2-}$ in the model ML^-, MHL, MH_2L^+ amd ML_2^{4-} causes greater variation in the equilibrium constants for ML^- and MH_2L^+, and hence the inclusion of the dimer results in a worse overall analysis of the experimental data.

3.4.3 Inclusion of ML_2^{4-} in Analysis of 1:1 Data

An attempt was made to fit the model ML^-, MHL, MH_2L^+ and ML_2^{4-} to the 1:1S and 1:1T titration data. Negative values for the equilibrium constant for ML_2^{4-} were obtained from both the 1:1S and the 1:1T data.

Table 3.28 Means and Standard Deviations of The Equilibrium Constants [1]

Combination of Data Sets	K^{M}_{ML}		K^{M}_{MHL}		$K^{M}_{MH_2L}$	
1:1, 1:0.845 and 1:1.2	5.448	(0.002)	3.30_7	(0.013)		
Higher ratio data sets	5.50_3	(0.03)	3.35_8	(0.02)	1.5_4	(0.13)
Higher ratio data sets + 1:1D and 1:1T	5.49_8	(0.03)	3.36_3	(0.02)	1.5_0	(0.14)

1. The equilibrium constants are recorded as logs.

Table 3.29 Agreement Factors (%) for the 1:2T Data When Analysed With $(ML)_2$ Included in Models

Model	Agreement Factor
MHL, $(ML)_2^{2-}$	2.78
ML^-, MHL, $(ML)_2^{2-}$	1.49
ML^-, MHL, MH_2L^+, $(ML)_2^{2-}$	1.33
ML^-, MHL, MH_2L^+, ML_2^{4-}, $(ML)_2^{2-}$	0.12
ML^-, MHL	1.42
ML^-, MHL, MH_2L^+	1.35
ML^-, MHL, MH_2L^+, ML_2^{4-}	0.13

These results are perhaps not surprising. The distribution curves calculated assuming the formation of the species ML^-, MHL, MH_2L^+ and ML_2^{4-}, indicated less than 0.5% ML_2^{4-} formed even at pH 5.

Summary

The titration data of solutions where citric acid is in more than two-fold excess of total nickel were analysed adequately in terms of the complexes ML^-, MHL, MH_2L^+, and ML_2^{4-}. For the solution where the ratio of nickel to citric acid was 1:1.5, there was an insignificant amount of MH_2L^+ formed. Similarly, the ML_2^{4-} species is formed in only very small amounts in the 1:1 solutions.

Analysis of the high ratio data with the species $(ML)_2^{2-}$ included was worse than when analysed on the basis of ML^-, MHL, MH_2L^+, and ML_2^{4-} alone.

The values of the equilibrium constants for ML^-, MHL and MH_2L^+ obtained from the higher ratio data agree well with those from the high concentration equimolar data, but not as well with the equimolar data with a nickel concentration of 1×10^{-3}M. This disagreement could not be explained on the basis of experimental errors or by the formation of other complex species.

3.5 ANALYSIS OF NICKEL-CITRIC ACID TITRATION DATA IN THE ALKALINE pH RANGE

Titration data for all the solutions discussed in Sections 3.3 and 3.4 extended into the alkaline region. However, only a preliminary analysis of the titration data with nickel:citric acid ratios close to 1:1 has been carried out.

3.5.1 Preliminary Analysis of Alkaline Titration Data of Nickel:Citric Acid 1:1 Solutions

Several workers have previously reported evidence for the species $MH_{-1}L$ in alkaline nickel-citric acid solutions (38 - 40, 42, 88, 117). However, where values for the equilibrium constant for the reaction

$$ML^{-} \rightleftharpoons MH_{-1}L^{2-} + H^{+}$$

are given, they vary widely (40, 42, 117).

Reference to the distribution curves for a 1:1 nickel: citric acid solution (Figures 3.3 amd 3.4) shows that at pH 7 the only species present are the free metal, M^{2+}, the free ligand, L^{3-}, and the complex ML^{-}. In the pH range 8 - 10 then, the following equilibria will occur:

$$1.\quad M^{2+} + L^{3-} \rightleftharpoons ML^{-} \qquad P_1$$

$$2.\quad ML^{-} \rightleftharpoons MH_{-1}L^{2-} + H^{+} \qquad P_2$$

$$3.\quad M^{2+} \rightleftharpoons MOH^{+} + H^{+} \qquad P_3$$

Equilibrium 3 allows for the hydrolysis of the free metal. The removal of the hydroxy proton from the triionized ligand, L^{3-}, was not considered important in this pH range, since the pK for its removal is around 12.0 (33).

The mass balance equations for the total metal, T_M, and total ligand, T_L, are

$$T_M = M + ML + MH_{-1}L + MOH \qquad 3.33$$

and

$$T_L = L + ML + MH_{-1}L$$

The square brackets (representing concentration) and the charges are omitted in these and subsequent equations, for clarity.

Equations 3.33 and 3.34 may be expressed in terms of the free metal and ligand concentrations, the hydrogen ion concentration and the equilibrium constants P_i.

$$T_M = M + P_3 M/H + P_1 ML + P_1 P_2 ML/H \qquad 3.35$$

and

$$T_L = L + P_1 ML + P_1 P_2 ML/H \qquad 3.36$$

Using the principle of electroneutrality, the following expression can be obtained:

$$2M^{2+} + Na^+ + H^+ + MOH^+ = Cl^- + OH^- + 3L^{3-} + ML^- + 2MH_{-1}L^{2-} \qquad 3.37$$

On rearrangement and substitution the concentration of chloride ions is given by

$$Cl^- = Na^+ + H^+ - 3L^{3-} - K_w/H^+ + M^{2+}(2 + P_3/H^+ - L^{3-}(P_1 + 2P_1P_2/H^+)) \qquad 3.38$$

Equations 3.35, 3.36 and 3.38 were solved using the least squares method. Given an approximate value for $P_2 = K^{ML}_{MH_{-1}L}$ the chloride concentration may be calculated (Ycalc) and then compared with the observed chloride concentration (Yobs) in order to get a better approximation for P_2. $P_1 = K^{M}_{ML}$ and is given the value of Table 3.27. $P_3 = K^{M}_{MOH}$ and in this analysis, a value of $\log P_3 = -9.49$ was used, being that appropriate for a background medium of 0.1 M KCl at 25°C (137).

3.5.2 The Value of $K^{ML}_{MH_{-1}L}$

The values of $K^{ML}_{MH_{-1}L}$ obtained from the five sets of titration data with near-equimolar nickel chloride and citric acid are reported in Table 3.30, along with the agreement factors. The mean and standard deviation of the log of the equilibrium constant are-9.13 and 0.08 respectively.

The fit of the model to the titration data is not good, the Rfactors all being greater than 2%. A systematic trend in the residuals was noticed, going from positive (Yobs > Ycalc) to negative (Yobs < Ycalc) as the pH increases. This indicates that the proposed model is not satisfactory.

It is possible that the 1:1 species may polymerize. Evidence for this has been reported for nickel-citric acid solutions (95). Polymeric complexes have also been reported for the iron(II) complex (95) and the copper(II) complex (47).

Until an improved model is developed, the value for the equilibrium constant $K^{ML}_{MH_{-1}L}$ cannot be regarded as accurate.

The same model was used to analyse the high ratio data of Section 3.4. However, in each case a negative value for the equilibrium constant was obtained.

It appears that the interpretation of the alkaline titration data is complex and therefore further work will be required to analyse these data.

Table 3.30 Values of $\log K^{ML}_{MH_{-1}L}$ Obtained From Titration Data of Near-Equimolar Nickel-Citric Acid Solutions

Solution Ratio	$\log K^{ML}_{MH_{-1}L}$	Rfactor %
1:0.84 [1]	-9.06	3.54
1:1 [1]	-9.15	2.26
1:1.2 [1]	-9.26	3.57
1:1D [2]	-9.14	2.89
1:1T [3]	-9.05	2.31

1. [Ni] = 1×10^{-3} M
2. [Ni] = 2×10^{-3} M
3. [Ni] = 3×10^{-3} M

4

Spectrophotometric Results

4.1 INTRODUCTION

The visible and near-infrared spectra of mixtures of nickel chloride and citric acid were recorded. Solutions were prepared with nickel chloride to citric acid ratios of 1:1 and 1:3 , and with total nickel concentrations of 0.002 and 0.004 $moll^{-1}$. The spectra of each solution were recorded over a range of pH's.

4.2 CHARACTERISTICS OF NICKEL-CITRATE SPECTRA

The nickel-aquo species $[Ni(H_2O)_6]^{2+}$ has three absorption bands in the visible-near-infrared region. A representative nickel-aquo spectrum is shown in Figure 4.1. The higher energy band is well defined with its absorption maximum at 398 nm. The middle band is split and has absorbance maximum at around 740 nm. The absorption band in the nir region is very broad and centered about 1200 nm.

When recording the spectra of mixtures of nickel chloride and citric acid, attention was directed toward the absorption bands in the visible region. The broadness of the nir band tends to mask any but the largest changes in its shape and position.

When comparing the spectra of various solutions, three features are of interest. The first is the difference in the position and shape of the absorption bands of the

Figure 4.1 Absorbance Spectrum of Nickel Chloride

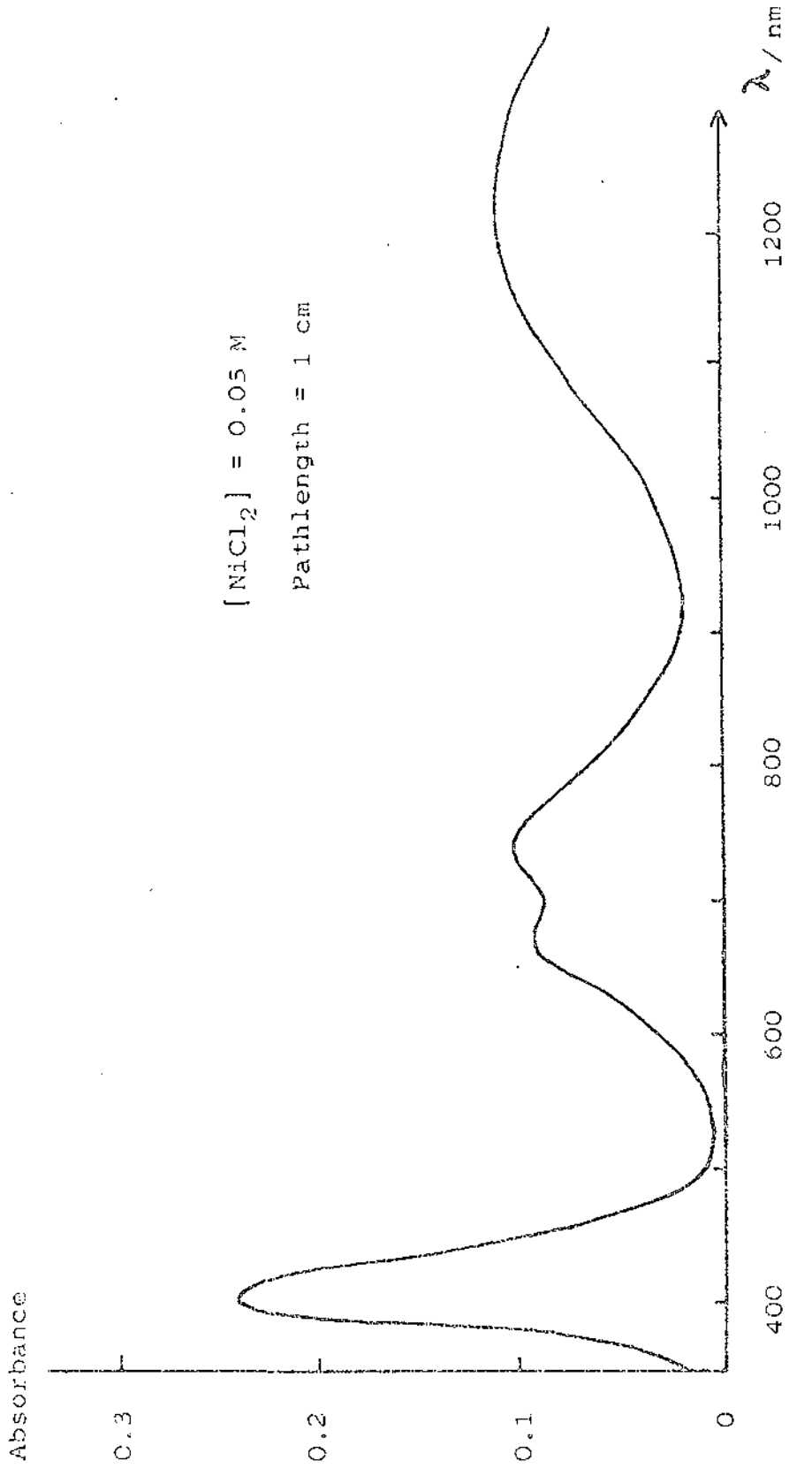

spectrum of a nickel-citric acid solution when compared with a nickel-aquo spectrum. The second feature is the change in the position and shape of the bands of a given solution as the pH changes. Thirdly, the spectra of solutions with different nickel to citric acid ratios may be compared.

4.2.1 The Spectra of Equimolar Nickel and Citric Acid Solutions at Various pH's

The spectrum of a nickel-citric acid mixture at pH 3 is similar to that of the nickel-aquo species, with only slightly enhanced absorbance and little shift in the positions of the maxima. This similarity is to be expected, since the distribution plots of Chapter 3 show that, at pH 3 , most of the metal is in the uncomplexed aquo form (see Figures 3.3 and 3.4). However, as the pH is increased, the absorbance at all wavelengths is enhanced, and the wavelength of maximum absorbance, λ_{max}, for each band changes.

Figure 4.2 shows how the shape of the absorption band at approximately 400 nm changes as the pH is varied. As the pH is increased from pH 2.5 to pH 4, the wavelength of maximum absorbance is decreased. In the case of a 1:1 solution, the wavelength of maximum absorbance shifts from 398 to 393 nm as the pH increases from 3 to 4. The wavelength of maximum absorbance is invariant as the pH increases from 5 to 8. As the pH is further increased into the alkaline region, the wavelength of maximum absorbance sharply increases. These changes are shown in Figure 4.3, which records the wavelength of maximum absorbance as the pH is varied.

The shift in the wavelength of maximum absorbance of the band at approximately 700 nm is characterized by changes in the asymmetry of the band (see Figure 4.4). Figure 4.5 shows this shift in wavelength of maximum absorbance as the pH changes. There is a dramatic decrease in the wavelength of maximum absorbance as the pH increases from 2.5 to 4 (740 to 680 nm). In the pH range 4 to 8, there is no change in the wavelength. As the pH increases above pH 8, the absorption maximum shifts to slightly longer wavelengths.

Figure 4.6 shows the changes in the absorbance at λ_{max}

Figure 4.2 Absorbance Spectra for the 400 nm Band of Nickel-Citric Acid Solutions as the pH is Varied

[Ni] = 0.004 M
Pathlength = 1 cm
Ni:Cit = 1:1

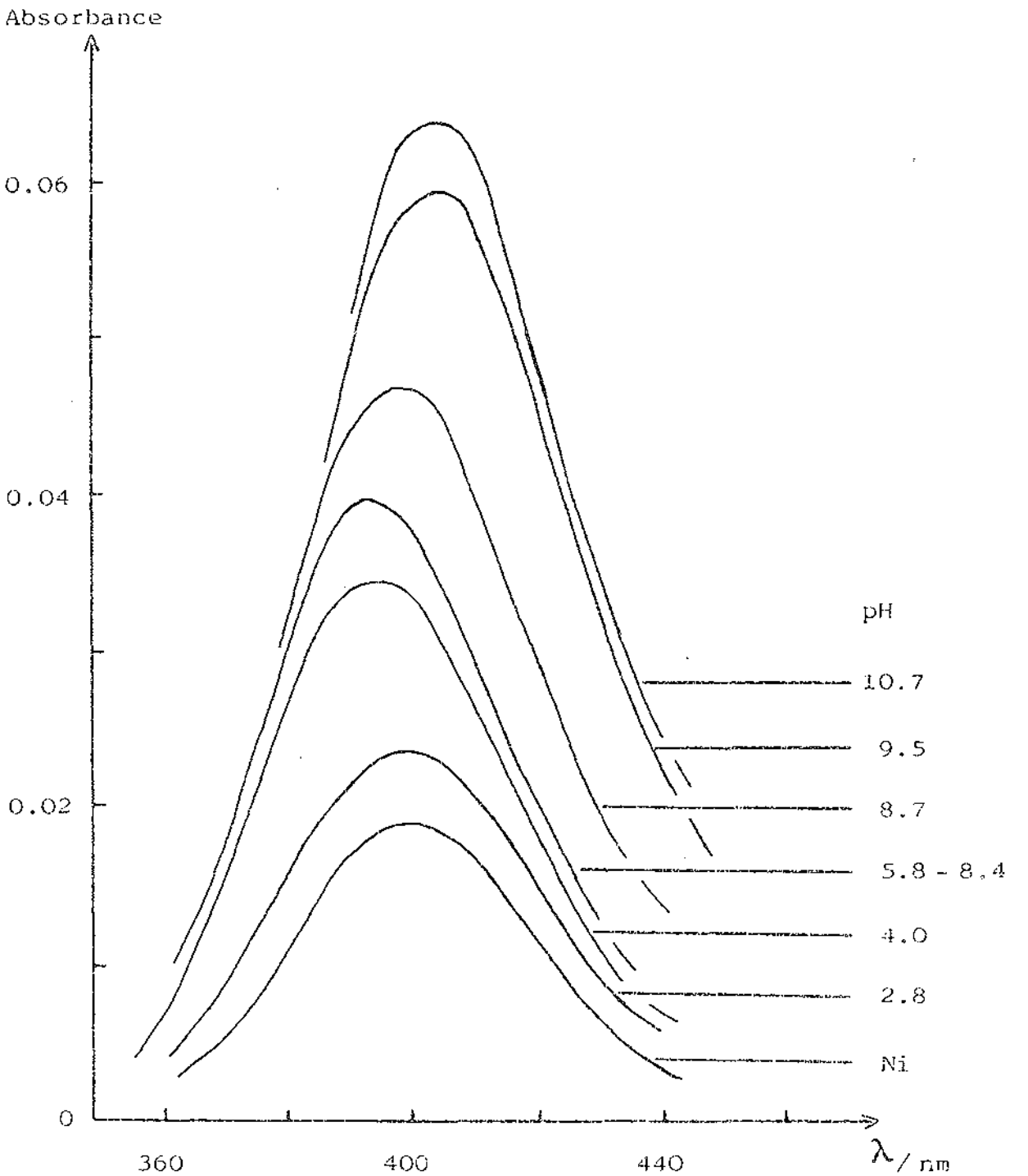

Figure 4.3 Wavelength of Maximum Absorbance for the 400 nm Band of Nickel-Citric Acid Solutions as a Function of pH

Nickel Conc ⊙ 0.002 M
o 0.004 M

Ni:Cit ratio 1:1

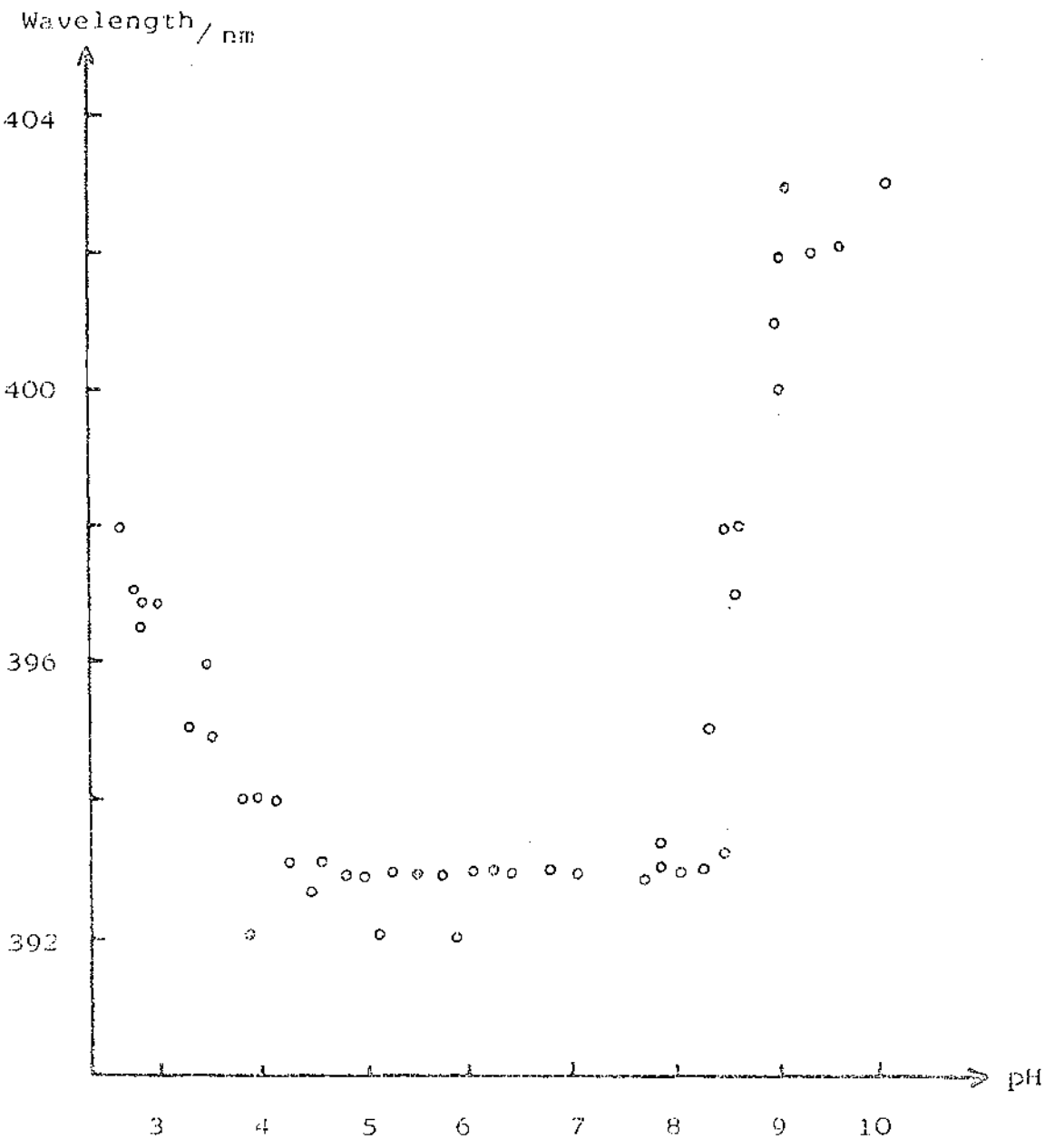

Figure 4.4 Absorbance Spectra for the 700 nm Band of the Nickel-Citric Acid Solutions as the pH is Varied

[Ni] = 0.004 M
Pathlength = 1 cm
Ni:Cit = 1:1

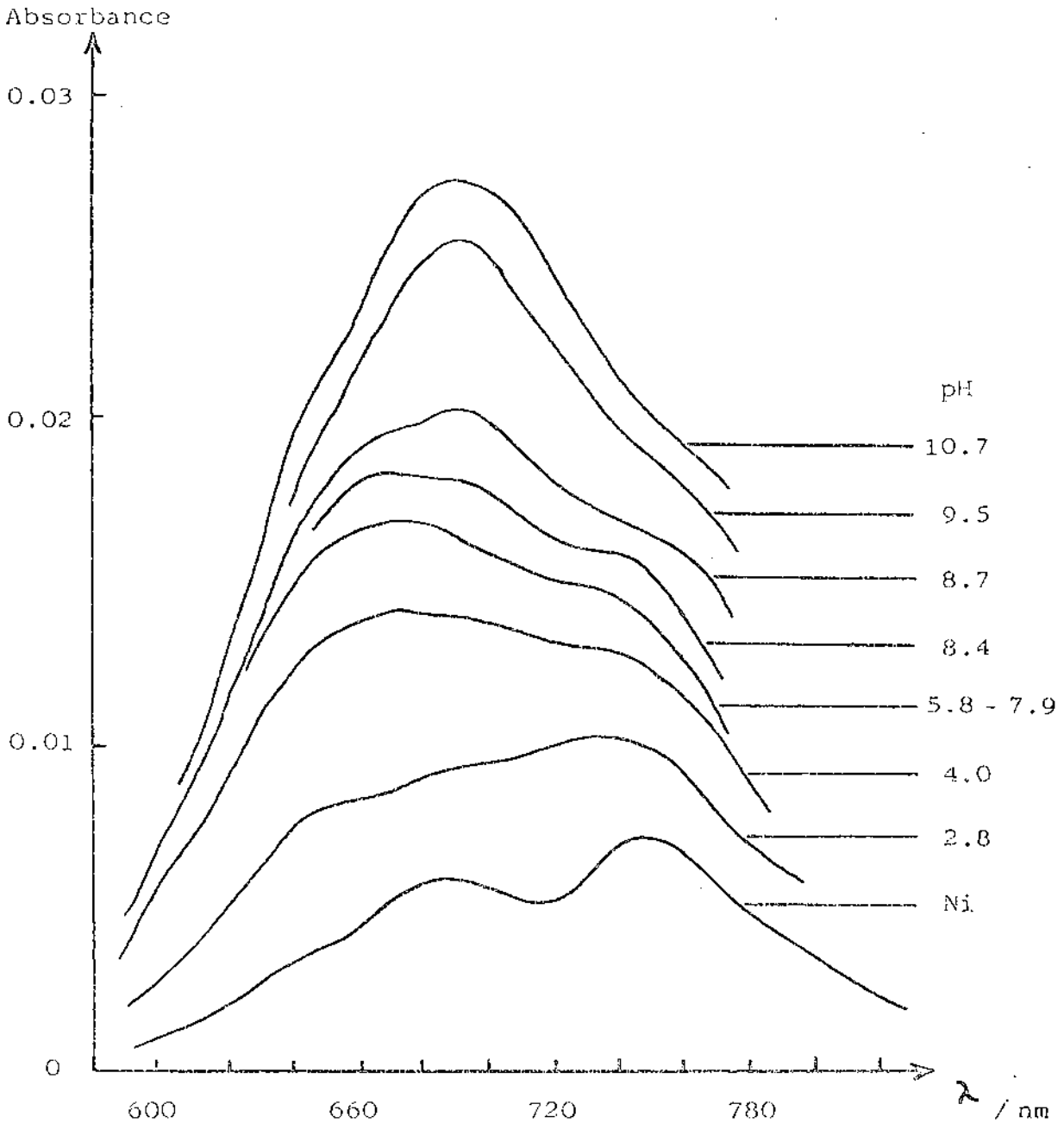

Figure 4.5 Wavelength of Maximum Absorbance for the 700 nm Band of Nickel-Citric Acid Solutions as a Function of pH

Ni conc o 0.002 M

o 0.004 M

Ni:Cit ratio 1:1

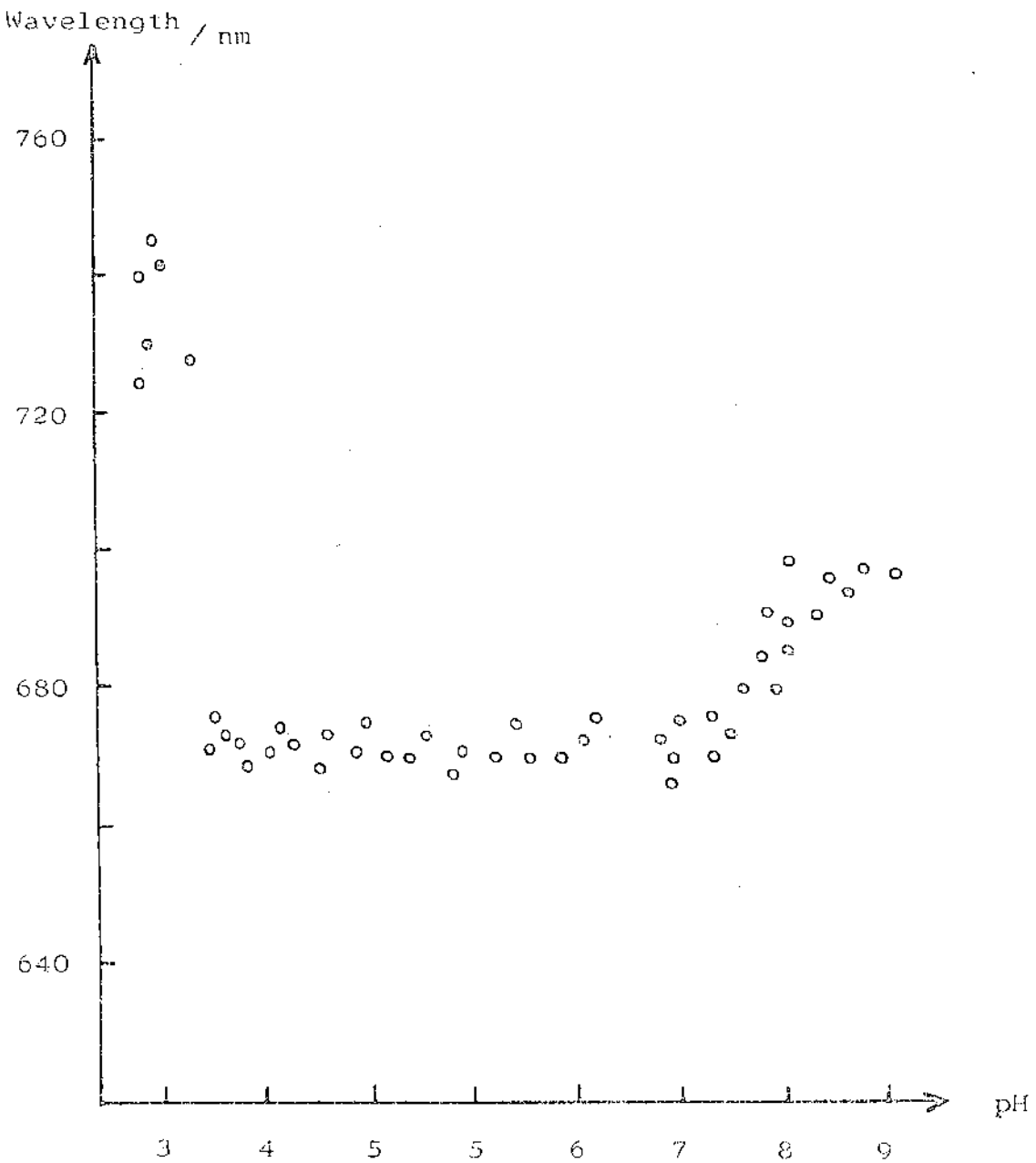

Figure 4.6 Absorbance of the 400 nm Band of Nickel-Citric Acid Solutions as a Function of pH

Ni conc 0.004 M

Ni:Cit ratio 1:1

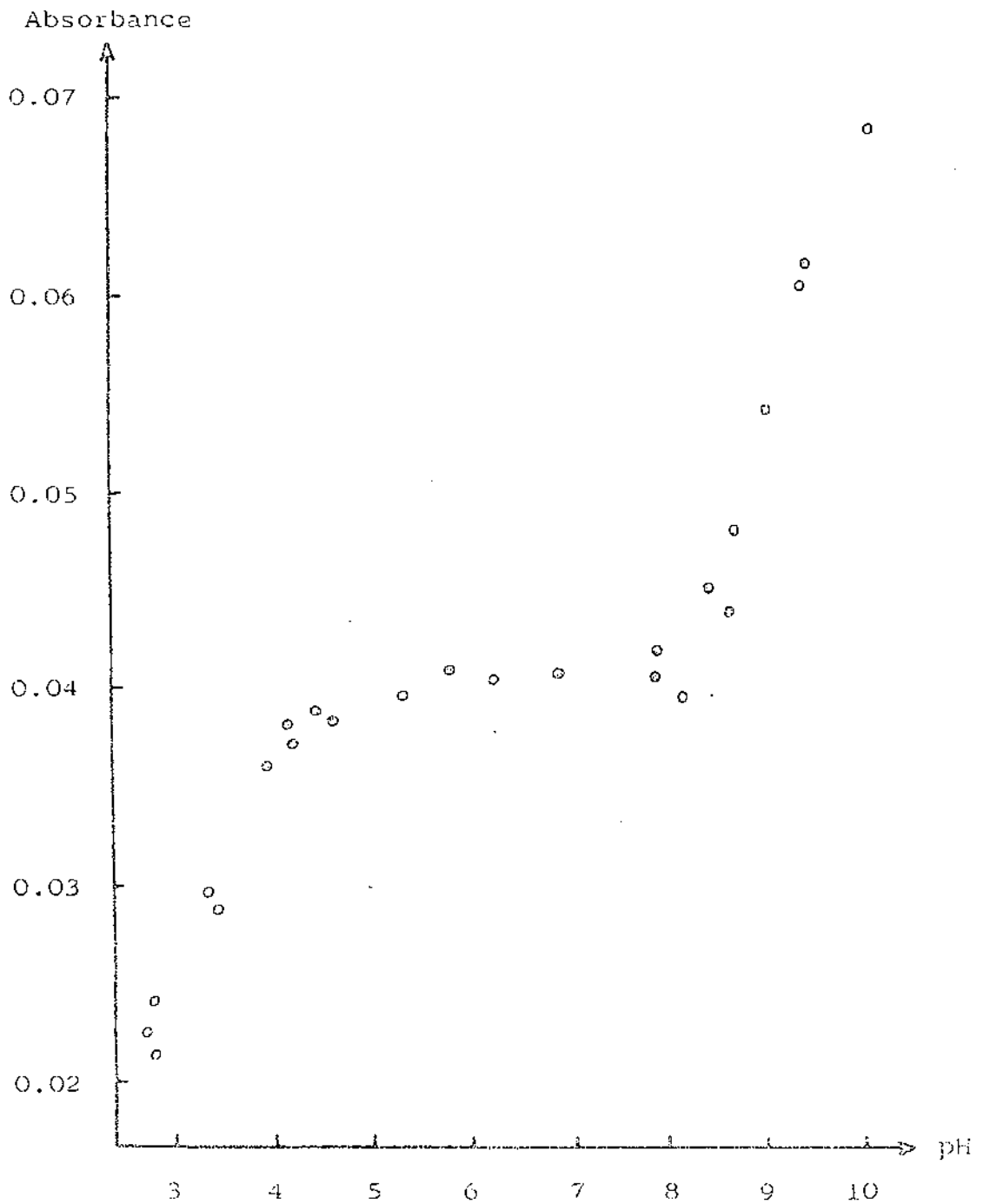

for the 400 nm band as the pH increases. The diagram records results from three experiments carried out at different times. The data from these experiments agrees well. The absorbance of this band increases as the pH increases from pH 2.5 to 5; is constant through the range 5 to 8; and increases dramatically as the solution becomes alkaline. The shape of the absorbance - pH plot for the 700 nm band is almost identical to that of the 400 nm band.

The shape of the absorbance -pH plot may be explained in terms of the equilibria involved. Reference to Figure 3.3 shows that in the case of a 1:1T solution, as the pH increases the concentration of complexed metal is increasing. By about pH 5, complex formation is near-complete and hence, the absorbance is constant until alkaline pH's, when new complexes, which must have a greater extinction than those in the acidic pH range, are formed (see Section 3.5).

Qualitatively similar results have been observed in earlier studies (39, 98,99). In these works, the pH was controlled by using a large excess of acetate and borax buffers. As acetate will complex with nickel ions (53), the nickel-citric acid equilibrium will be affected. The absorbance was measured at only a few selected wavelengths and, as shown in Figures 4.3 and 4.5, the wavelength of maximum absorbance is by no means fixed as the pH is varied. In addition, nickel concentrations much higher than those used in this study were used.

4.2.2 Effects of Excess Citric Acid on the Absorption Spectra of Nickel-Citric Acid Solutions

The position and shape of the absorption bands in the spectra of solutions where the nickel to citric acid ratios are 1:1 and 1:3 are not the same. Figure 4.7 records the spectra of a nickel chloride solution, and nickel-citric acid solutions with ratios 1:1, 1:2 and 1:3, and total metal concentration of 0.05 M. The pH of the complex solutions is near neutral. The graph shows that, as the concentration of citric acid exceeds total nickel, the absorbance of the 400 nm band decreases, and there are changes in the shape of the 700 nm band. However, for all

Figure 4.7 Absorbance Spectra of Nickel-Citric Acid Solutions of Varying Ratio

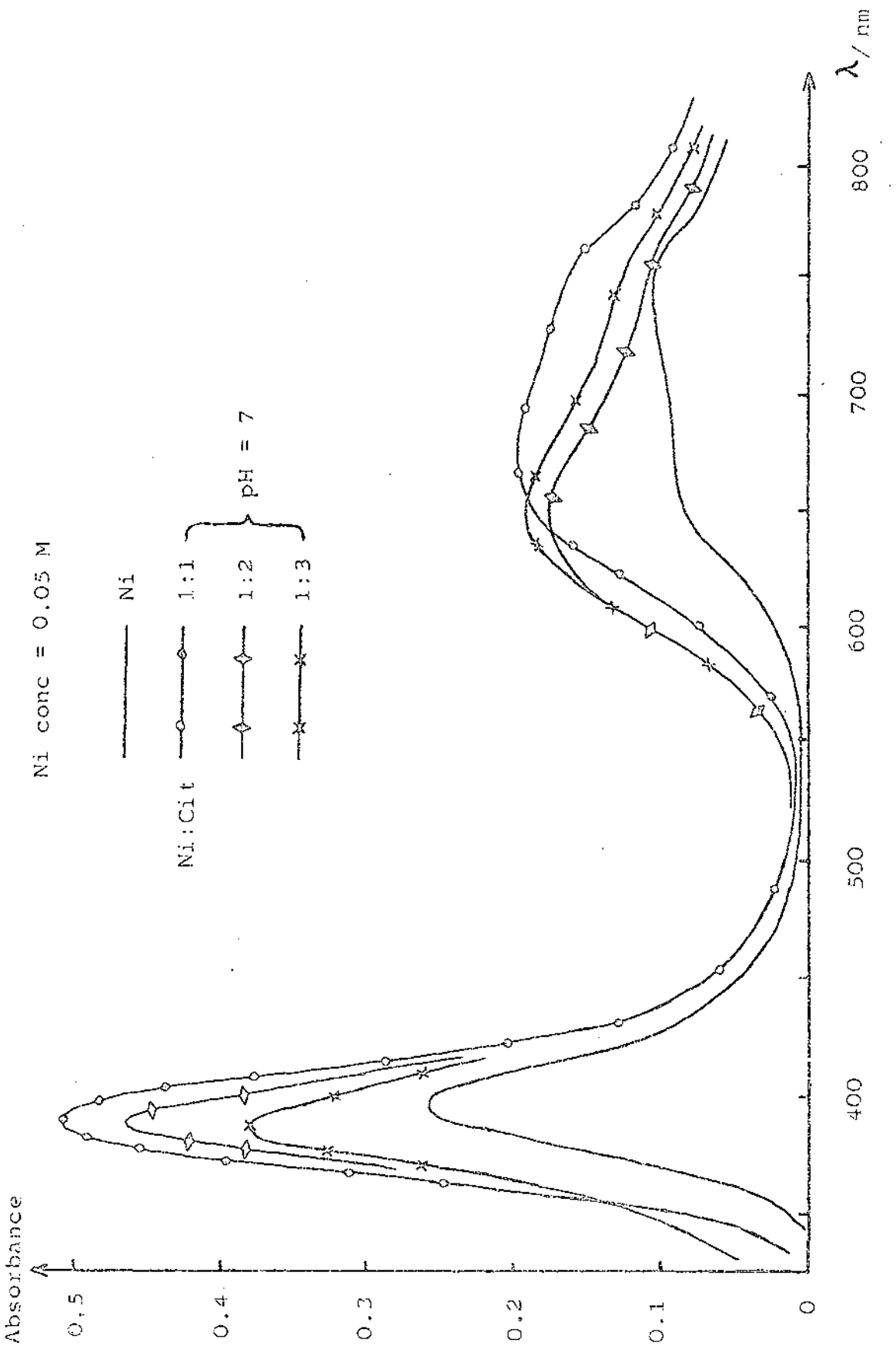

complex solutions, the absorbance at both bands is greater than that of nickel alone.

The shifts in the wavelength of maximum absorption at both bands for the solutions discussed above were such that changes in the colour of the solution when the nickel-citric acid ratio was increased from 1:1 to 1:3 were noticeable to the eye.

Figure 4.8 shows how the absorbance of a 1:1 and a 1:3 solution differ at various pH's for the 400 nm band. At any pH between 2.5 and 4, the absorbance of a 1:3 solution is greater than that of a 1:1 solution. In the pH range 5 to 9 where the absorbance is constant, the "plateau" for the 1:3 solution is below that of the 1:1 solution. In the alkaline region, both solutions show a dramatic increase in absorbance as the pH increases, but at any given pH, the absorbance of the 1:3 solution is less than the 1:1 solution. The changes in absorbance for the 700 nm band were similar, though smaller in magnitude, to those for the 400 nm band.

Reference to the distribution curves for a 1:1 and a 1:3 solution (Figures 3.4 and 3.8), provides a reason for the differences between the spectra of the 1:1 and 1:3 solutions in the acid pH range. Complex formation is greater at low pH's in a 1:3 solution than it is in a 1:1 solution; hence the greater absorbance at any given pH in a 1:3 solution.

The formation of ML_2^{4-} becomes significant at about pH 5 in the 1:3 solution, and it is at this pH that the absorbance of the 1:3 solution begins to decrease when compared to the 1:1 solution, where ML_2^{4-} is not found in significant amounts.

The wavelength of maximum absorbance at any given pH shifts to higher energies if citric acid is in excess. This is shown for the 700 nm band in Figure 4.9. There is a distinct shift of 10-15 nm towards shorter wavelengths when nickel to citric acid ratios change from 1:1 to 1:3. A possible shift of 2 to 3 nm in the case of the band at 400 nm is somewhat difficult to define, since the uncertainty in reading the wavelength of the spectra is of that order (1-2 nm).

Figure 4.8 Absorbance at 400 nm Band of Nickel-Citric Acid Solutions With Ratio 1:1 and 1:3 as a Function of pH

Ni conc 0.004 M

Ni:Cit ratio o 1:1

× 1:3

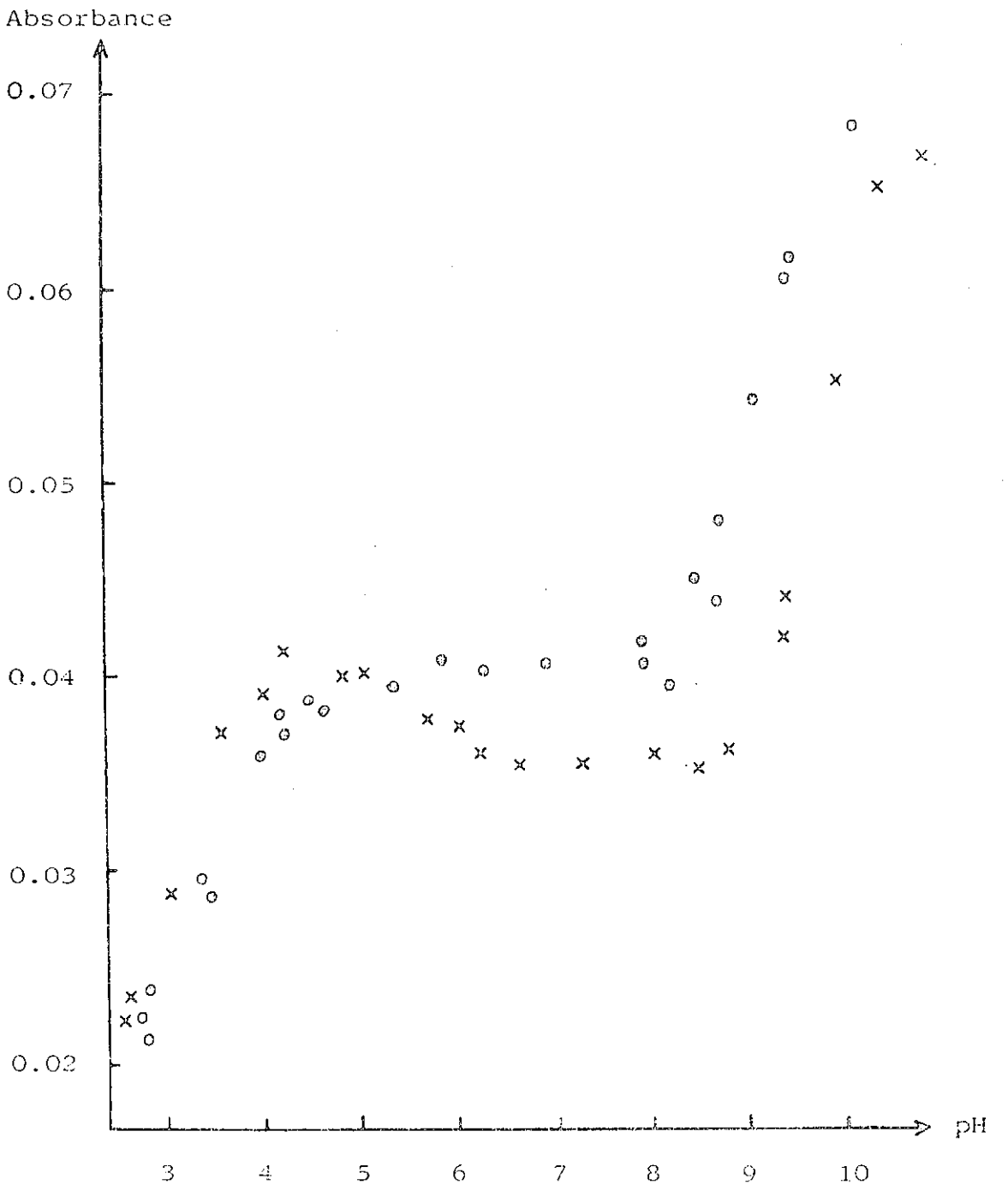

Figure 4.9 Wavelength of Maximum Absorbance for the 700 nm Band of Nickel-Citric Acid Solutions With Ratio 1:1 and 1:3 as a Function of pH

Ni conc 0.004 M

Ni:Cit ratio o 1:1

× 1:3

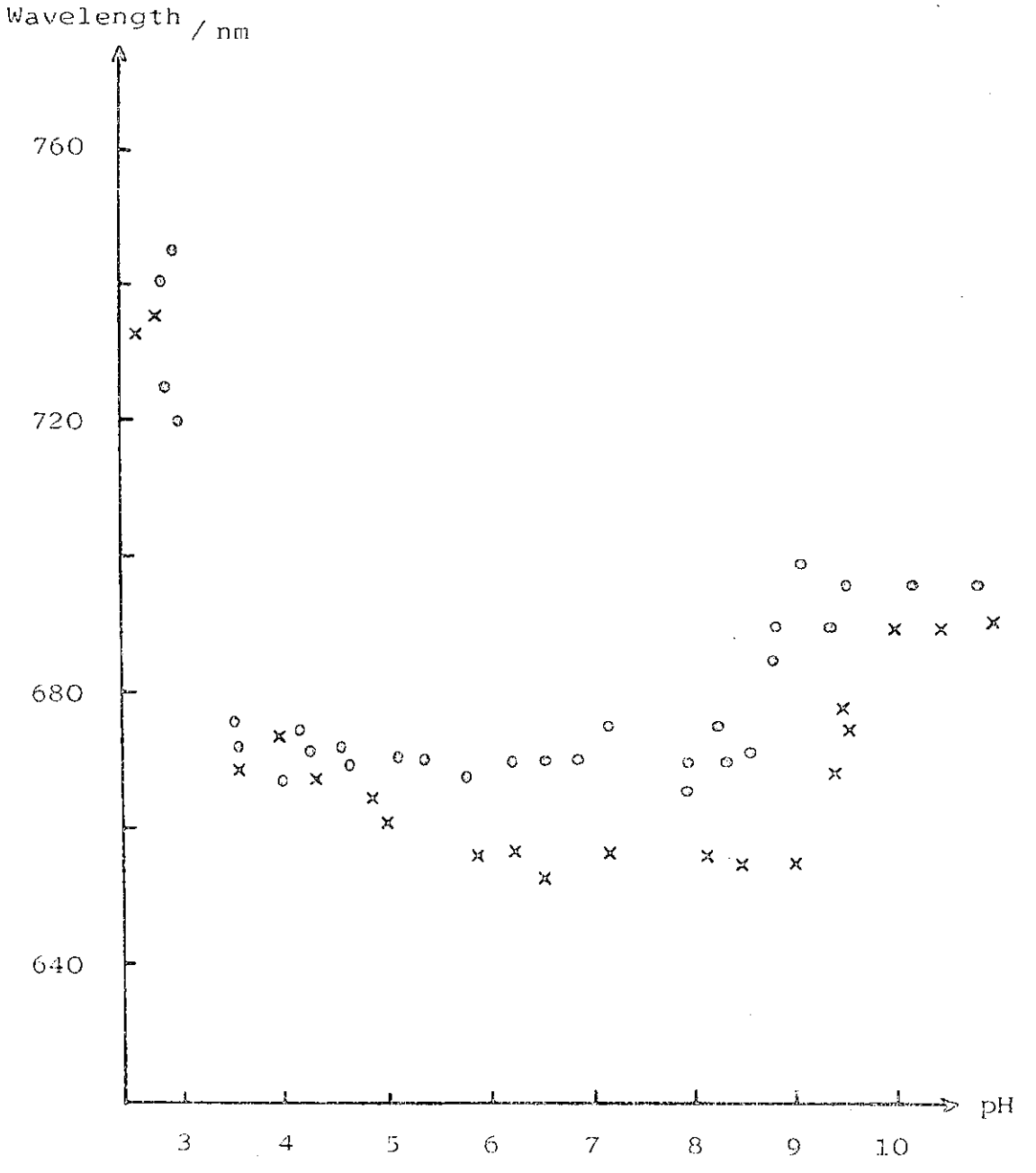

Similar changes in the absorbance when excess citric acid is present have been reported for solutions where the metal concentration was higher and buffers were used to control the pH (39). This previous study measured the absorbance at selected fixed wavelengths (400 nm and 700 nm), and hence, did not take account of the shifts in the wavelength of maximum absorbance.

Summary

The magnitude of the absorbance and the λ_{max} values for nickel-citric acid solutions are dependent upon the pH of the solution.

When excess citric acid is present, the spectra of nickel chloride and citric acid solutions are not the same as when equimolar amounts of nickel and citric acid are present. The difference in the spectra is highlighted by: (i) a smaller absorbance for the excess citric acid solutions in the pH range 5 to 9; and (ii) shifts of the absorption bands to shorter wavelengths for the solutions containing excess citric acid.

5

Discussion

The results of this investigation have been presented in the previous two chapters. The aim of the investigation was to undertake a more thorough study of the equilibria between nickel ions and citric acid over a wide range of pH. However, time did not permit the complete analysis of the alkaline titration data.

5.1 THE STRUCTURE OF CITRIC ACID

Citric acid has three carboxylic acid groups and one hydroxy group (as shown in Figure 5.1).

Figure 5.1 Structure of Citric Acid

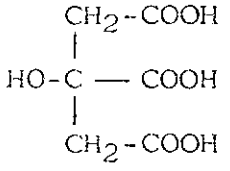

As such, citric acid has four potential donor groups in complex formation. The carboxylic acid groups can be ionized, and the resulting carboxylate groups may be coordinated. In this case, the negative charge is delocalized over the group:

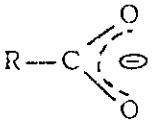

The hydroxy group may also be coordinated, in which case the pK for the removal of the hydroxy proton would be lowered, and hence it is possible for the coordination of $-O^-$

The large number of donor groups makes citric acid a multidentate ligand capable of forming chelate complexes. Each of the complexes characterized during this study, ML^-, MHL, MH_2L^+ and ML_2^{4-}, may be a chelate complex as a result of a combination of the above-mentioned types of coordinate bonds. In addition, the multidentate feature of the ligand means that different complexes with the same stoichiometry may be formed. These will depend on which combination of donor groups is involved.

5.2 THE STABILITY AND STRUCTURE OF NICKEL-CITRATE COMPLEXES

Stability constants are reported in Table 5.1 for the formation of nickel complexes with the following carboxylic acids: citric, tricarballylic, malic, succinic, glutaric and acetic acids. The values for citric acid are the average of those of Table 3.27. The structure and systematic name of each acid is given in Table 5.2.

5.2.1 Stability and Structure of ML^-

In the pH range 4-7, the complex ML^- dominates. In the complex species, the proton will have been lost from each of the three carboxylate groups, hence the ligand carries a 3- charge. In this pH range, the hydroxy proton is intact. Therefore, the ligand is of the form

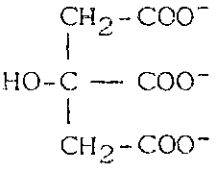

Evidence for the formation of chelate complexes can be drawn from the stability of the complex ML^- ($\log K^M_{ML} = 5.5$). If only one carboxylate group was coordinated, then a formation constant similar in magnitude to that for the nickel-acetate complex, ML would be expected. Reference to Table 5.1 shows that the nickel-citrate complex is several orders of magnitude more stable than the nickel-acetate complex.

Using models it is apparent that triionized citric acid can coordinate in several ways, three of which are feasible. One of these involves coordination through the hydroxy group and two carboxylate groups, the central group and one terminal group. The second involves the two terminal carboxylate groups and the hydroxy group, while the third involves coordination through all three carboxylate groups. Sketches of these three structures are shown in Figures 5.2, 5.3 and 5.4 respectively.

Table 5.1 Formation Constants of Complexes of Nickel With Several Carboxylic Acids

Acid		Log of Equilibrium Constant K^{M}_{ML}	K^{M}_{MHL}	$K^{M}_{MH_2L}$		Reference
Citric	H_3L	5.50	3.36	1.5	(B_2 = 7.9)	this work
Tricarballylic	H_3L	2.7	1.6	1.0		35
Malic	H_2L	3.3	1.4			101
Succinic	H_2L	1.6				101
Glutaric	H_2L	1.6				102
Acetic	HL	1.65	(B_2 = 2.96)			104

Table 5.2 Structure and Systematic Names of Several Carboxylic Acids

Common Name	Structure	Systematic Name [103]
Citric	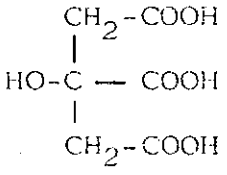	2-hydroxy 1,2,3-propane-tricarboxylic acid
Tricarballylic	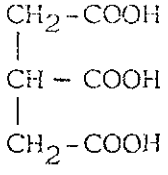	1,2,3-propanetricarboxylic acid
Malic	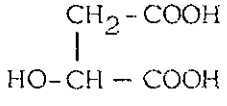	hydroxy- ethanedicarboxylic acid
Succinic	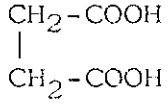	1,2-ethanedicarboxylic acid
Glutaric	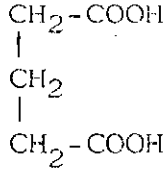	1,3-propanedicarboxylic acid
Acetic	CH_3-COOH	ethanoic acid

Figure 5.2 Possible Structure of the Complex ML^-

A: Coordination hydroxy

central and terminal carboxylate

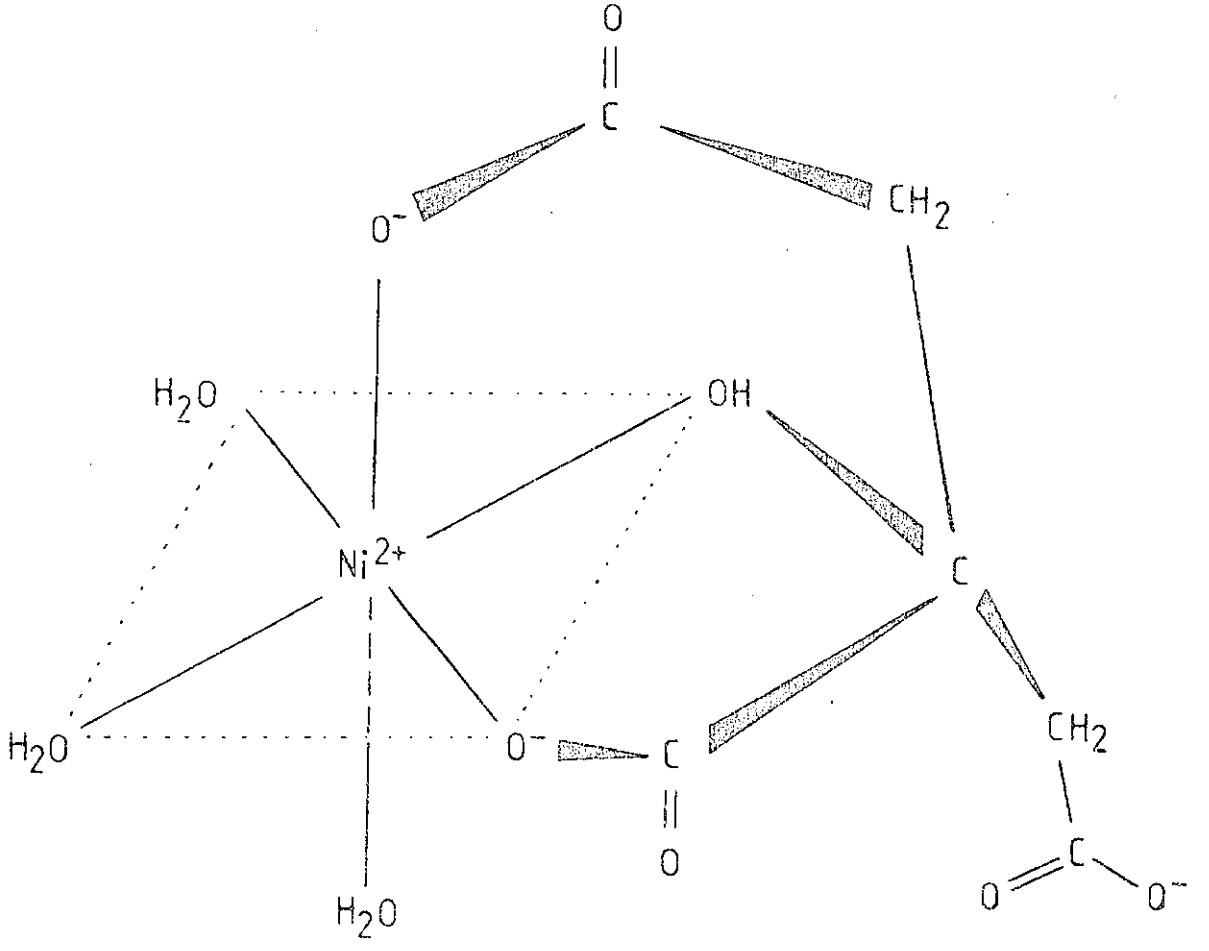

Figure 5.3 Possible Structure for the Complex ML^-

B: Coordination hydroxy

two terminal carboxylates

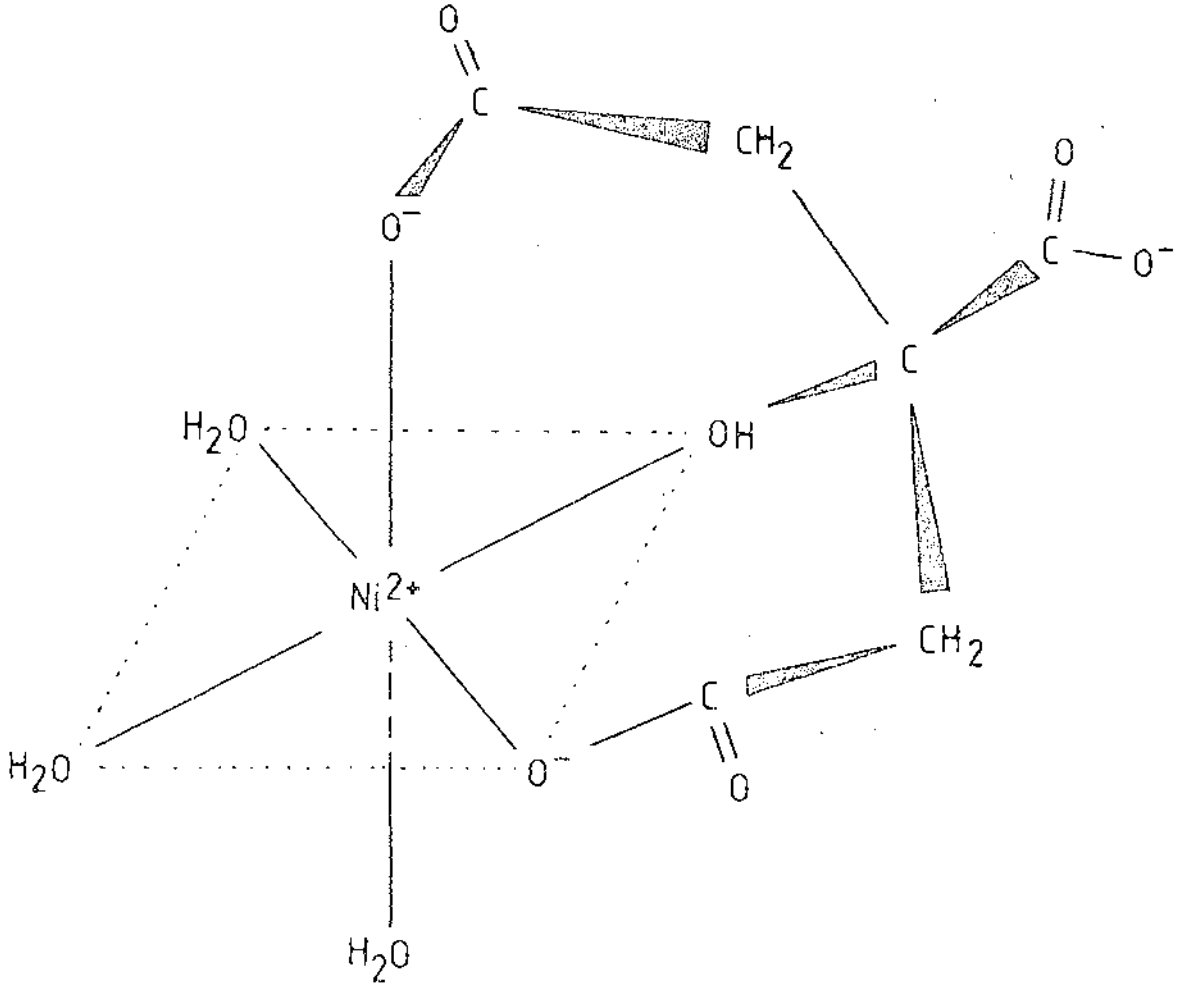

Figure 5.4 Possible Structure for the Complex ML^-

C: Coordination three carboxylates

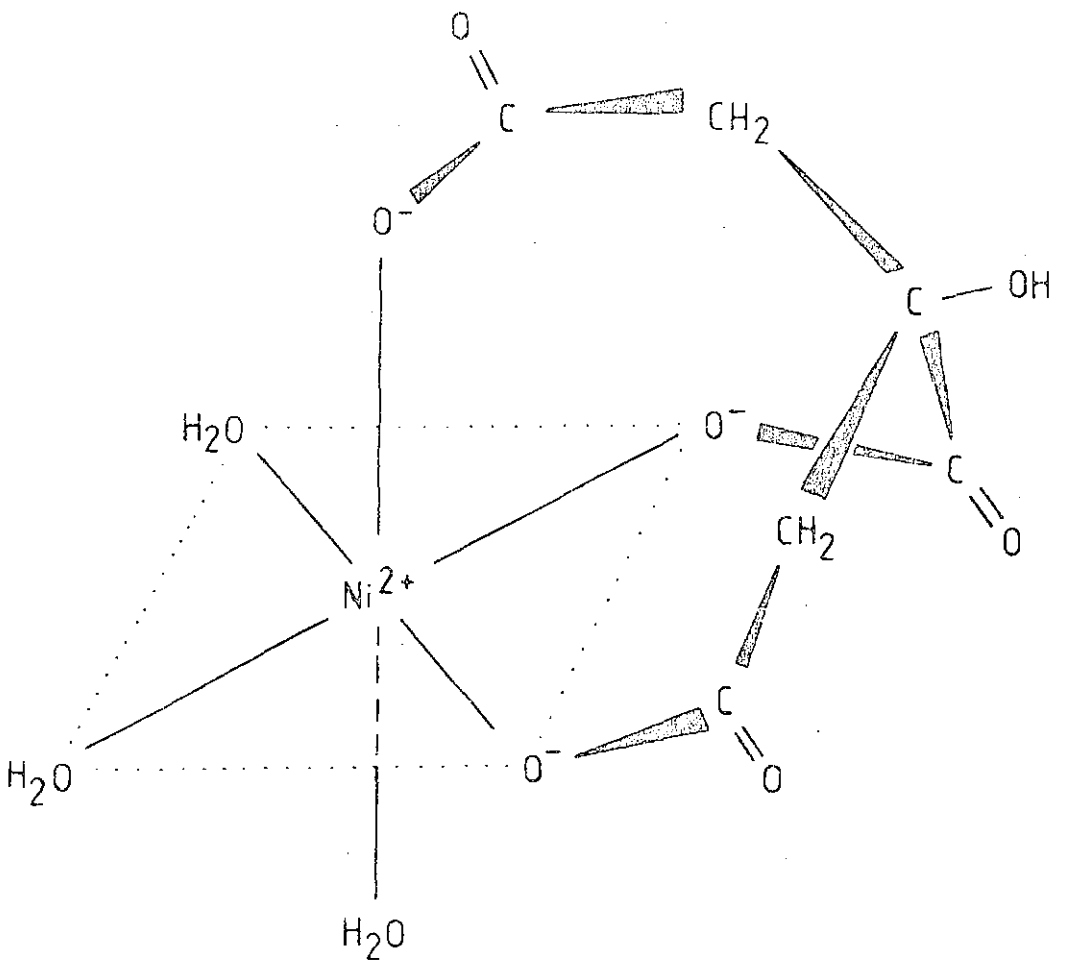

The question arises as to which of these structures is the most likely form of the complex ML^-.

Citric acid and tricarballylic acid each have three carboxylic acid groups, but citric acid has a hydroxy group attached to the central carbon atom, while tricarballylic acid has a proton in this position (see Table 5.2). Reference to Table 5.1 shows that the nickel-citrate complex ML^- is at least two orders of magnitude more stable than the corresponding tricarballylate complex, in spite of tricarballylate being a stronger base than citrate (35). This provides some evidence for implicating the hydroxy group of citric acid in the coordination of L^{3-} to the nickel (II) ion. A similar comparison is also noticed for malic acid (having a hydroxy group) and succinic acid (see Tables 5.1 and 5.2).

It is well known that the stability of a chelate complex is related to the size of, and the number of chelate rings formed (113,114,115,116). In general, five-membered rings tend to be the most stable, with the stability decreasing as the ring size becomes larger (114). The stability of complexes also increases with the number of chelate rings (113). Reference to Figures 5.2, 5.3 and 5.4 shows that the three complexes each have two chelate rings, but the rings are not all of the same size. The complex with the central and terminal carboxylate groups coordinated along with the hydroxy group has one five-membered ring and one six-membered ring. The complex with the hydroxy group and the two terminal carboxylates coordinated has two six-membered rings. The tri-carboxlyate coordinated complex has two seven-membered rings.

On the basis of ring size effects, the complex with the hydroxy group, the central and terminal carboxylate groups coordinated would be the most favoured.

Coordination of the hydroxy group in nickel-citrate complexes has been implicated previously (99,117).

Supportive evidence for the coordination of the hydroxy group can be drawn from an x-ray structural study of iron(II)-citrate complexes (94). This study character-

ized a tridentate chelate of triionized citrate and iron(II) in which the protonated hydroxy group, the central and one terminal carboxylate group are coordinated to the iron(II) ion. The third carboxylate group was involved in a bridging between iron(II) ions, completing a polymeric structure.

It should be noted that using the techniques in this work there is no way to determine which, (or what combination), of the three proposed structures dominates in the solution. The formation constant for ML^- is a "macroconstant", comprising the "microconstants" for each contributing species for ML^-.

5.2.2 Stability and Structure of MHL

This is the complex where one of the three carboxylate groups is protonated. Comparisons with the MHL complexes of tricarballylic, malic, succinic and glutaric acids can provide information regarding the likely structure of the nickel-citrate MHL complex (see Tables 5.1 and 5.2).

A comparison of the stability of the citrate complex MHL ($\log K^M_{MHL} = 3.36$) and the nickel-tricarballylate complex ($\log K^M_{MHL} = 1.6$) indicates that the hydroxy group of citric acid is again involved in coordination.

The citrate complex MHL is at least an order of magnitude more stable than the ML complexes of succinic and glutaric acids (see Table 5.1). All three complexes have two ionized carboxylate groups, and the fact that the citrate complex is the more stable lends further support to the involvement of the hydroxy group in coordination. If the hydroxy group was not involved, one might expect the stability of the citrate complex to be similar to that of the succinate and glutarate complexes (having regard to the basicity of each ligand).

Coordination of the two ionized carboxylate groups of MHL may take place in two ways. Firstly, if the central carboxylate and one terminal group are coordinated along with the hydroxy group, then there are two chelate rings, one five-membered, the other six-membered. Secondly, the coordination of the two terminal carboxylate groups

along with the hydroxy group results in two six-membered rings. These two complexes have the same coordination as those of Figures 5.2 and 5.3 respectively, but the free carboxylate groups are protonated.

The stabilities of the nickel-citrate complex, MHL, and the malate complex, ML, are similar. This similarity in stability suggests that the mode of coordination may be similar for the two ligands. As noted earlier, and in other works (35,101), coordination of malate is thought to involve the hydroxy group. The likely mode of coordination in the protonated citrate complex is with the central, and one terminal carboxylate group coordinated along with the hydroxy group.

Coordination of the two terminal carboxylate groups along with the hydroxy group of citric acid would result in two six-membered rings, slightly less favourable than the complex with the central carboxylate group coordinated. Comparison of the citrate system with that of hydroxyglutaric acid would provide evidence as to whether or not this mode of coordination is likely. Unfortunately, no data were available on complexes of nickel and hydroxyglutaric acid.

However, it is considered that the structure with the central and terminal carboxylate groups and the hydroxy group is the most favoured structure for the complex MHL.

5.2.3 Stability and Structure of MH_2L^+

This complex has only one coordinated carboxylate group. It will be noted that the stability of this complex is similar to that of the corresponding malate complex, MHL (having the hydroxy group and one carboxylate group, see Table 5.1 and 5.2), and of greater stability than the corresponding tricarballylate complex.

These comparisons suggest that the hydroxy group is coordinated in the citrate complex. On the basis of ring size effects, the central carboxylate group is probably coordinated. This would result in a five-membered ring, whereas coordination of a terminal carboxylate group along with the hydroxy group results in a six-membered ring and would be of lower stability.

5.2.4 Stability and Structure ML_2^{4-}

No previous equilibrium constants have been reported for the formation of the bis nickel-citrate complex, ML_2^{4-}. Possible reasons for this have been discussed in Section 1.2. The stepwise formation constants are $\log K^{M}_{ML} = 5.5$ and $\log K^{ML}_{ML_2} = 2.4$ As is usually found in complex formation (118, 119, 120), $K^{ML}_{ML_2}$ is less than K^{M}_{ML}.

Comparison of the stepwise formation constant for ML_2^{4-} ($\log K^{ML}_{ML_2} = 2.4$) with the corresponding copper-citrate value ($\log K^{CuL}_{CuL_2} = 2.2$ (33)) shows that the value for nickel is of the expected magnitude, but is in apparent conflict with the Irving-Williams Order (121), which predicts that copper complexes are more stable than nickel complexes. However, octahedral copper(II) complexes which have an electronic configuration $3d^9$ are subject to Jahn-Teller distortion (122, 123). This would account for the lower stability of the bis species for copper. This apparent reversal of the order of stability of nickel and copper complexes has also been observed for other complexes e.g. tris-ethylenediamine complexes of copper and nickel (124).

Reference to Figures 5.2, 5.3 and 5.4 shows that any of the three structures are able to accept a second ligand. In each case, the first ligand occupies three coordinate sites of the octahedron. A possible structure for one of the feasible bis structures is given in Figure 5.5. It will be noted that this structure has two uncoordinated carboxylate groups. There would appear to be no reason why one or both of these groups could not be protonated.

However, analysis of titration data failed to characterize a complex where both $M(HL)_2^{2-}$, or only one, MHL_2^{3-}, of these carboxylate groups was protonated.

Figure 5.5 One Possible Structure for the Bis Complex ML_2^{4-}

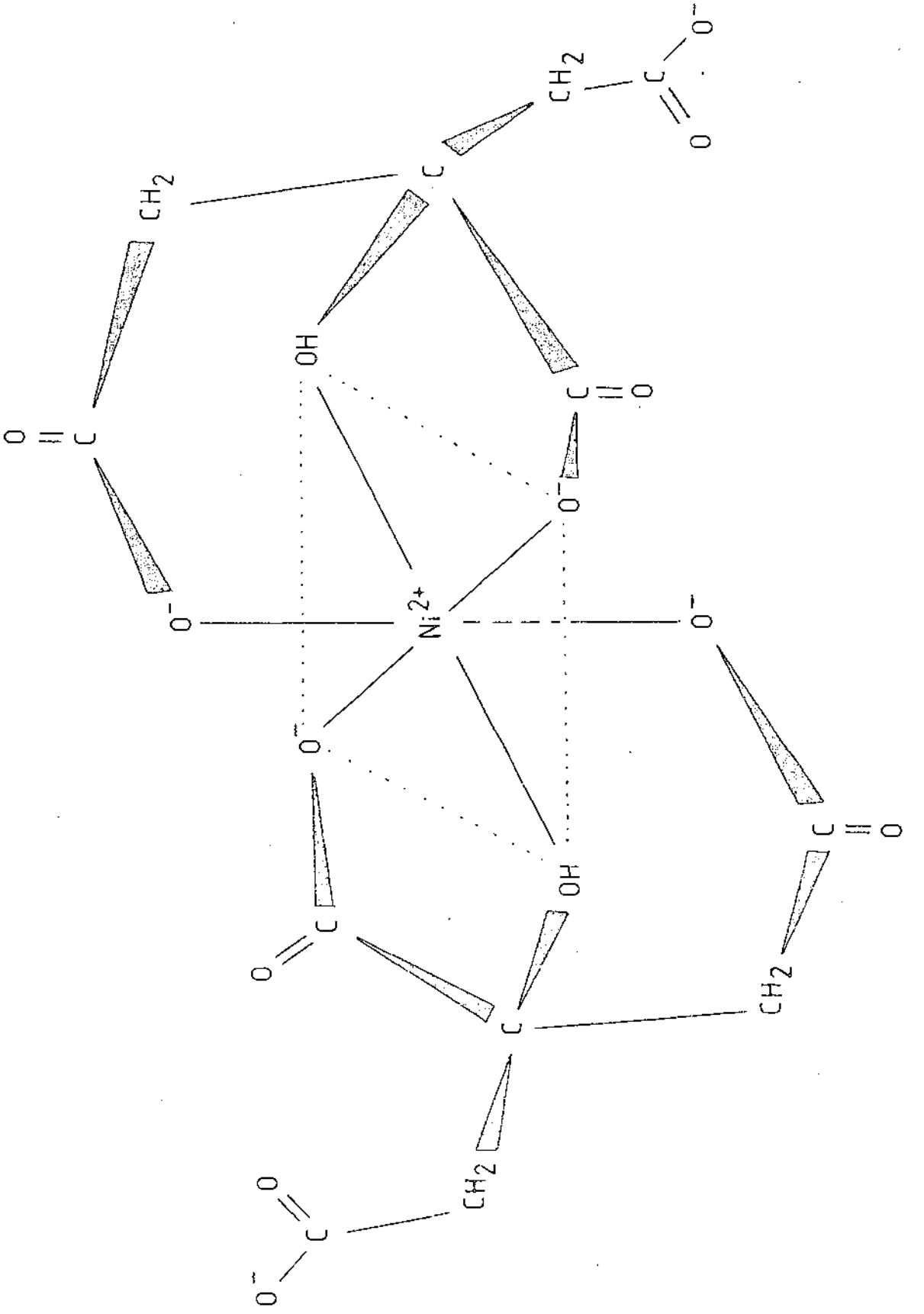

5.3 THE SPECTRA OF NICKEL-CITRIC ACID SOLUTIONS

5.3.1 Band Assignments

The spectra of the nickel-citric acid mixtures are typical of octahedrally coordinated nickel. There are three absorption bands in the visible-nir region of the spectrum at wavelengths of 1100, 700 and 400 nm. Using the energy level diagram for the d^8 configuration, these bands are assigned to the three spin allowed transitions, $^3A_{2g} \rightarrow {}^3T_{2g}$, $^3A_{2g} \rightarrow {}^3T_{1g}(F)$ and $^3A_{2g} \rightarrow {}^3T_{1g}(P)$(125). These transitions can be seen on Figure 5.6 (126).

Figures 4.1 and 4.7 show that the band at approximately 700 nm is split in the case of the nickel-aquo spectra. This is due to spin orbit coupling, which mixes the $^3T_{1g}(F)$ and ^1E_g states which are very close in energy at the ligand field energy, (Δ_o), given by $6H_2O$, approximately 900 cm^{-1} (125, 127). This can be seen on the energy diagram (Figure 5.7) where the $\Delta_o(H_2O)$ is marked.

In the presence of citric acid, the band at about 700 nm becomes more symmetrical (see Figures 4.4 and 4.7). This is indicative of coordination of ligands of greater ligand field strength then H_2O. It is evident from Figure 5.7 that as Δ_o increases, the energy states $^3T_{1g}(F)$ and ^1E_g separate and the mixing of these two states becomes less likely.

5.3.2 Calculation of the Extinction Coefficients and the Ligand Field Strength of L^{3-} in the Complex ML^-

The absorbance of several solutions with equimolar nickel chloride and citric acid was measured at about pH 7. This ensured that, to a first approximation, the only species present is ML^- (see Figure 3.3).

The extinction coefficient, ϵ, is a quantity related to the absorbance and concentration of the absorbing species. The relationship is quantitatively described by the Beer-Lambert Law, $A = \epsilon bc$, where A is the absorbance, c the concentration, and b the pathlength of the incident radiation through the absorbing solution (128). The extinction coefficient is also dependent upon the wavelength of the incident radiation, and should always be given along with the wavelength.

Figure 5.6 Energy Levels for d^8 Configuration and Allowed Transitions for Ni (II)

1. $^3A_2 \longrightarrow {}^3T_2$
2. $^3A_2 \longrightarrow {}^3T_1(F)$
3. $^3A_2 \longrightarrow {}^3T_1(F)$

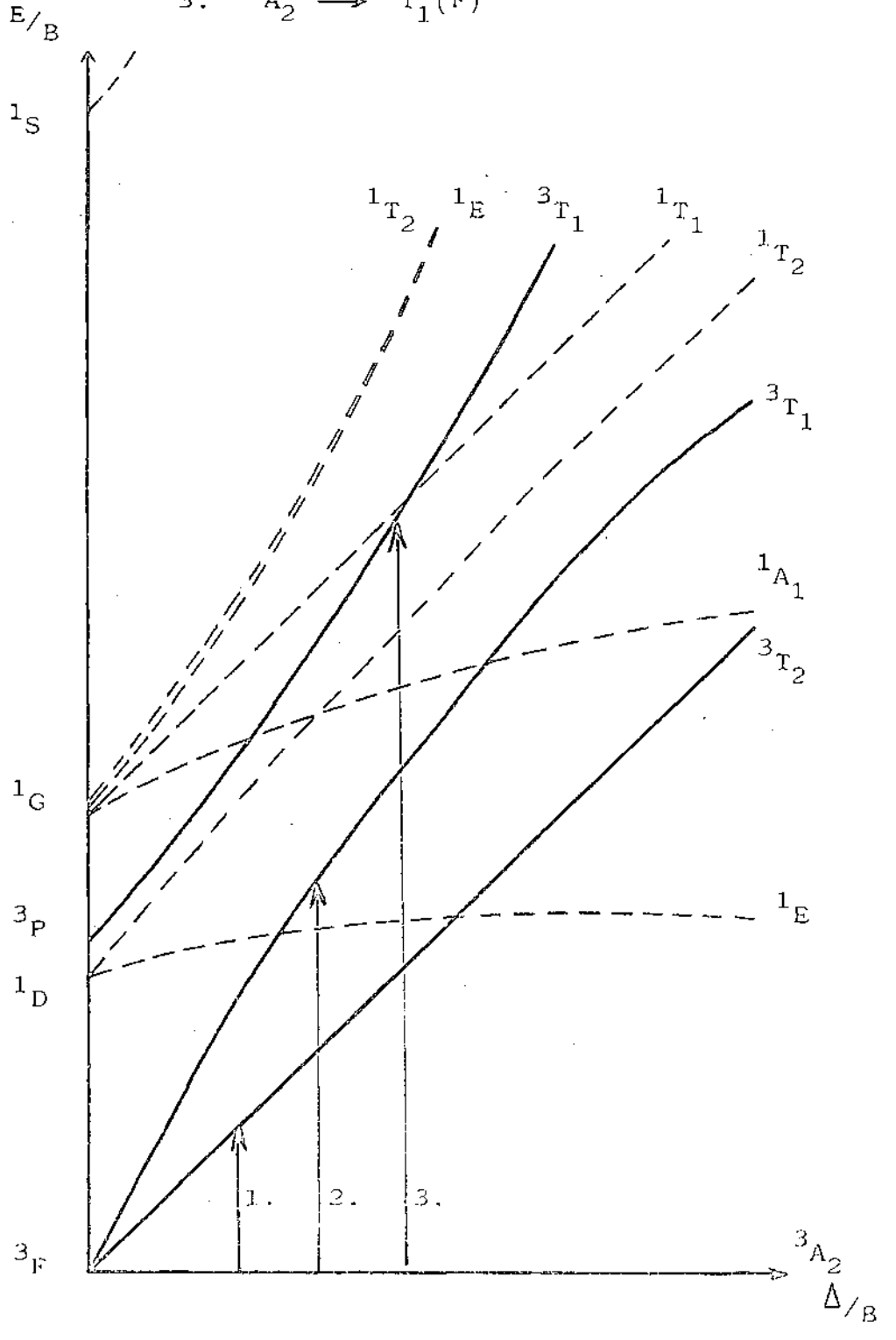

Figure 5.7 Calculation of Ligand Field Strength for L^{3-}

B = 1080 cm^{-1} for free Ni(II) ion

Energy of Transitions for NiL^{-} 25,400
14,900
8,500 cm^{-1}

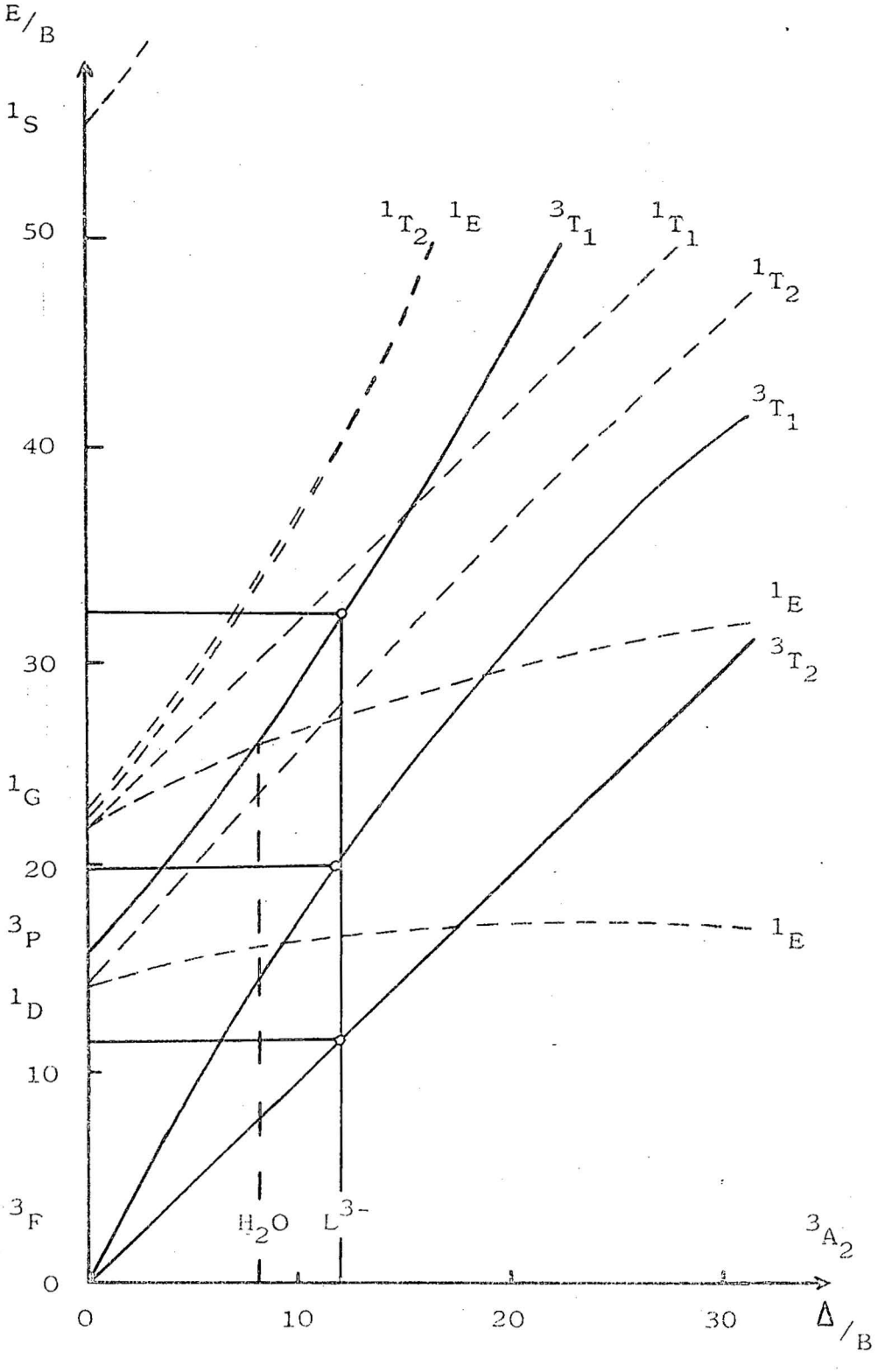

The extinction coefficients calculated for the nickel-citrate species ML^-, at the wavelengths of maximum absorbance are: 10.83 (393 nm), 4.20 (670 nm) and 3.5 (1150 nm). The unit of the extinction coefficient is $1mol^{-1}\,cm^{-1}$. These values are several times greater than those for the nickel-aquo species, $[Ni(H_2O)_6]^{2+}$, which has the extinction coefficients of 5.0 (393 nm), 1.76 (670 nm) and 1.80 (1150 nm).

Since in an equimolar nickel-citrate solution at pH 7 the only species present is ML^-, it is possible to calculate the ligand field strength (Δ_o) of the ligand L^{3-}. The position of the bands for such a solution are 393, 670 and 1170 nm. These correspond to energies of 25,400, 14,900 and 8,500 cm^{-1} respectively. These energies give a reasonable fit to the Tanabe-Sugano diagram with a Racah Parameter of B=760 and a Δ_o of 1190 cm^{-1} (see Figure 5.7). This value of Δ_o for the citrate ligand L^{3-} is greater than that for the nickel-aquo species, Δ_o = 870 cm^{-1} (129).

5.3.3 Interpretation of 1:1 Nickel:Citric Acid Spectra

The spectra of equimolar nickel-citric acid solutions are dependent upon the pH. As the pH increased to near neutral, the absorbance increased, and the wavelength of maximum absorbance shifted to shorter wavelengths (see Figures 4.2, 4.3, 4.4 and 4.5).

As citrate ions become coordinated around the central nickel(II) ion, the octahedral field becomes distorted. (Water molecules around nickel form an almost perfect octahedron). As the octahedron becomes distorted, the symmetry of the complex is lowered. Generally, as the symmetry of an octahedrally coordinated complex becomes less regular, the extinction coefficient increases (130, 131). A typical example is the cis and trans isomers for the cobalt (III) complexes of the type CoA_4B_2 (132).

The increase in the intensity of the absorption spectrum with pH results from the increased extinction coefficient of the nickel-citrate 1:1 complexes as compared to the nickel-aquo complex (e.g. at 393 nm $\epsilon(ML^-)$ = 10.83 and ϵ(Ni-aquo) = 5.0 $1mol^{-1}cm^{-1}$). This indicates that the

Table 5.3 Extinction Coefficient for ML^- Calculated From the Absorbance Data of Several 1:1 Nickel:Citric Acid Solutions at pH = 7

Total [Ni] / 10^{-3} M	Wavelength					
	393 nm		670 nm		1150 nm	
	A	ϵ	A	ϵ	A	ϵ
1.90	0.021	11.02	0.0079	4.20		
1.90	0.020	10.50	0.0076	3.99	0.0065	3.41
3.81	0.042	11.03	0.016	4.20	0.014	3.67
3.81	0.041	10.76	0.017	4.41		

octahedral field of the complex ML^- is distorted compared to that of the nickel-aquo complex.

The shift of the absorption maxima to shorter wavelengths (higher energies) is indicative of the coordination of ligands with a greater ligand field strength. While it is generally accepted that the carboxylate group has a ligand field energy less than water (127, 133, 134, 135), it is also noted that the dicarboxylate groups, oxalate and malate, have ligand field strengths approximately equal to water (127, 133). The results of this work show that a combination of either three carboxylate groups, or two carboxylate groups and the hydroxy group, have a greater ligand field strength than water

$$(\Delta_o(H_2O) = 870 \text{ cm}^{-1}, \quad \Delta_o(L^{3-}) = 1190 \text{ cm}^{-1}).$$

The shift in the peaks of the spectrum is greatest in the pH range 5 - 8, where only ML^- is present (see Figures 3.3, 4.3 and 4.5). The approximately linear decrease in λ_{max} in the pH range 3 to 5 would result from the increase in coordination of the ligand as the complex species moves through the series MH_2L^+, MHL and ML^-, as the pH increases.

5.3.4 Interpretation of the Spectra When Excess Citric Acid is Present

Two features exist to distinguish the spectrum of, say, a 1:3 nickel:citric acid solution from that of an equimolar solution. The absorbance of a 1:3 solution through the pH range 5 - 8 is less than that of a 1:1 solution, and the absorption bands are shifted to shorter wavelengths (see Figures 4.7, 4.8 and 4.9). Both these features are consistent with the formation of a bis species.

In a 1:3 nickel:citric acid solution at pH 7, the only complex species present are ML^- and ML_2^{4-}. This is shown in Figure 3.8. In such a solution the total absorbance will be the sum of the absorbance of each absorbing species.

$$A_{total} = A_{ML} + A_{ML_2} \qquad 5.1$$

$$= b(\epsilon_{ML}C_{ML} + \epsilon_{ML_2}C_{ML_2})$$

where b is the pathlength, ϵ_i and C_i are the extinction coefficient and concentration of species i respectively (136).

Using equation 5.1, the extinction coefficients for the complex ML_2^{4-} were calculated at a number of wavelengths. The values obtained were 8.9 (393 nm), 4.6 (666 nm), and 6.4 (1150 nm). It should be noted that these values are only approximate, and will not correspond to those of the absorption maximum of a solution of pure ML_2^{4-}. They are therefore not a very useful aid in coming to any conclusions regarding the symmetry of ML_2^{4-} compared to that of ML^-.

The shift of the absorption maxima to higher energies when excess citric acid is present is consistent with the greater ligand field strength for the ligand relative to H_2O.

5.3.5 Interpretation of the Spectra in the Alkaline Region

The spectra of alkaline nickel:citrate solutions have two features when compared to those of acidic solutions: greatly enhanced absorbance, and a slight shift to longer wavelengths (see Figures 4.2 to 4.6).

It has been suggested (39) that the hydroxy proton is removed from the 1:1 complex ML^- at alkaline pH's. This is quite likely. However, it would not account for the large increase in absorbance, as the formation of $MH_{-1}L^{2-}$ would not necessarily result in much further distortion of the octahedral field (see Figures 5.2 to 5.4).

Polymeric complexes of copper and citrate have been reported in the alkaline pH range (47). It has been suggested that the structure of these complexes involve the bridging of complex units of stoichiometry

$M_2(H_{-1}L)_2$ by hydroxy groups. It is possible that similar complexes exist for nickel.

A complex of nickel and tetraionized citrate has been crystallized from alkaline solution (94). X-ray techniques indicate a large anionic complex in which two tetrahedra of complexed Ni(II) ions are joined together by bridging citrate carboxyl groups. The faces of the tetrahedra are capped by ionized citrate hydroxy oxygen atoms. Such a complex species would have a large extinction coefficient due to the tetrahedral ligand field about the Ni(II) ions. This is consistent with the experimental observations of this work.

It is evident that a good deal of further work is required in order to fully determine the nature of the interaction of nickel and citrate ions in alkaline solutions.

5.4 SUMMARY

Titration data of nickel:citrate ratio near 1:1 have been analysed satisfactorily in terms of the complexes ML^-, MHL, and MH_2L^+, while when excess citric acid is present, a further species, ML_2^{4-} is formed.

The spectrophotometric results can readily be interpreted in terms of the above complexes. The differences between the spectra of solutions with equimolar nickel and citric acid, and solutions where citric acid is in excess, can be explained by the presence of ML_2^{4-} in the latter solutions.

The most probable structure for the complex ML^- involves the coordination of the hydroxy group along with the central and one terminal carboxylate groups.

Analysis of both potentiometric and spectrophotometric results indicate a bis species exists in solutions where citric acid is present in greater concentrations than nickel ions. Hence, in plants with excess citric acid over nickel, bis species are likely to exist.

Suggestions for Further Work

Other carboxylic acids have been implicated in nickel-accumulating plants. Studies of the solution chemistry of mixtures of these acids and nickel ions are not widespread. It would be worthwhile to investigate these systems and those of mixed acids, since plants often have more than one carboxylic acid present, in high concentrations.

Appendix 1

Algebra of Least Squares

Linear Observational Equations

A set of m equations, linear in the unknown parameters $x_1, x_2, \ldots x_n$, $m > n$, may be expressed in a matrix notation

$$A\underline{x} = \underline{b} \qquad 1$$

where A is an (mxn) matrix, $\underline{x}$ a vector of order n and $\underline{b}$ a vector of order m. The elements of A and $\underline{b}$, a_{ij} and b_i, are subject to experimental error if the system of equations 1 arise from experimental observations. When this is the case, an exact solution to equation 1 cannot be obtained, and some means by which the "best" solution is obtained must be used.

A vector of residuals, $\underline{r}$, is defined so that

$$\underline{r} = \underline{b} - A\underline{x} \qquad 2$$

The best solution is, that $\underline{x}$ for which the sum of squares of residuals is a minimum, i.e. minimise

$$M = \underline{r}^T\underline{r} \qquad 3$$

where $\underline{r}^T$ is the transpose or the vector $\underline{r}$. The minimising condition,

$$\frac{dM}{d\underline{x}} = \underline{0} \qquad 4$$

where $\underline{0}$ is the zero vector, gives rise to the normal equations (106)

$$A^TA\underline{x} = A^T\underline{b} \qquad 5$$

The normal equations can be solved directly to obtain estimates of $\underline{x}$ by premultiplication of $A^T \underline{b}$ by $(A^T A)^{-1}$.

$$\underline{x} = (A^T A)^{-1} A^T \underline{b} \qquad 6$$

Non-Linear Observational Equations

Consider the case where the functions, f_i, depend on the unknowns, x_j, in some non-linear manner:

$$f_i = f_i(x_1, x_2, \ldots x_n) \qquad 7$$

$$f_i = f_i(\underline{x}) \qquad 8$$

where $\underline{x}$ is a vector of order n.

The set of non-linear equations, f_i, may be "linearised" by employing the Taylor expansion (107). Expansion of f_i about the point $(x_1^0 \ldots x_n^0)$ and neglecting the second and higher order derivatives gives rise to

$$f_i \doteqdot f_i(x_1^0 \ldots x_n^0) + \frac{\partial f_i}{\partial x_i}(x_1 - x_1^0) + \frac{\partial f_i}{\partial x_i}(x_2 - x_2^0) + \ldots$$

or

$$f_i - f_i^0 \doteqdot \sum_{j=1}^{n} \frac{\partial f_i}{\partial x_i}(x_j - x_j^0)$$

or

$$\Delta f_i \doteqdot \sum_{j=1}^{n} \frac{\partial f_i}{\partial x_i} \Delta x_j \qquad 9$$

The problem is now of the form $A\underline{x} = \underline{b}$. However, since the non-linear terms of the Taylor expansion were neglected, it is necessary to iterate, that is, to repeat the solution of equation 9 with successive approximations, $\underline{x}_p$, until an $\underline{x}_p$ is obtained for which all elements of $\Delta \underline{x}_p$, the correction vector for the p-th iteration, are negligible. Convergence, though not always guaranteed, can be forced, by reducing the changes $\Delta \underline{x}_p$ indicated in each iteration, p, by a sufficiently small factor.

This process is carried out by the program ORGLS.

Inversion of the Matrix

Solution of the normal equations, 5, requires inversion of the matrix $A^T A$. This was accomplished by employing the Choleski process (108). A symmetric matrix A can be factorized,

$$A = L L^T$$

where L is a lower triangular matrix. The inverse of A is given by

$$A^{-1} = (L L^T)^{-1}$$

$$= (L^T)^{-1} (L^{-1})$$

Now $(L^T)^{-1} = (L^{-1})^T$. Therefore to form the inverse of matrix A, the three steps in the process are:

1. factorize the matrix into its lower triangular matrix
2. invert the lower triangular matrix
3. premultiply this matrix by its transpose.

This process is incorporated in the computer program ORGLS. The matrix inversion is carried out by the program MATINV (see Appendix Two).

Appendix 2

Computer Programs

The FORTRAN computer programs listed below were used on a Burroughs B-6700 computer.

Program ORGLS

This program was modified from the program ORGLS of W.R Busing and H.A. Levy (109). The listing below shows the program adopted to calculate the equilibrium constants for the nickel-citric acid complexes as defined in Section 3.2. (The program ORGLS was also used to calculate the protonation constants of citric acid. The appropriate changes to the subroutines PRELIM and CALC have not been shown).

The program consists of five sections: the mainline, and the four subroutines PRELIM, CALC, TEST and MATINV. PRELIM carries out preliminary calculations on the titration data, e.g. calculation of Yobs from the data. In CALC, the value of the observed quantity is calculated from the parameters, P, the hydrogen ion concentration, X, and the free ligand and metal concentrations, FLIG and FMET respectively. The calculated quantity, Ycalc, is then passed back to the mainline. MATINV incorporates the matrix inversion process (see Appendix One). TEST is used to apply checks to the parameters at the end of each least squares cycle e.g. test for convergence, and zero or negative parameters.

Program COMICS

This program is an adapted version of the program COMICS of D.D. Perrin and I.G. Sayce (110). Changes are

restricted to the incorporation of the subroutines STORE and PLOT to enable the distribution curves to be plotted. The program calculates the equilibrium concentration of defined species given the appropriate overall stability constants for each species (56).

ORGLS

```
C       PROGRAM ORGLS
C
C       GENERAL LEAST-SQUARES (WITH FORTRAN MATRIX INVERTER).
C
C       DIMENSIONS FOR NV(MAX)=100,NP(MAX)=200,NO(MAX)=1000,NX(MAX)=5
C
FILE    5=FILE5, UNIT=READER
FILE    6=FILE6, UNIT=PRINTER
        DIMENSION TMET(100), TLIG(100)

        DIMENSION FLIG(100),FMET(100)
        DIMENSION VOL(100)
        DIMENSION AM(700)
        DIMENSION TITLE(20),P(20),X(2,100),YO(100),SIGYO(100),KI(20)
        DIMENSION ZP(20),SQDT(20)
        DIMENSION DP(20) ,SGSIG(2), V(50),DC(20) ,DV(50),DD(200)
        DIMENSION DIAG(50),PD(50),ROW(50)
        COMMON AM,V,DC,DV,DP,YC,P,X
        COMMON NC,NV,NX,ID,IW,IP,IT,NP,ISENT,NO,NM,NCY,IC
        COMMON SQRTW, DPK,PSAVE,YO,JK,ISING,II,IID,POI,IJ,IJD,POLD
        COMMON SIGP,ISTOP,NT,NFCD
        COMMON TITLE,SIGYO,KI,SGSIG,DD,DIAG,PD,ROW
C
C       FORMAT STATEMENTS
C
   17 FORMAT('0 PARAMETERS CANNOT BE PUNCHED ON CARDS ')
   20 FORMAT(I2)
   21 FORMAT('0' 5X,I1,5X,E10.4,5X,F8.4)
   29 FORMAT(//'OCONVERSION OF THE PARAMETERS TO LOG VALUES'/'0      I
     1          P(I)            LOG(P(I))')
   40 FORMAT('0'20A4)
 51     FORMAT(20A4)
 52     FORMAT(////1H020A4)
 53     FORMAT(/I3)
 54     FORMAT(32HONUMBER OF CYCLES IN THIS JOB ISI2/37HONUMBER OF PARAMET
     1ERS TO BE VARIED ISI3/51HONUMBER OF INDEPENDENT VARIABLES PER OBSE
     2RVATION ISI2)
 58     FORMAT(31HODERIVATIVES PROGRAMMED BY USER)
   59 FORMAT('ONUMERICAL DERIVATIVES UNLESS PARAMETER INCREMENT IS ZERO'
     1)
 61     FORMAT(31HOWEIGHTS TO BE SUPPLIED BY USER)
 62     FORMAT(34HOUNIT WEIGHTS TO BE SET BY PROGRAM)
 63     FORMAT(36HOPARAMETERS TO BE READ AS INPUT DATA)
 64     FORMAT(34HOPARAMETERS TO BE TAKEN FROM CYCLEI2,16H OF PREVIOUS JOB
     1)
   66 FORMAT(I3,77X/(6E10.3))
 67     FORMAT(29HONUMBER OF PARAMETERS READ ISI3)
   68 FORMAT(I1,F9.3,F10.3,E10.3)
   69 FORMAT('ONUMBER OF OBSERVATIONS READ IS',I4)
 70     FORMAT(72I1)
   71 FORMAT(5E10.3)
 72     FORMAT(46HOCALCULATED Y BASED ON PARAMETERS BEFORE CYCLEI2)
 73     FORMAT('0  Y(OBS)            Y(CALC)          OBS-CALC          SIG(O)           (O
     1-C)/SIG(O)          X(I)             FLIG(I)          FMET(I)         PH            VO
     1L  WIT')
   79 FORMAT(' ',8(E10.4,4X),F5.3,3X,F5.3,X,I3)
 80     FORMAT(51HOAGREEMENT FACTORS BASED ON PARAMETERS BEFORE CYCLE I2/
     120HOSUM(W*(O-C)**2) IS E11.3/'OSQRT(SUM(W*(O-C)**2)/(NO-NV)) IS '
     2 E11.4/'0 SUM(W*O**2) IS ',E11.4/'0 RFACTOR   SQRT(SUM(W*(O-C)**2)
     3/SUM(W*O**2)) IS ',F7.4)
   81 FORMAT(60HOESTIMATED AGREEMENT FACTORS BASED ON PARAMETERS AFTER C
     1YCLE I2/20HOSUM(W*(O-C)**2) IS E11.3/35HOSQRT(SUM(W*(O-C)**2)/(NO
     2-NV)) IS E11.4/'ORFACTOR IS ',F7.4)
 83     FORMAT(62H MATRIX HAS A ZERO DIAGONAL ELEMENT CORRESPONDING TO PAR
     1AMETERI3,16H OF THOSE VARIED)
 85     FORMAT(40H SINGULARITY RETURN FROM MATRIX INVERTER)
 86     FORMAT(37HOPARAMETERS AFTER LEAST SQUARES CYCLEI2/'0                    OLD
     1          CHANGE                  NEW                   ERROR'/1H )
 88     FORMAT(1H I3,5X,E10.4,15X,E10.4)
 89     FORMAT(1H I3,4(5X,E10.4))
 90     FORMAT(66HOSUBROUTINE TEST INDICATES THAT JOB IS TO BE TERMINATED
     1FOR REASONI2)
```

```
   91 FORMAT('OREASON 2          PARAMETER INCREMENTS SMALL ENOUGH FOR
     1EQUATE REFINEMENT')
   92 FORMAT('0              INPUT DATA'//'0          P(I)          K(I)
     1DF(I)')
   93 FORMAT(1H ,I3,5X,E16.8,5X,I4,3X,E11.3)
   94 FORMAT(31HOCORRECTED PARAMETERS NOT TO BE SAVED FOR LATER USE)
   95 FORMAT(31HOCORRECTED PARAMETERS TO BE WRITTEN ON PRIVATE TAPE)
   96 FORMAT(31HOCORRECTED PARAMETERS TO BE WRITTEN FOR CARD OUTPUT)
   97 FORMAT(19HOCORRELATION MATRIX)
   98 FORMAT(1HO13,10F9.4/(1H 3X,10F9.4))
   99 FORMAT('OREASON 1      NEGATIVE OR ZERO PARAMETER FOUND')
      INTEGER RDR,PTR
      RDR=5
      PTR=6
C
C     READ TITLE AND CONTROL DATA --- IONIC STRENGTH AISTR ,
C     TITRATION NUMBER TIT, NO. OF CYCLES IN JOB NC , NO. OF PARAS. TO
C     BE VARIED NV , NO.OF DETERMINATIONS OF THE VARIABLE X ,
C     DERIVATIVE INDICATOR ID, WEIGHT INDICATOR IW , IP AND IT ARE
C     OUTPUT CONTROL PARAMETERS
C
      INTL=0
      READ(RDR,20) KODE
   30 READ(RDR,51)(TITLE(I),I=1,20)
      WRITE(PTR,52)(TITLE(I),I=1,20)
      READ(5,51) (SUBT(I),I=1,20)
      WRITE(6,40) (SUBT(I),I=1,20)
      READ(RDR,53) NC,NV,NX,ID,IW,IP,IT
      WRITE(PTR,54)NC,NV,NX
      IF(ID)206,204,206
  204 WRITE(PTR,56)
      GO TO 207
  206 WRITE(PTR,59)
  207 IF(IW)210,208,210
  208 WRITE(PTR,61)
      GO TO 211
  210 WRITE(PTR,62)
  211 IF(IP)212,212,214
  212 WRITE(PTR,63)
      GO TO 215
  214 WRITE(PTR,64)IP
  215 IF(IT-1)216,216,221
  216 WRITE(PTR,94)
      GO TO 301
  218 WRITE(PTR,95)
      GO TO 301
  221 WRITE(PTR,96)
C
C     READ TRIAL PARAMETERS P , AND NO. OF PARAS. NP
C
  301 IF(IP)401,401,501
  401 READ(RDR,66,NP,(P(I),I=1,NP)
      GO TO 601
  501 DO 503 J=1,IP
  503 CONTINUE
  601 WRITE(PTR,67)NP
C
C     READ OBSERVATIONS TO SENTINEL
C
      J=0
  801 J=J+1
      READ(5,68) ISENT,VOL(J),X(1,J),SIGYU(J)
      IF(ISENT)801,801,1101
 1101 NO=J-1
      WRITE(PTR,69)NO
C     READ KEY INTEGERS AND PARAMETER INCREMENTS IF SPECIFIED
      IF(NC)1601,1601,1301
 1301 READ(RDR,70)(KI(I),I=1,NP)
 6601 IF(ID)1501,1611,1501
 1501 READ(RDR,71)(DP(I),I=1,NP)
      GO TO 1621
 1601 DO 1602 I=1,NP
 1602 KI(I)=0
```

```
1611   DO 1612 I=1,NP
1612   DP(I)=0.0
C
C      INITIALIZE PROBLEM AND ENTER SUBROUTINE PRELIM IF PROVIDED
CC
C
1621   NM=(NV*(NV+1))/2
       SGSIG(1)=1.0
C
       CALL PRELIM(YO,X,WO,SIGYO,VOL,C,D,TLIG,TMET)
C
C      PUT OUT TRIAL PARAMETERS, KEY INTEGERS, AND PARAMETER INCREMENT
       WRITE(PTR,92)
       DO 1653 I=1,NP
1653   WRITE(PTR,93)I,P(I),KI(I),DP(I)
C
C      START LOOP TO PERFORM NC CYCLES AND ONE FINAL CALCULATION OF Y
C
       NCY=NC+1
       DO 2501 IC=1,NCY
C      CLEAR ARRAYS AM AND V EXCEPT ON LAST CYCLE
       IF(IC-NCY)1851,2001,2001
1851   DO 1852 I=1,NM
1852   AM(I)=0.0
       DO 1902 I=1,NV
1902   V(I)=0.0
C
C      INITIALIZE FOR CYCLE IC AND PUT OUT CAPTION FOR LIST OF Y(CALC)
C
 2001  SGSIG(2)=SGSIG(1)
       SIG=0.0
       SUMYO=0.0
       WRITE(PTR,72)IC
       WRITE(PTR,73)
C
C      START LOOP THROUGH NO OBSERVATIONS
C
 2201  DO 3101 I=1,NO
C
C
C      ENTER USERS SUBROUTINE TO COMPUTE Y(CALC) AND DERIVATIVES
C
       CALL CALC(I,X,YC,P,C,D,FLIG,FMET,TLIG,TMET,NIT)
C
C      OBTAIN WEIGHT AND CALCULATE QUANTITIES FROM Y(OBS)-Y(CALC)
       IF(IW)2001,2501,2601
 2501  SQRTW=1.0/SIGYO(I)
       GO TO 2701
 2601  SIGYO(I)=1.0
       SQRTW=1.0
 2701  DY=YO(I)-YC
       WDY=SQRTW*DY
       SIG=SIG+WDY*WDY
       WYO=YO(I)*SQRTW
       SUMYO=SUMYO+WYO*WYO
       PACID=(-ALOG10(X(1,I)))
C
C      PUT OUT Y(CALC) AND OTHER INFORMATION FOR ONE OBSERVATION
C
 2070  WRITE(PTR,79) YO(I),YC,DY,SIGYO(I),WDY,X(1,I),FLIG(I),TMET(I),P
      1O,VOL(I),NIT
C
CC
C      DY-PASS DERIVATIVE AND MATRIX SET-UP ON FINAL CALC OF Y
       IF(IC-NCY)3001,3101,3101
C
C      START LOOP TO STORE AN ARRAY OF NV DERIVATIVES
C
 3001  J=1
       DO 4101 K=1,NP
       IF(KI(K))4101,4101,3201
 3201  IF(ID)3401,3301,3401
C      OBTAIN DERIVATIVE FROM THOSE PROGRAMMED BY USER
```

```
 3301 DV(J)=SQRTW*DC(K)
      GO TO 4001
C     OBTAIN DERIVATIVE NUMERICALLY UNLESS PARAMETER
C     INCREMENT IS ZERO
 3401 DPK=DP(K)
      IF(DPK)3601,3301,3601
 3601 PSAVE=P(K)
      P(K)=PSAVE+DPK
C
      CALL CALC(I,X,YD,P,C,D,FLIG,FMET,TLIG,TMET,NIT)
C
      DV(J)=SQRTW*(YD-YC)/DPK
      P(K)=PSAVE
 4001 J=J+1
 4101 CONTINUE
C     END LOOP TO OBTAIN DERIVATIVES
C
C     START LOOP TO STORE MATRIX AND VECTOR.
C     1604 OR GLS STORAGE SCHEME IS REVERSE OF 7090 OR GLS
C
      JK=1
      DO 5001 J=1,NV
 4301 TEMP=DV(J)
      IF(TEMP)4501,4401,4501
C     BY-PASS IF DERIVATIVE IS ZERO
 4401 JK=JK+NV+1-J
      GO TO 5001
 4501 DO 4801 K=J,NV
      AM(JK)=AM(JK)+TEMP*DV(K)
      JK=JK+1
 4801 CONTINUE
      V(J)=V(J)+TEMP*WDY
 5001 CONTINUE
C     END LOOP TO STORE MATRIX AND VECTOR
 5101 CONTINUE
C     END LOOP THROUGH NO OBSERVATIONS
C
C     COMPUTE AND PUT OUT AGREEMENT FACTORS
C
      RFACT=SQRT(SIG/SUMYD)
      SQSIG(1)= SQRT(SIG/FLOAT(NO-NV))
      WRITE(PTR,60)IC,SIG,SQSIG(1),SUMYD,RFACT
C     BY-PASS MATRIX INVERSION AND PARAMTER OUTPUT ON FINAL CYCLE
      IF(IC-NCY)5401,6701,8701
C
C     START LOOP TO TEST FOR ZERO DIAGONAL ELEMENT
C
 5401 ISING=0
      II=1
      IID=NV
      DO 5801 I=1,NV
      IF(AM(II))5701,5601,5701
 5601 ISING=1
      WRITE(PTR,63)I
 5701 II=II+IID
      IID=IID-1
 5801 CONTINUE
C     END LOOP TO TEST FOR ZERO DIAGONAL ELEMENT
C     TERMINATE JOB IF ZERO DIAGONAL ELEMENT WAS FOUND
      IF(ISING)10301,6001,10301
C
C     ENTER SUBROUTINE TO REPLACE MATRIX WITH INVERSE
C
 6001 CALL MATINV(AM,NV,ISING)
      IF(ISING)6201,6301,6201
C     TERMINATE JOB IF SINGULAR MATRIX WAS FOUND
 6201 WRITE(PTR,65)
      GO TO 10301
C
C     START LOOP FOR MATRIX VECTOR MULTIPLICATION FOR
C     PARAMETER CHANGES
C
 6301 DO 7201 I=1,NV
```

```
      PDI=0.0
      IJ=1
      IJD=NV+1
      DO 7001 J=1,NV
      PDI=PDI+AN(IJ)*V(J)
      IF(J-I)6701,6801,6901
 6701 IJ=IJ+IJD
      IJD=IJD-1
      GO TO 7001
C
C     SAVE DIAGONAL ELEMENTS OF INVERSE MATRIX
C
 6801 DIAG(I)=AN(IJ)
 6901 IJ=IJ+1
 7001 CONTINUE
      PD(I)=PDI
      SIG=SIG-PDI*V(I)
 7201 CONTINUE
C     END LOOP FOR MATRIX VECTOR MULTIPLICATION
C
C     RECOMPUTE AGREEMENT FACTOR USING MODIFIED SIG
C
 3655 SQSIG(1)= SQRT(SIG/FLOAT(ND-NV))
      RFACT=SQRT(SIG/SUMY0)
C     PUT OUT CAPTION FOR LIST OF CORRECTED PARAMETERS
 3666 WRITE(PTR,52)(TITLE(I),I=1,20)
      WRITE(PTR,66)IC
C
C     START LOOP TO CORRECT AND PUT OUT PARAMETERS
C
      J=1
      DO 6001 I=1,NP
      IF(KI(I))7001,7001,7701
 7001 WRITE(PTR,80)I,P(I),P(I)
      GO TO 8001
 7701 POLD=P(I)
      P(I)=POLD+PD(J)
 6111 SIGP=SQRT(DIAG(J))*SQSIG(1)
      WRITE(PTR,89)I,POLD,PD(J),P(I),SIGP
      J=J+1
 6001 CONTINUE
C     END LOOP TO CORRECT AND PUT OUT PARAMETERS
C
C     PUT OUT ESTIMATED AGREEMENT FACTORS
      WRITE(PTR,81)IC,SIG,SQSIG(1),RFACT
C
C     ENTER USERS SUBROUTINE TO TEST AND MODIFY PARAMETERS
C     OR END JOB
 6112 ISTOP=0
      CALL TEST(ISTOP,P,SQSIG,NP)
C
C     WRITE CORRECTED PARAMETERS ON AUXILIARY TAPE IF
C     DESIRED
      IF(IT-1) 8403,6204,6204
 6204 WRITE(6,17)
 8403 IF(ISTOP) 6501,6501,8401
 6401 WRITE(PTR,90)ISTOP
      IF(ISTOP-1) 8410,6410,6411
 6410 WRITE(PTR,99)
      GO TO 8701
 6411 WRITE(PTR,91)
      GO TO 8701
 6501 CONTINUE
C     END LOOP THROUGH NC CYCLES AND FINAL CALC OF Y
C
C     TERMINATE JOB
 8701 IF(NC)10501,10501,8601
C
C
C     CONVERSION OF THE CONSTANTS TO LOG VALUES
C
 8601 WRITE(PTR,29)
      DO 8522 I=1,NP
```

```
      IF(P(I)) 18,18,19
   18 ZP(I)=1.0
      GO TO 8522
   19 ZP(I)=ALOG10(P(I))
 8522 WRITE(PTR,22) I,P(I),ZP(I)
C     CALCULATE AND PUT OUT CORRELATION MATRIX
      WRITE(PTR,52)(TITLE(I),I=1,20)
      WRITE(PTR,97)
      DO 9101 I=1,NV
      DIAG(I)=1.0/SQRT(DIAG(I))
 9101 CONTINUE
      IJ=1
      DO 10201 I=1,NV
      DO 9601 J=1,NV
      ROW(J)=0.0
 9601 CONTINUE
      DO 10001 J=1,NV
      ROW(J)=AM(IJ)*DIAG(I)*DIAG(J)
      IJ=IJ+1
10001 CONTINUE
      WRITE(PTR,96)I,(ROW(J),J=1,NV)
10201 CONTINUE
10301 CONTINUE
      INTE=INTE+1
      IF(INTE-KODE) 30,10301,10501
10501 STOP
      END
```

CALC

```
      SUBROUTINE CALC(I,X,Y,P,C,D,FLIG,FMET,TLIG,TMET,N)
C
C     NICKEL-CITRIC ACID TITRATION DATA
C     PROGRAM TO CALCULATE YCALC FROM THE
C
      DIMENSION FLIG(100),FMET(100),TLIG(100),TMET(100)
      DIMENSION X(2,100),P(20)
      DIMENSION YC(100)
      REAL K1,K2,K3
      REAL M,MNEW(100),M0,M1,M2
      REAL L,LNEW(100),L0,L1,L2
      DATA K1,K2,K3/5.106E5,2.328E4,6.070E2/
      A=1.+K1*X(1,I)+K2*K1*X(1,I)**2+K3*K2*K1*X(1,I)**3
      B=K1*X(1,I)+2.*K2*K1*X(1,I)**2+3.*K3*K2*K1*A(1,I)**3
      IF(I.EQ.1) GO TO 1
      L=LNEW(I-1)
      M=MNEW(I-1)
      GO TO 2
C     CALCULATE AN APPROX LIG AND MET CONC FOR THE FIRST POINT
C     BY ASSUMING NO COMPLEX FORMATION.
C     FOR OTHER POINTS ASSIGN FMET AND FLIG OF THE PREVIOUS POINT
    1 L=TLIG(I)/A
      M=TMET(I)
    2 AA=P(2)*P(3)*(K1*X(1,I))**2
      BB=P(2)*K1*X(1,I)
      CC=K1*P(2)*P(6)*X(1,I)
      DD=K1*K2*P(5)*X(1,I)**2
C     ENTER NR ROUTINES FOR METAL AND LIGAND CONCENTRATIONS
      N=1
C     SET UP COEFFICIENTS FOR LIGAND
    3 L2=2.*P(7)*M**2+2.*M*(AA+P(1)*P(4)+CC)
      L1=A+M*(P(1)+BB+DD)
      L0=-TLIG(I)
C     SET UP COEFFICIENTS FOR METAL
      M2=2.*P(7)*L**2
      M1=L**2*(AA+P(1)*P(4)+CC)+L*(BB+DD+P(1))+1.
      M0=-TMET(I)
C     CALCULATE AN APPROXIMATE VALUE FOR FMET
      FM=M0*M1*M+M2*M**2
      FMD=M1+2.*M2*M
      MNEW(I)=M-FM/FMD
      M=MNEW(I)
C     CALCULATE AN APPROXIMATE VALUE FOR FLIG
      FL=L0+L1*L+L2*L**2
      FLD=L1+2.*L2*L
      LNEW(I)=L-FL/FLD
      D=0.00001*LNEW(I)
C     IF CONVERGENCE IS OKAY CALCULATE CALC  ELSE GO AROUND AGAIN
      IF(ABS(L-LNEW(I)).LE.D) GO TO 4
      L=LNEW(I)
      N=N+1
      IF(N.LE.40) GO TO 3
    4 FLIG(I)=LNEW(I)
      FMET(I)=MNEW(I)
      Y=FLIG(I)*(B+FMET(I)*(2.*DD+BB+FLIG(I)*(2.*AA+CC)))
      RETURN
      END
```

PRELIM

```
      SUBROUTINE PRELIM(YO,X,ND,SIGYO,VOL,C,D,TLIG,TMET)
C
C     PRELIM CALCULATES P(H+), TOTAL CONCENTRATIONS FOR
C     EACH POINT AND YO,S
C
      DIMENSION TLIG(100),PMET(100),TLIG(100),TMET(100)
      DIMENSION X(2,100),P(20)
      DIMENSION YO(100),SIGYO(100),VOL(100)
      REAL IACID,ILIG,IMET
      READ(5,16) IACID,ILIG,IMET,ALK,PIVOL,GAMMA
      WRITE(6,17) ILIG,IMET,ALK
      DO 11 I=1,ND
      X(1,I)=X(1,1)-0.052
      X(1,I)=10.**(-X(1,I))
      Q=PIVOL/(PIVOL+VOL(I))
      ALKA=VOL(I)*ALK/(PIVOL+VOL(I))
      IACID=IACID*Q
      TMET(I)=IMET*Q
      TLIG(I)=ILIG*Q
   11 YO(I)=IACID-ALKA+1.007E-14/(X(1,I)*GAMMA)-X(1,I)
   16 FORMAT(3(E10.3),F10.4,F10.3,F10.3)
   17 FORMAT(//'0   LIGAND CONCENTRATION IS ',E11.4/'0   METAL CONCENTR
     1TION IS  ',E11.4/'0   ALKALI CONCENTRATION IS',F8.4//)
      RETURN
      END
```

TEST

```
      SUBROUTINE TEST(ISTOP,P,SQSIG,NP)
C
      DIMENSION P(10),SQSIG(2)
      I=1
    2 IF(P(I)) 3,4,4
    3 ISTOP=1
      GO TO 8
    4 I=I+1
      IF(I-NP) 5,5,6
    6 A=ALOG10(SQSIG(2))-ALOG10(SQSIG(1))
      IF(A) 11,12,12
   11 A=-A
   12 IF(A.LT.0.0005) GO TO 7
      GO TO 8
    7 ISTOP=2
    8 CONTINUE
      RETURN
      END
```

MATINV

```
      SUBROUTINE MATINV(AM,N,NFAIL)
C
      DIMENSION AM(700)
C     ********** SEGMENT 1 OF CHOLESKI INVERSION **********
C     ***** FACTOR MATRIX INTO LOWER TRIANGLE X TRANSPOSE *****
      K=1
      IF(N-1)10,9,9
    9 AM(1)=1.0/AM(1)
      GO TO 204
C     ***** LOOP M OF A(L,M) *****
    9 DO 7 M=1,N
      IMAX=M-1
C     ***** LOOP L OF A(L,M) *****
      DO 6 L=M,N
      SUMA=0.0
      KLI=L
      KMI=M
      IF(IMAX)23,23,1
C     *****SUM OVER I=1,N-1 A(L,I)*A(M,I) *****
    1 DO 2 I=1,IMAX
      SUMA=SUMA+AM(KLI)*AM(KMI)
      J=N-I
      KLI=KLI+J
    2 KMI=KMI+J
C     *****TERM=A(L,M)-SUM *****
   23 TERM=AM(K)-SUMA
      IF(L-M)3,3,5
    3 IF(TERM)10,10,4
C     ***** A(M,M)=SQRT(TERM) *****
    4 DENOM= SQRT(TERM)
      AM(K)=DENOM
      GO TO 6
   10 NFAIL= 6
      GO TO 300
C     ***** A(L,M)=TERM/A(M,M) *****
    5 AM(K)=TERM/DENOM
    6 K=K+1
    7 CONTINUE
C     ********** SEGMENT 2 OF CHOLESKI INVERSION **********
C     *****INVERSION OF TRIANGULAR MATRIX*****
  100 AM(1)=1.0/AM(1)
      KDM=1
C     ***** STEP L OF B(L,M) *****
      DO 104 L=2,N
      KDM=KDM+N-L+2
C     ***** RECIPROCAL OF DIAGONAL TERM *****
      TERM = 1.0/AM(KDM)
      AM(KDM)=TERM
      KMI=0
      KLI=L
      IMAX=L-1
C     ***** STEP M OF B(L,M) *****
      DO 103 M=1,IMAX
      K=KLI
C     ***** SUM TERMS *****
      SUMA=0.0
      DO 102 I=1,IMAX
      II=KMI+I
      SUMA=SUMA-AM(KLI)*AM(II)
  102 KLI=KLI+N-I
C     ***** MULT SUM * RECIP OF DIAGONAL *****
      AM(K)=SUMA*TERM
      J=N-M
C
      KLI=K+J
  103 KMI=KMI+J
  104 CONTINUE
C     ********** SEGMENT 3 OF CHOLESKI INVERSION **********
C     *****MULTIPLY LOWER TRIANGLE BY TRANSPOSE*****
  200 K=1
      DO 203 N=1,N
      KLI=K
      DO 202 L=M,N
```

```
      KMI=K
      IMAX=N-L+1
      SUMA=0.0
      DO 201 I=1,IMAX
      SUMA=SUMA+AM(KLI)*AM(KMI)
      KLI=KLI+1
201   KMI=KMI+1
      AM(K)=SUMA
202   K=K+1
203   CONTINUE
204   NFAIL=0
300   RETURN
      END
```

COMICS

```
C       PROGRAM COMICS
C
C       INPUT DATA
C
C       1 NUMBER OF SETS OF EXPERIMENTAL CONDITIONS TO BE RUN
C       2 TITLE OF  THE  EXPERIMENT    (CAN USE COLS 1-80)
C       3 KODE TO INDICATE IF A DISTRIBUTION PLOT IS REQUIRED
C         WHEN KODE=1 SUBROUTINE PLOT IS CALLED
C       NFLAG TO INDICATE IF PRINTING OF CONCENTRATIONS IS REQUIRED
C         WHEN NFLAG=1 DETAILED PRINITING OF CONCENTRATIONS IS INCLUDED
C       4 NUMBER OF LIGANDS  NL
C         NUMBER OF METALS  NM
C         NUMBER OF COMPLEXES  NM  (INCLUDING PROTONATED FORMS OF LIGAND
C        AND HYDROLYSED METAL)
C         NUMBER OF PROTONATED LIGAND COMPLEXES  N1
C       5 A CARD FOR EACH COMPLEX SPECIES LSITING THE NUMBER OF MOLECULES
C         OF LIGAND(1 2 3 ETC UP TO 10) THE NUMBER OF IONS OF METAL THE
C         NUMBER OF HYDROXYL IONS(A POSITIVE INTEGER) OR OF PROTONS(A
C         NEGATIVE INTEGER) THE LOGARITHM OF THE CUMULATIVE ASSOCIATION
C         CONSTANT OF THE SPECIES
C       6 THE TOTAL CONCENTRATION OF EACH LIGAND
C       7 THE TOTAL CONCENTRATION OF EACH METAL
C       8 READ A CARD CONTAINING THE INITIAL PH APH INCREMENT AND
C         THE TOTAL NO OF POINTS
C       9 TITLE CARD FOR DISTRIBUTION PLOT
C      10 KODE TO INDICATE IF PLOT IS TO INCLUDE PROTONATED LIGAND SPECIES
C         KODE = 1 PRINT PROTONATED LIGAND SPECIES
C         (GIVEN BY ITEM1) HAS BEEN REACHED
C      11 THEN RETURN TO ITEM2 UNTIL TOTAL NUMBER OF EXPERIMENTS
C
      DIMENSION C(200),Y1(10),Y2(10),Y3(10),Y4(10),BTOT(10),CLTOT(10),
     1TX(10),VX(10),ML(10,200),MM(10,200),MN(200),AL(10,200),AM(10,200),
     2AN(200),B(200),L(200),DM(10),DMT(10),TITLE(20)
      DIMENSION PH(100),PMET(100),PLIG(100),COMP(100,100)
C
      COMMON C,Y1,Y2,Y3,Y4,BTOT,CLTOT,TX,VX,ML,MM,MN,AL,AM,AN,NL,NM,N,B,
     1UX,IPT
C
    1 FORMAT(I2)
    2 FORMAT(2I2,8X,F10.4)
    6 FORMAT('  ',I3,2X,2I(2X,I2),3X,F9.4)
    8 FORMAT(10E8.3)
    9 FORMAT('  TOTAL CONCN OF METAL(',I2,') =',E10.4)
   10 FORMAT('  TOTAL CONCN OF LIGAND(',I2,') =',E10.4)
   11 FORMAT(13X,2HC1,9X,2HC2,9X,2HC3,9X,2HC4,9X,2HC5,9X,2HC6,9X,2HC7,9X
     1,2HC8,9X,2HC9,9X,3HC10)
   12 FORMAT(4(I2,1X))
   17 FORMAT(2F10.3,7X,I3)
   30 FORMAT(///' PH =',F8.3)
   33 FORMAT('0COMP   L1   L2   L3   L4   L5   L6   L7   L8   L9  L10   M1   M2   M3
     1   M4   M5   M6   M7   M8   M9  M10   OH   LOG BETA')
   34 FORMAT(' FREE METALS')
   35 FORMAT(9X,10(1X,1PE10.3))
   36 FORMAT(' FREE LIGANDS')
   37 FORMAT(' COMPLEX SPECIES')
   43 FORMAT(1X,I3,1H=,I3,10(1X,1PE10.3))
   44 FORMAT(11,4X,I1)
   45 FORMAT(///'0                    TOTAL CONCENTRATIONS OF LIGANDS AND METALS
     1'/)
  130 FORMAT(20A4)
  131 FORMAT('0',20A4///)
  999 FORMAT(1H1)
C
      WRITE(6,999)
      READ(5,1) NJ
      NJ=0
  100 READ(5,130) (TITLE(I),I=1,20)
      WRITE(6,131) (TITLE(I),I=1,20)
      READ(5,44) KODE,NFLAG
      WRITE(6,33)
      READ(5,12) NL,NM,N,N1
      DO 7 J=1,N
```

```
      READ(5,2) ((ML(I,J),I=1,10),(MM(I,J),I=1,10),MN(J),E(J)
    7 WRITE(6,6) J,(ML(I,J),I=1,10),(MM(I,J),I=1,10),MN(J),E(J)
      WRITE(6,45)
      READ(5,6) (CLTOT(I),I=1,10)
      READ(5,6) (BTOT(I),I=1,10)
      WRITE(6,10) (I,CLTOT(I),I=1,NL)
      WRITE(6,9) (I,BTOT(I),I=1,NM)
      HX=ALOG(10.0)
      IPT=1
      DO 4 J=1,N
      AN(J)=MN(J)
      DO 4 I=1,10
      AL(I,J)=ML(I,J)
    4 AM(I,J)=MM(I,J)
      DO 13 I=1,N
   13 B(I)=EXP(HX*E(I))
      DO 14 I=1,NM
   14 Y1(I)=BTOT(I)*0.000001
      DO 15 I=1,NL
   15 Y3(I)=CLTOT(I)*0.000001
      JJ=1
      READ(5,17) PH(JJ),PHIN,TOTP
   16 UX=EXP(HX*PH(JJ))
      IF(IPT-1) 18,16,27
   18 DO 19 I=1,NM
   19 VX(I)=BTOT(I)
      DO 20 I=1,NL
      DMY(I)=1.0
      DO 22 J=1,N
      IF(ML(I,J)) 22,22,200
  200 DO 21 K=1,NM
      IF(MM(K,J)) 22,21,22
   21 CONTINUE
      DM(I)=(EXP(HX*E(J)))*UX**MN(J)
      DMY(I)=DMY(I)+DM(I)
   22 CONTINUE
   20 CONTINUE
      DO 23 I=1,NL
   23 TX(I)=CLTOT(I)/DMY(I)
C
   27 CALL COGS(NI,NFLAG)
C
      IF(NFLAG) 46,46,47
   47 WRITE(6,30) PH(JJ)
      WRITE(6,11)
      WRITE(6,34)
      WRITE(6,35) (VX(I),I=1,NM)
      WRITE(6,36)
      WRITE(6,35) (TX(I),I=1,NL)
      WRITE(6,37)
      KP=0
   40 KP=KP+1
      KN=10*KP
      KM=KN-9
      IF(KN-N) 41,42,42
   41 WRITE(6,43) KM,KN,(C(I),I=KM,KN)
      GO TO 40
   42 WRITE(6,43) KM,N,(C(I),I=KM,N)
C
   46 CALL STORE(JJ,VX,TX,C,NM,NL,N,FMET,FLIG,COMP)
C
      IF(JJ.GE.TOTP) GO TO 38
      JJ=JJ+1
      PH(JJ)=PH(JJ-1)+PHIN
      GO TO 16
   38 IF(KODE) 31,31,39
C
   39 CALL PLOT(TOTP,PH,FLIG,FMET,COMP,N,BTOT,CLTOT,NI)
C
   31 NJD=NJD+1
      WRITE(6,99)
      IF(NJD-NJ) 106,32,32
   32 STOP
      END
```

COGS

```
      SUBROUTINE COGS(N1,NFLAG)
C
      DIMENSION TERM(200),TERMM(200),C(200),Y1(10),Y2(10),Y3(10),Y4(10),
     1BTOT(10),CLTOT(10),TX(10),VX(10),ALO(10),BO(10),TY(10),VY(10),ML(1
     20,200),MM(10,200),MN(200),AL(10,200),AM(10,200),AN(200),B(200)
C
      COMMON C,Y1,Y2,Y3,Y4,BTOT,CLTOT,TX,VX,ML,MM,MN,AL,AM,AN,NL,NM,N,B,
     1UX,IPT
C
   99 FORMAT(' NUMBER OF ITERATIONS =',I4)
  998 FORMAT(' ITERATION DID NOT CONVERGE')
C
      NIT=0
      DO 1 K=1,N
    1 TERM(K)=B(K)*UX**MN(K)
    2 DO 3 K=1,N
    3 TERMM(K)=TERM(K)
      DO 4 K=1,N
      DO 4 J=1,NM
    4 TERMM(K)=TERMM(K)*VX(J)**MM(J,K)
      DO 5 K=1,N
      DO 15 J=1,NL
   15 TERMM(K)=TERMM(K)*TX(J)**ML(J,K)
    5 C(K)=TERMM(K)
      NIT=NIT+1
      IF(NIT.LE.N) GO TO 19
      DO 7 I=1,NM
      BO(I)=VX(I)
      DO 8 K=1,N
    8 BO(I)=BO(I)*AM(I,K)*C(K)
      RATIO=BO(I)/BTOT(I)
      VY(I)=VX(I)/SQRT(RATIO)
    7 Y2(I)=ABS(BO(I)-BTOT(I))
   19 DO 9 I=1,NL
      ALO(I)=TX(I)
      DO 10 K=1,N
   10 ALO(I)=ALO(I)+AL(I,N)*C(K)
      RATIO=ALO(I)/CLTOT(I)
      TY(I)=TX(I)/SQRT(RATIO)
    9 Y4(I)=ABS(ALO(I)-CLTOT(I))
      IF(NIT-999) 11,11,999
   11 DO 12 I=1,NM
      IF(Y1(I)-Y2(I)) 14,12,12
   12 CONTINUE
      DO 13 I=1,NL
      IF(Y3(I)-Y4(I)) 14,13,13
   13 CONTINUE
      IPT=IPT+1
      IF(NFLAG.NE.1) GO TO 18
      WRITE(6,99) NIT
   18 RETURN
   14 DO 16 I=1,NL
   16 TX(I)=TY(I)
      DO 17 I=1,NM
   17 VX(I)=VY(I)
      GO TO 2
  999 WRITE(6,998)
      IPT=1
      RETURN
      END
```

PLOT

```
      SUBROUTINE PLOT(TOTP,PH,FLIG,FMET,COMP,N,BTOT,CLTOT,N1)
C
C     THIS VERSION WILL PLOT DISTRIBUTION CURVES FOR A ONE METAL ONE
C     LIGAND SYSTEM WITH UP TO 20 COMPLEXES
      DIMENSION PH(100),FLIG(100,10),FMET(100,10),COMP(100,100),BTOT(1
     1,CLTOT(10)
      DIMENSION LINE(101),NCOMP(20)
      DIMENSION SUBTLE(20)
      INTEGER OUT,BLANK,SYM(20)
      DATA OUT,BLANK,SYM/' ','.','M','L','A','B','C','D','E','F','G','H
     1','I','J','K','N','O','P','Q','R','S','T'/
      READ(5,20) (SUBTLE(I),I=1,20)
      WRITE(6,21) (SUBTLE(I),I=1,20)
      READ(5,19) NODE
      WRITE(6,22)
      WRITE(6,23)
C     IF THERE ARE NO METAL SPECIES SET BTOT(1) = 1
      IF(N1.NE.N) GO TO 16
      BTOT(1)=1
C     DRAW THE Y AXIS
   16 DO 11 J=1,101
   11 LINE(J)=OUT
      WRITE(6,24) LINE
      DO 1 JJ=1,TOTP
C     CALCULATE THE PERCENT COMPOSITION FOR EACH SPECIES
      FMET(JJ,1)=FMET(JJ,1)*100./BTOT(1)
      FLIG(JJ,1)=FLIG(JJ,1)*100./CLTOT(1)
      DO 4 I=1,N1
    4 COMP(JJ,I)=COMP(JJ,I)*100./CLTOT(1)
      NN=N1+1
      DO 5 I=NN,N
    5 COMP(JJ,1)=COMP(JJ,1)*100./BTOT(1)
C     CLEAR ARRAY LINE
      DO 12 K=1,101
   12 LINE(K)=BLANK
C     CONVERT PERCENTAGES TO FIXED POINT AND ROUND OFF
      NMET=FMET(JJ,1)
      IF((FMET(JJ,1)-NMET).LT.0.50) GO TO 7
      NMET=NMET+1
    7 NLIG=FLIG(JJ,1)
      IF((FLIG(JJ,1)-NLIG).LT.0.50) GO TO 8
      NLIG=NLIG+1
    8 DO 9 I=1,N
      NCOMP(I)=COMP(JJ,1)
      IF((COMP(JJ,1)-NCOMP(I)).LT.0.50) GO TO 9
      NCOMP(I)=NCOMP(I)+1
    9 CONTINUE
C     CHECK IF PROTONATED LIGAND AND METAL SPECIES ARE TO BE
C     PLOTTED TOGETHER
      IF(NODE) 2,2,3
    3 DO 10 I=1,N
   10 LINE(NCOMP(I)+1)=SYM(I+2)
      LINE(NLIG+1)=SYM(2)
      LINE(NMET+1)=SYM(1)
      LINE(1)=OUT
      LINE(101)=OUT
      GO TO 13
    2 DO 14 I=NN,N
   14 LINE(NCOMP(I)+1)=SYM(I+2)
      LINE(NMET+1)=SYM(1)
      LINE(1)=OUT
      LINE(101)=OUT
   13 WRITE(6,25) PH(JJ),LINE
    1 CONTINUE
      DO 15 I=1,101
   15 LINE(I)=OUT
      WRITE(6,24) LINE
   19 FORMAT(I1)
   20 FORMAT(20A4)
   21 FORMAT('1',20A4)
   22 FORMAT('0                                        PERCENTAGE OF SPECIES IN S
     1OLUTION')
   23 FORMAT('0          0          10          20          30          40
```

```
     *   50          60          70          80          90          100')
  24 FORMAT(' ',10X,101A1)
  25 FORMAT(' ',4X,F5.2,1X,101A1)
     RETURN
     END
```

STORE

```
      SUBROUTINE STORE(JJ,VX,IX,C,NM,NL,N,FMET,FLIG,COMP)
C
C     THIS ROUTINE STORES THE CALCULATED FREE LIGAND FREE METAL
C     AND COMPLEX CONCENTRATIONS FOR EACH PH VALUE. THESE VALUES
C     ARE THEN USED BY SUBROUTINE PLOT
      DIMENSION VX(100),IX(100),C(100),FMET(100,10),FLIG(100,10),COMP(1
     10,100)
      DO 1 I=1,NM
    1 FMET(JJ,I)=VX(I)
      DO 2 I=1,NL
    2 FLIG(JJ,I)=IX(I)
      DO 3 I=1,N
    3 COMP(JJ,I)=C(I)
      RETURN
      END
```

Bibliography

1. Schroeder, H.A. and Nason, A.P.
   Clin. Chem. 17, 461-74, 1971.

2. Mertz, W.
   Fed. Proc. 29, 1482-88, 1970.

3. Schartz, M.K.
   In "Nuclear Activation Techniques in Life Sciences"
   International Atomic Energy Agency, Vienna, 1972.

4. Committee on Medical and Biologic Effects of
   Environmental Pollutants.
   "Medical and Biologic Effects of Environmental
   Pollutants - Nickel",
   National Academy of Sciences, Washington, D.C., 1975
   Page 88.

5. Brooks, R.R.
   In "Environmental Chemistry", Ed. J.O'M. Brockis,
   Plenum Press, New York, 1977.

6. Nielsen, F.H.
   In "Newer Trace Elements in Nutrition", Eds. W. Mertz
   and W.E. Cornatzer, Marcel Dekker, New York, 1971

7. Sunderman, F.W., Decsy, M.I., McNeely, D.
   Ann. N.Y. Acad. Sci. 199, 300-12, 1972.

8. Nielson, F.H.
   In "Trace Element Metabolism in Animals-2"
   Ed. W.G. Hoekstra, Univ. Park. Press, Maryland, 1974

9. Underwood, E.J.
"Trace Elements in Human and Animal Nutrition", 4th Edn,
Academic Press, New York, 1977.
Chapter 6.

10. Pfeiffer, C.C.
"Mental and Elemental Nutrients",
Keats Publishing, Connecticut, 1975.
Chapter 30.

11. See reference 4, page 5.

12. Jaffré, T. Brooks, R.R., Lee, J., and Reeves, R.D.
Science 193, 579-80, 1976.

13. Lee, J., Brooks, R.R., Reeves, R.D., Boswell, C.R., Jaffré, T
Plant and Soil 46, 675-80, 1977

14. Mishra, D. and Kar, M.
Botanical Review 40, 395-452, 1974.

15. See reference 4, page 52.

16. Brooks, R.R.
In "Biogeochemistry of Nickel", Ed. J.O. Nriagu,
Ann Arbor Science, Michigan, 1979.

17. Brooks, R.R., Morrison, R.S., Reeves, R.D., Dudley, T.R.
Proc. Roy. Soc. London, Section B, (in press).

18. Brooks, R.R. and Kerston, W.
Unpublished work.

19. Tiffin, L.O.
Plant Physiol. 48, 273-7, 1971.

20. Tiffin, L.O.
Plant Physiol. 45, 280-3, 1970.

21. Thompson, J.F. and Tiffin, L.O.
Plant Physiol 53 Suppl., 23, 1974.

22. Kelly, P.C., Brooks, R.R., Dilli, T., and Jaffré, T.
Proc. Roy, Soc. London B189, 69-80, 1975.

23. Pelosi, P., Fiorentini, R., and Galoppini, C.
Agri. Biol. Chem 40, 1641-2, 1976.

24. Pancaro, L., Pelosi, P., Vergnano Gambi, O. and Galoppini, C.
G. Bot. Ital. (in press).

25. Lee, J., Reeves, R.D., Brooks, R.R. and Jaffrē, T.
Phytochemistry 17, 1033-5, 1978.

26. Lee, J., Reeves, R.D., Brooks, R.R. and Jaffrē, T.
Phytochemistry 16, 1503-5, 1977.

27. Lee, J.
Ph.D. Thesis, Massey University, Palmerston North, NZ, 1977.

28. Mathys, W.
Physiologic Plantarum 40, 130-6, 1977

29. Lee, J.
M.Sc. Thesis, Massey University, NZ, 1974.

30. Farago, M.E., Clark, A.J. and Pitt, M.J.
Co-ord. Chem. Rev. 16, 1-8, 1975.

31. Rossotti, F.J.C. and Rossotti, H.
"The Determination of Stability Constants",
McGraw-Hill, London, 1961.
Page 1.

32. Brooks, R.R., Lee, J., Reeves, R.D. and Jaffrē, T.
J. Geochem Explor. 7, 49-57, 1977.

33. Petit-Ramel, M.M. and Khalil, I.
Bull. Soc. Chim. France 7-8, 1255-8, 1974.

34. Field, T.B., Coburn, J., McCourt, J.L. and McBryde, W.A.E.
Anal. Chim. Acta. 74, 101-6, 1975.

35. Campi, E., Ostacoli, G., Meirone, M. and Saini, G.
J. Inorg. Nuclear Chem. 26, 553-64, 1964.

36. Li, N.C., Lindenbaum, A. and White, J.M.
J. Inorg. Nuclear Chem. 12, 122-8, 1959.

37. Kereichuk, A.S. and Churikova, T.M.
Russ. J. Inorg. Chem. 17, 1300-3, 1972.

38. Grigor'eva, V.V. and Tsimbler, S.M.
Russ. J. Inorg. Chem. 13, 259-63, 1968

39. Heitner-Wirguin, C., Friedman, D., Goldschmidt, J.M.E. and Shamir, J.
Bull. Soc. Chim. France, 864-7, 1958.

40. Patnaik, R.K. and Pani, S.
J. Indian Chem. Soc. 42, 793-8, 1965.

41. Khoperiya, T.N. and Glonti, Z.Sh.
Russ. J. Phys. Chem. 46, 329-32, 1972.

42. Migal, P.K. and Sycheu, A.Ya.
Zhur. Neorg. Kkim. 3, 314-24, 1958.

43. Migal, P.K. and Sycheu, A.Ya.
Zhur. Neorg. Khim. 1, 1008-12, 1956.

44. Heitner-Wirguin, C. and Eliezer, I.
Bull. Soc. Chim. France 24, 149-52, 1957.

45. Bottari, E.
Annali di Chimica 65, 375-94, 1975.

46. Field, T.B, McCourt, J.L. and McBryde, W.A.E.
Can. J. Chem. 54, 3119-24, 1974.

47. Rajan, K.S. and Martell, A.E.
J. Inorg. Nuclear Chem. 29, 463-71, 1967.

48. Heitner, C. and Eliezer, I.
Bull. Soc. Chim. France 23, 174-7, 1956.

49. Patnaik, R.K. and Pani, S.
J. Indian Chem. Soc. 38, 364-78, 1961.

50. Tsimbler, S.M. and Grigor'eva, V.V.
Russ. J. Inorg. Chem. 15, 1397-9, 1970.

51. Wang, S.M. and Li, N.C.
J. Inorg, Nuclear Chem. 27, 2093-101, 1965.

52 Li, N.C. and White, J.M.
J. Inorg. Nuclear Chem. 16, 131-7, 1960.

53. Chemical Society of London,
"Stability Constants of Metal Ion Complexes"
Special Publication 17(1964), 25(1971),
Chemical Society, London.

54. Vogel, A.I.
"A Textbook of Quantitative Inorganic Analysis", 3rd Edn,
Longman, London, 1961.
Pages 125 and 479.

55. See reference 54, page 307.

56. Hedwig, G.R.
Massey University, Palmerston North, N.Z.
Unpublished work.

57. Bates, R.G.
"Determination of pH, Theory and Practice", 2nd Edn.,
John Wiley and Sons, New York, 1973.
Page 97.

58. Keller, R.A.
"Basic Tables in Chemistry"
McGraw-Hill, New York, 1967.
Page 149.

59. Perrin, D.D.
Chem. and Ind., 661, 1966.

60. See reference 57, page 29.

61. See reference 57, page 72.

62. See reference 54, page 172.

63. See reference 57, page 48.

64. McBryde, W.A.E.
Analyst 94, 337-46, 1969.

65. See reference 57, page 73.

66. Hedwig, G.R. and Powell, H.J.K.
Anal. Chem. 43, 1206-12, 1971.

67. Rand, R.N.
Clin. Chem. 15, 839-63, 1969.

68. Johnson, E.A.
Photoelectric Spectrometry Group Bulletin 17, 505-7, 1967

69. Milazzo, G.
NBS Spec Publ 408, 127-45, 1975.

70. Haupt, G.W.
J. Opt. Soc. Amer. 42, 441-7, 1952.

71. Slavin, W.
J. Opt. Soc. Amer. 52, 1399-1401, 1962.

72. Ewing, G.W.
"Instrumental Methods of Chemical Analysis", 4th Edn.
McGraw-Hill, Tokyo, 1975.
Page 41.

73. Dick, J.G.
"Analytical Chemistry",
McGraw-Hill, Tokyo, 1973.
Page 239.

74. See reference 73, page 242.

75. Gran, G.
Acta. Chim. Scand., 559-77, 1950.

76. Gran, G.
Int. Congress Anal. Chem. 77, 661-71, 1952.

77. Rossotti, F.J.C. and Rossotti, H.
J. Chem. Education 42, 375-8, 1965.

78. See reference 57, page 95.

79. Pearce, K.N. and Creamer, L.K.
Aust. J. Chem. 28, 2409-15, 1975.

80. Kankare, J.J.
Anal. Chem. 44, 2376-9, 1972.

81. Warner, R.C. and Weber, I.
J. Amer. Chem. Soc. 75, 5086-94, 1953.

82. Briggs, T.N. and Stuehr, J.E.
Anal. Chem. 47, 1916-20, 1975.

83. Pearce, K.N.
Ph.D. Thesis, Massey University, NZ, 1972.

84. Vaňura, P. and Kuča, A.
Coll. Czech. Chem. Comm. 43, 1460-75, 1978.

85. Hamm, R.E., Shull, C.M., and Grant, D.M.
J. Amer. Chem. Soc. 76, 2111-14, 1954.

86. Timberlake, C.F.
J. Chem. Soc., 5078-85, 1964.

87. Kereichuk, A.S.
Russ. J. Inorg. Chem. 16, 1346-8, 1971.

88. Besse, G., Chabard, J., Voissière, G., Petit, J.
and Berger, J.
Bull. Soc. Chim. France 11, 4166-9, 1970.

89. See reference 4, page 81.

90. Baes, C.F. and Mesmer, R.E.
"The Hydrolysis of Cations"
Wiley and Sons, New York, 1976.

91. Kereichuk, A.S. and Churikova, I.M.
Zh. Neorg. Khim. 23, 1686-8, 1978.

92. Brooks, R.R., Lee, J. and Jaffrẽ, T.
J. Ecol. 62, 493-9, 1974.

93. Rautkina, V.I.
Refer Chemical Abstracts 73, 41368b, 1970.

94. Strouse, J., Layten, S.W. and Strouse, C.E.
J. Amer. Chem. Soc. 99, 562-72, 1977.

95. Strouse, J.
J. Amer. Chem. Soc. 99, 573-80. 1977.

96. Conte, S.D. and de Boor, C.
"Elementary Numerical Analysis"
McGraw-Hill, Kogakasha, 1972.

97. Camden, B., Paulin, A., Quinn, K. and Ramsay, A.
"Numerical Methods"
Eton Press, Christchurch, NZ, 1975.

98. Bobtelsky, M. and Heitner, C.
Bull. Soc. Chim. France, 494-502, 1951.

99. Bobtelsky, M. and Jordan, J.
J. Amer. Chem. Soc. 67, 1824-31, 1945.

100. Nielson, F.H.
In "Trace Elements in Human Health and Disease - Vol II"
Ed. A.S. Prasad, Academic Press, New York, 1976

101. Campi, E.
Ann. Chim. (Italy) 53, 96-116, 1963.

102. Yasuda, M., Yamasaki, K. and Ohtaki, H.
Bull. Chem. Soc. Japan 33, 1067-70, 1960

103. Windholz, M. (Ed)
"The Merck Index", 9-th Edn.,
Merck and Co., New Jersey, 1976.

104. Watelle-Marion, G.
Compt. rend. 246, 3610-13, 1958.

105. Vacca, A., Sabatini, A. and Gristina, M.A.
Coord. Chem. Rev. 8, 45-53, 1972.

106. Rollet, J.S. (Ed)
"Computing Methods in Crystallography"
Pergamon Press, Oxford, 1965.
Page 33.

107. Greenspan, H.B. and Benny, D.J.
"Calculus, An Introduction to Applied Mathematics"
McGraw-Hill, New York, 1973.
Page 329.

108. See reference 106, page 20.

109. Busing, W.R. and Levy, H.A.
"General Least Squares Program"
ORNL-TM-271, Chemistry Division, Oak Ridge National Laboratory, Oak Ridge, Tennessee. 1962

110. Perrin, D.D. and Sayce, I.G.
Talanta 14, 833-42, 1967.

111. Jurs, P.C.
Anal. Chem. 42, 747-50, 1970.

112. Hugus, Z.Z.
In "Advances in the Chemistry of the Coordination Compounds"
Ed. S. Kirschner, MacMillan, 1961.
Page 388.

113. Rossotti, F.J.C.
In "Modern Coordination Chemistry"
Eds. J. Lewis and R.G. Wilkens,
Interscience, New York, 1960.
Page 57-64.

114. Beck, M.T.
"Chemistry of Complex Equilibria"
Van Nostrand Reinhold, London, 1970.
Page 263.

115. Douglas, B.E. and McDaniel, D.H.
"Concepts and Models of Inorganic Chemistry"
Xerox, Lexington, 1965.
Page 400.

116. Cotton, F.A. and Wilkinson, G.
"Advanced Inorganic Chemistry", 3-rd Edn.
Interscience, New York, 1972.
Page 650.

117. Patnaik, R.K. and Pani, S.
J. Ind. Chem. Soc. 34, 619-28, 1957.

118. See reference 113, page 34.

119. See reference 116, page 649.

120. See reference 114, page 34.

121. Irving, H. and Williams, R.P.G.
J. Chem. Soc., 3192-210, 1953.

122. See reference 116, pages 592 and 912.

123. Orgel, L.E.
"An Introduction to Transition-Metal Chemistry
Ligand Field Theory", 2-nd Edn.
Methuen, London, 1967.
Page 63.

124. Ashcroft, S.F. and Mortimer, C.T.
"Thermochemistry of Transition Metal Complexes"
Academic Press, London, 1973.
Page 27.

125. See reference 116, page 894.

126. See reference 116, page 1118.

127. Jørgensen, C.K.
"Modern Aspects of Ligand Field Theory"
North-Holland, Amsterdam, 1971.
Page 347.

128. See reference 72, page 37.

129. See reference 127, page 378.

130. Hare, C.R.
In "Spectroscopy and Structure of Metal Chelate Compounds"
Eds. K Nakamoto and P.J. McCarthy,
Wiley, New York, 1968.
Page 106.

131. See reference 123, page 95.

132. See reference 116, page 885.

133. See reference 130, page 97.

134. Dunn, T.M.
In "Modern Coordination Chemistry"
Eds. J. Lewis and R.G. Wilkens,
Interscience, New York, 1960.
Page 266.

135. See reference 123, page 98.

136. See reference 72, page 72.

137. Ksandr, Z. and Hegtnãnek, M.
Cited by Perrin, D.D
J. Chem. Soc., 3644-8, 1964.
Also see Chemical Abstracts 50, 3150g, 1956.